



ANP-10287NP
Revision 0

**Incore Trip Setpoint and Transient Methodology for U.S. EPR
Topical Report**

November 2007

AREVA NP Inc.

Copyright © 2007

**AREVA NP Inc.
All Rights Reserved**

Abstract

This report documents the analytical methodology used to determine the setpoints for the incore-based departure from nucleate boiling (DNB) and linear power density (LPD) limiting safety system setting (LSSS), limitation, and limiting conditions for operation (LCO) functions in the U.S. EPR. These functions represent graduated layers of defenses against violation of the DNB and LPD specified acceptable fuel design limits (SAFDL) during the design basis events they are designed to protect.

The DNB setpoints are established such that the DNB-limiting pin in the core will not experience departure from nucleate boiling during DNB basis events, at 95 percent probability, with 95 percent confidence, considering all uncertainties. The LPD setpoints are established such that the location in the core with peak linear power density will not exceed either fuel centerline melt or clad strain limits during LPD basis events, at 95 percent probability and with 95 percent confidence, considering all applicable uncertainties.

Nature of Changes

Item	Date	Change Section(s) or Page(s)	Description
0	November, 2007	All	Initial release

Contents

		<u>Page</u>
1.0	INTRODUCTION	1-1
2.0	REGULATORY REQUIREMENTS	2-1
2.1	Holistic Protection of Fuel SAFDL in U.S. EPR.....	2-2
	2.1.1 Monitoring (LCO) Functions	2-2
	2.1.2 Limitation Functions	2-3
	2.1.3 Trip (LSSS) Functions.....	2-3
3.0	LOW DNBR CHANNEL LIMITING SAFETY SYSTEM SETTINGS	3-1
3.1	Design Basis	3-1
3.2	Functional Description	3-2
	3.2.1 Process Variable Input	3-2
	3.2.2 Plant Constant Inputs.....	3-3
	3.2.3 Algorithm.....	3-3
	3.2.4 Setpoints	3-3
	3.2.5 Reactor Trip Signal Scenarios	3-6
	3.2.6 Function Blocks.....	3-7
	3.2.7 Inhibition.....	3-7
3.3	Interface with Other Trips.....	3-8
4.0	LIMITING CONDITIONS FOR OPERATION ON DNB	4-1
4.1	Design Basis	4-1
4.2	Functional Description	4-1
	4.2.1 Process Variable Input	4-2
	4.2.2 Plant Constants.....	4-3
	4.2.3 Algorithm.....	4-4
	4.2.4 Setpoints	4-4
4.3	Inhibition	4-4
5.0	STATIC DNBR SETPOINT METHODOLOGY.....	5-1
5.1	Statement of Problem	5-1
5.2	Clarification of Terminology	5-3
5.3	Uncertainties Affecting DNBR Monitoring and Protection	5-4
	5.3.1 Cold Leg Temperature Measurement	5-5

5.3.2	Pressurizer Pressure Measurement.....	5-6
5.3.3	Inlet Flow Rate	5-6
5.3.4	SPND Measurement	5-7
5.3.5	CHF Correlation	5-8
5.3.6	Online Algorithm.....	5-9
5.3.7	Power Calorimetric.....	5-11
5.3.8	Transient SPND Decalibration	5-11
5.3.9	Reconstructed Power Distribution (AMS).....	5-15
5.3.10	Thermal Hydraulic Conditions for SPND Data.....	5-16
5.3.11	SPND Calibration Frequency	5-17
5.3.12	Assembly Geometry Deviations	5-18
5.3.13	Rod Bow	5-18
5.3.14	Assembly Bow.....	5-19
5.3.15	Epistemic	5-19
5.4	Coverage Method for Establishing DNBR/Quality Setpoints.....	5-20
5.4.1	Coverage Method.....	5-21
5.4.2	Calculation of Reference DNBR.....	5-25
5.4.3	Calculation of Reference Exit Quality.....	5-27
5.4.4	Calculation of Sensed DNBR	5-29
5.4.5	Calculation of Sensed Exit Quality	5-30
5.4.6	Treatment of Inoperable SPNDs	5-30
5.5	Testing Method for Confirming Existing Setpoints	5-31
5.5.1	General Flow of Testing Process	5-32
5.5.2	Testing Method for LSSS versus LCO Functions.....	5-34
6.0	HIGH LPD CHANNEL LIMITING SYSTEM SAFETY SETTING	6-1
6.1	Design Basis	6-1
6.2	Functional Description	6-2
6.2.1	Process Variable Input.....	6-2
6.2.2	Plant Constant Inputs.....	6-2
6.2.3	Algorithm.....	6-3
6.2.4	Setpoints	6-5
6.2.5	Inhibition.....	6-5
6.3	Interface with Other Trips.....	6-5
7.0	LIMITING CONDITIONS FOR OPERATION ON LPD.....	7-1
7.1	Design Basis	7-1
7.2	Functional Description	7-1

7.2.1	Process Variable Input	7-1
7.2.2	Plant Constant Inputs	7-2
7.2.3	Algorithm	7-2
7.2.4	Setpoints	7-4
7.2.5	Inhibition	7-5
8.0	STATIC LPD SETPOINT METHODOLOGY	8-1
8.1	Statement of Problem	8-1
8.2	Uncertainties Impacting LPD Monitoring and Protection	8-2
8.2.1	SPND Measurement	8-2
8.2.2	Power Calorimetric	8-3
8.2.3	Transient SPND Decalibration	8-3
8.2.4	Reconstructed Power Distribution (AMS)	8-3
8.2.5	Thermal Hydraulic Conditions for SPND Data	8-3
8.2.6	SPND Calibration Frequency	8-3
8.2.7	Pellet Manufacturing Deviations	8-4
8.2.8	Rod Bow	8-4
8.2.9	Assembly Bow	8-4
8.2.10	Epistemic	8-5
8.3	Coverage Method for Establishing LPD Setpoints	8-5
8.3.1	Calculation of Reference LPD	8-8
8.3.2	Calculation of Sensed LPD	8-11
8.3.3	Treatment of Inoperable SPNDs	8-12
8.4	Methodology for Confirming Existing LPD Setpoints	8-12
9.0	TRANSIENT ANALYSIS FOR INCORE TRIPS	9-1
9.1	Overview	9-1
9.2	Initial Conditions Credited in the Transient Analysis	9-2
9.3	Treatment of Power Distributions	9-5
9.4	Method for Performing Undershoot/Overshoot Assessments	9-6
9.5	Method for Δ (DNBR) and Δ (LPD) Allowances	9-10
9.5.1	Establishing New Δ (DNBR) and Δ (LPD) Allowances	9-10
9.5.2	Confirming Δ (DNBR) and Δ (LPD) Allowances	9-13
9.6	Method for Establishing Limitation Function Setpoints	9-14
10.0	SAMPLE CALCULATIONS	10-1
10.1	Static Setpoint Sample Calculation – LSSS Functions	10-1

10.1.1	Trip Configuration Inputs.....	10-1
10.1.2	Uncertainty Inputs	10-1
10.1.3	Power Distribution Inputs	10-2
10.1.4	Thermal Hydraulic Statepoint Inputs	10-3
10.1.5	Sample Calculation Results	10-3
10.2	Static Setpoint Sample Calculation – LCO Functions	10-4
10.2.1	LCO Configuration Inputs.....	10-4
10.2.2	Uncertainty Inputs	10-4
10.2.3	Power Distribution Inputs	10-5
10.2.4	Thermal Hydraulic Statepoint Inputs	10-5
10.2.5	Sample Calculation Results	10-5
10.3	Transient DNBR Undershoot Evaluation.....	10-5
10.4	Transient Δ (DNBR) Evaluation	10-6
11.0	REFERENCES	11-1
APPENDIX A STATISTICAL METHODOLOGY		A-1
A.1	Description of Statistical Tolerance Limits.....	A-1
A.1.1	Overview	A-1
A.1.2	Coverage Approach for Single Setpoint	A-1
A.1.3	Testing Approach for Multiple Setpoints	A-5
A.1.4	Sample Size Considerations	A-7
APPENDIX B PRINCIPLES OF SPND CALIBRATION.....		B-1
B.1	Overview	B-1
B.1.1	LPD Calibration Factors	B-1
B.1.2	DNBR Calibration Factors	B-2
APPENDIX C DESCRIPTION OF ONLINE DNBR ALGORITHM		C-1
C.1.1	Power Shape Reconstruction.....	C-1
C.1.2	Filtering of Process Input Signals.....	C-1
C.1.3	Calculation of the Inlet Mass Velocity.....	C-2
C.1.4	[.....	C-3
C.1.5	[.....	C-5
C.1.6	[.....	C-6
C.1.7	[.....	C-7
C.1.8	Calculate Uniform Critical Heat Fluxes.....	C-8
C.1.9	Calculate Non-Uniform Flux Factors	C-8
C.1.10	Calculate DNBRs	C-9

C.1.11	Filter MDNBR and Exit Quality Signals	C-10
C.2	Calculation of SPND Imbalance	C-10
APPENDIX D	RANDOM SAMPLING FROM CUMULATIVE DISTRIBUTION FUNCTIONS	D-1
APPENDIX E	METHODOLOGY FOR ASSESSING MEASURED POWER DISTRIBUTION UNCERTAINTIES	E-1
E.1	Aeroball Measurement System	E-1
E.2	MEDIAN Power Distribution Reconstruction Methodology	E-2
E.3	Determination of Two-Group Optimal Fluxes	E-3
E.4	Extrapolation of the Node Fluxes	E-4
E.5	Application of Spacer Grid Axial Form Functions	E-5
E.6	Inferred Relative Power Distribution Uncertainties	E-7
E.7	Sample Power Distribution Uncertainty Calculation	E-8
E.7.1	F_Q Power Distribution Uncertainty	E-9
E.7.2	$F_{\Delta H}$ Power Distribution Uncertainty	E-10
E.7.3	Assembly Axial Offset Distribution Uncertainty	E-10
E.7.4	Local Peaking Factor Uncertainty	E-11
E.7.5	Combined Power Distribution Uncertainties	E-11
E.7.6	Summary	E-13

List of Tables

	<u>Page</u>
Table 3-1 Basis Events for the Low DNBR Channel LSSS	3-10
Table 3-2 Plant Constants Used in the Low DNBR Channel LSSS.....	3-11
Table 3-3 Setpoint Logic for the Low DNBR Channel LSSS	3-16
Table 3-3 Low DNBR Channel Setpoint Adjustments for SPND String Failures	3-16
Table 3-4 Function Blocks in the Low DNBR Channel LSSS	3-17
Table 4-1 Basis Events for the DNB LCO	4-5
Table 4-2 Plant Constants for the DNB LCO.....	4-6
Table 4-3 DNB LCO Setpoint Adjustments for SPND Failures.....	4-7
Table 6-1 Basis Events for the High LPD Channel LSSS.....	6-9
Table 6-2 High LPD Channel LSSS Constants	6-10
Table 6-3 High LPD Channel LSSS Logic for Failed SPNDs	6-11
Table 7-1 Basis Events for the LPD LCO	7-7
Table 7-2 LPD LCO Constants.....	7-8
Table 10-1 Input Data for the Static Sample Problem	10-8
Table 10-2 SPND Imbalance Thresholds for Sample Problem	10-9
Table 10-3 Input Uncertainties for the Sample Problem.....	10-10
Table 10-4 Parameter Ranges for LSSS Setpoint Sample Calculation.....	10-11
Table 10-5 T/H Setpoint Statepoints for LSSS Sample Calculation	10-12
Table 10-6 Parameter Ranges for LCO Setpoint Sample Calculation.....	10-12
Table 10-7 T/H Setpoint Statepoints for LCO Sample Calculation	10-13
Table 10-8 Results from Sample LSSS Coverage Calculation.....	10-13
Table 10-9 Results from Sample LCO Coverage Calculation	10-14
Table A-1 [.....].....	A-8
Table E-1 Inferred Relative Power Distribution Summary Statistics.....	E-14

Table E-2 χ^2 Test of Normality, Local Peaking Factor DataE-18

Table E-3 Summary of Mean and Standard Deviations (%C-M)E-18

Table E-4 Inferred Relative Power Distribution Uncertainties.....E-19

List of Figures

	<u>Page</u>
Figure 2-1 Monitoring/Protection System Functionality in U.S. EPR	2-4
Figure 3-1 Low DNBR Channel Symmetric Trip Scenario	3-18
Figure 3-2 Low DNBR Channel Imbalance (DNBR _{IMB/RD}) Trip Scenario	3-19
Figure 3-3 Low DNBR Channel Dropped Rod (DNBR _{RD}) Trip Scenario	3-20
Figure 5-1 Establishing the DNBR Trip Setpoint	5-36
Figure 5-2 Establishing the Exit Quality Trip Setpoint	5-37
Figure 5-3 Establishing the DNB LCO Setpoint.....	5-38
Figure 5-4 DNBR and Exit Quality Coverage Method	5-39
Figure 5-5 Testing Method for Confirming Setpoints	5-40
Figure 6-1 High LPD Channel LSSS Functional Diagram	6-7
Figure 6-2 Core Layout for the High LPD Channel LSSS.....	6-8
Figure 7-1 LPD LCO Functional Diagram.....	7-6
Figure 8-1 Establishing the LPD Trip Setpoint	8-14
Figure 8-2 Establishing the LPD LCO Setpoint	8-15
Figure 8-3 LPD Coverage Method for Establishing Setpoints	8-16
Figure 9-1 Example of APS LCO “Barn”.....	9-17
Figure 9-2 Transient Analysis Process Flow	9-18
Figure 9-3 DNBR Undershoot Assessment.....	9-19
Figure 9-4 LPD Overshoot Assessment.....	9-20
Figure 9-5 Method for Establishing New Δ (DNBR) Allowances.....	9-21
Figure 10-1 DNBR Algorithm Uncertainty.....	10-14
Figure 10-2 Exit Quality Algorithm Uncertainty.....	10-15
Figure 10-3 Bank Withdrawal At Power Considering Incore Trips.....	10-16
Figure 10-4 Δ (DNBR) Calculation for Four-Pump Loss of Coolant Flow	10-17
Figure B-1 SPND Calibration for LPD	B-5

Figure B-2 Generation of SPND Power for DNBRB-6

Figure B-3 SPND Calibration for DNBRB-7

Figure E-1 Layout of Incore Nuclear Instrumentation in U.S. EPR.....E-20

Figure E-2 Plant G1 Assembly Guide Tube ConfigurationE-21

Figure E-3 Plant G2 Assembly Guide Tube ConfigurationE-22

Figure E-4 FQ Relative Difference Compared to Normal DistributionE-23

Figure E-5 $F\Delta H$ Relative Difference Compared to Normal DistributionE-24

Figure E-6 AO Relative Difference Compared to Normal DistributionE-25

Nomenclature

Acronym	Definition
AMS	Aeroball Measurement System
AO	Axial Offset
AOO	Anticipated Operational Occurrences
APS	Axial Power Shape
CDF	Cumulative Distribution Function
CFR	Code of Federal Regulations
CHF	Critical Heat Flux
CRDM	Control Rod Drive Mechanism
(M)DNB(R)	(Minimum) Departure from Nucleate Boiling (Ratio)
EFPD	Effective Full Power Days
GDC	General Design Criteria
HCPL	High Core Power Level
(H)LPD	(High) Linear Power Density
IMB	(SPND) Imbalance
LCO	Limiting Conditions for Operation
LOCA	Loss of Coolant Accident
LPD	Linear Power Density
LPF	Local Peaking Factor
LSSS	Limiting Safety System Setting
LTSP	Limiting Trip Setpoint
MSLB	Main Steam Line Break
MSSV	Main Steam Safety Valves
NRC	Nuclear Regulatory Commission
PA	Postulated Accident
PDF	Probability Density Function
PZR	Pressurizer
PS	Protection System
PWR	Pressurized Water Reactor
RCCA	Rod Cluster Control Assembly
RCP	Reactor Coolant Pump
RCSL	Reactor Control, Surveillance, and Limitation System
RD	Rod Drop

RT	Reactor Trip
RTD	Resistance Temperature Detector
RTP	Rated Thermal Power
SAFDL	Specified Acceptable Fuel Design Limit
SGFF	Spacer Grid Axial Form Function
SPND	Self-Powered Neutron Detector
SRP	Standard Review Plan

1.0 INTRODUCTION

This topical report describes the analytical methodology used to establish setpoints for the incore trip and Limiting Conditions for Operation (LCO) functions in the U.S. EPR. Specifically, it describes the methods to be used for the following Limiting Safety System Settings (LSSS) and LCO functions:

- Low DNBR Channel LSSS
- Low DNBR Limitation
- DNB LCO
- High LPD Channel LSSS
- High LPD Limitation
- LPD LCO

The DNB and LPD LCO functions are designed to maintain acceptable margins to the DNB and LPD safety limits, while the Low DNBR and High LPD Channel LSSS functions provide active protection against penetration of the DNB and LPD safety limits during trip basis events. The Low DNBR and High LPD Limitation functions are designed to generate a partial trip in response to an encroachment upon the Low DNBR and High LPD trip setpoints, respectively.

This methodology describes the process for propagating constituent uncertainties related to these functions into a limiting trip setpoint (LTSP) setting. A number of the input uncertainties to this process are the result of channel uncertainty calculations. The methodology for generating channel uncertainties is outside the scope of this topical report, and is documented in a separate topical report (Reference 5).

The U.S. EPR Incore Trip Setpoint and Transient Methodology Topical Report will be used to develop setpoints associated with the protection system functions discussed herein. AREVA NP plans to reference this topical report in its Design Certification application for the U.S. EPR.

2.0 REGULATORY REQUIREMENTS

The LSSSs and LCOs that are the subject of this report are designed for safe operation in accordance with the specifications outlined in the 10 CFR 50, Appendix A (Reference 1). In particular, General Design Criteria (GDC) II:10 and II:13 (multiple fission barrier protection), and Criteria III:20, III:25, and III:29 (protection and reactivity control systems) stipulate that the SAFDLs should be protected by these functions during normal operation and anticipated operational occurrences (AOO). The SAFDLs are experimental or analytical limits on the fuel and cladding which preclude fuel damage, set conservatively with respect to the safety limits. The SAFDLs germane to the incore based trips for the U.S. EPR are the following:

1. Departure from nucleate boiling
2. Fuel centerline melt

The setpoint analysis must demonstrate that, with 95 percent confidence, the probability of violating either of the SAFDLs is less than or equal to 5 percent (i.e., satisfying the 95/95 criterion).

The DNB acceptance criterion is given on page 4.4-5 of Section 4.4 of Reference 2 and is as follows:

Standard Review Plan (SRP) Section 4.2 specifies the acceptance criteria for the evaluation of fuel design limits. One criterion provides assurance that there is at least a 95-percent probability at the 95-percent confidence level that the hot fuel rod in the core does not experience a DNB or transition condition during normal operation or AOOs.

Section 4.2.II.2(e) of Reference 2 also stipulates that fuel centerline melting is not permitted for AOOs in order to preclude fuel failure.

2.1 *Holistic Protection of Fuel SAFDL in U.S. EPR*

The relationship between LSSS and LCO functions is defined in 10 CFR 50.36. The U.S. EPR implements the LSSS and LCO in a graduated fashion, relative to contemporary plant designs. Figure 2-1 graphically depicts the evolutionary implementation of SAFDL protection for the incore trip functions discussed in this report.

The U.S. EPR has four layers of incore plant setpoints which protect the SAFDLs. These will be discussed in the following subsections.

2.1.1 *Monitoring (LCO) Functions*

The monitoring (LCO) functions are designed to protect the SAFDL by partially defining an envelope of acceptable initial conditions in terms of either DNBR or LPD. The functions thus preserve sufficient initial thermal margin such that the consequences of a transient event initiated within that operational envelope can be accommodated. The DNBR and LPD LCO functions are specifically designed to protect against the following types of AOO events:

- Events relying solely upon initial DNBR or LPD margin to prevent penetration of the SAFDLs
- Events requiring a combination of initial DNBR or LPD margin and a system trip¹ to prevent penetration of the SAFDLs

More generally, the ensemble of initial operational envelopes defined by the DNB LCO, LPD LCO, and the other LCOs, plus the ensemble of system trips must prevent penetration of the SAFDL for AOOs in which the Low DNBR Channel or High LPD Channel trips are not effective. Notably, this includes particular cases in the transient spectra that might slip into “cracks” in the holistic DNB or LPD protection.

¹ Throughout this document, the terminology “system trip” will be used to generically describe any trip other than the Low DNBR Channel or High LPD Channel trips.

The monitoring (LCO) functions on LPD and DNBR are implemented in terms of distinct setpoints (LCO1 and LCO2), which represent graduated thresholds for compensatory actions. The LCO functions are implemented in the Reactor Control, Surveillance, and Limitation System (RCSL) system.

2.1.2 *Limitation Functions*

The limitation functions are a plant-specific feature of the U.S. EPR design. The purpose of the limitation functions are to intercede in situations in which the plant operating state encroaches upon the incore trip setpoints. The limitation function will automatically apply rapid corrective actions with the purpose of bringing the plant into a controlled state, prior to the actuation of the full protection system (PS) trip. In contrast to the full reactor trip, a partial trip leaves the plant in an operational situation amenable to relatively rapid correction of the root cause of the thermal margin degradation, and resumption of full-power operation. Ultimately, the limitation functions are designed to increase plant availability.

Limitation functions are formulated in the PS, using concurrent signals with the LSSS functions. The signals are then compared against different setpoints for determination of limitation function violation and the issuance of a partial trip signal. The partial trip signal generated by the PS is then passed to the RCSL system for processing. The partial trip generates a fast turbine runback and the dropping of select rod cluster control assembly (RCCA) banks until the power is stabilized around 50 percent rated thermal power (RTP).

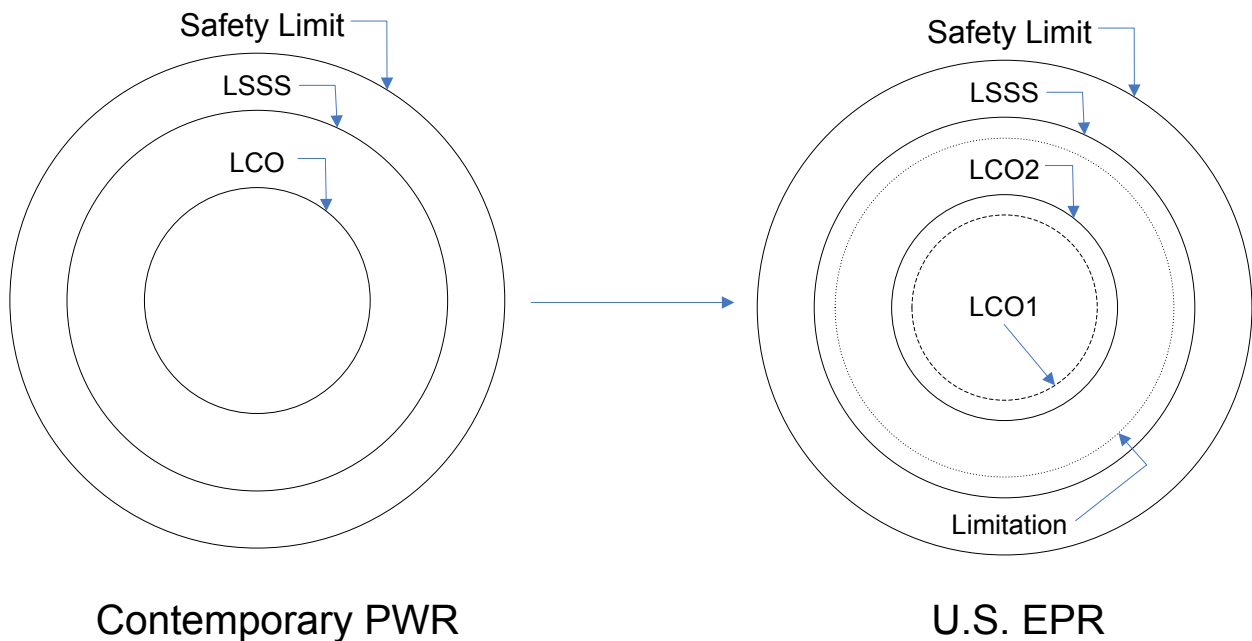
2.1.3 *Trip (LSSS) Functions*

The LSSS functions are designed to provide active intervention during normal and off-normal conditions in which the SAFDLs are approached. This is accomplished by monitoring either the LPD or DNBR in the reactor core, and comparing it against setpoint values that conservatively protect the safety limit. Violation of the LSSS function setpoint will produce a reactor trip signal.

Potential instances of full reactor trip are minimized via the use of limitation functions, as noted in Section 2.1.2.

In contrast to contemporary U.S. pressurized water reactor (PWR) designs, the U.S. EPR incore trips have two LCO setpoints, representing thresholds for graduated compensatory actions. If the first LCO setpoint is violated, initial passive automatic actions are performed (generally alarms and rod blocks). If the secondary LCO setpoint is subsequently violated, more active actions are taken to bring the plant into an acceptable operating state, including generator demand reduction and control bank insertion.

Figure 2-1 Monitoring/Protection System Functionality in U.S. EPR



3.0 LOW DNBR CHANNEL LIMITING SAFETY SYSTEM SETTINGS

Per the Standard Review Plan (Reference 2), Section 4.4, the SAFDL on DNB requires that at a minimum 95 percent probability, with minimum 95 percent confidence level, the limiting fuel rod in the core will not experience DNB during normal operation or transient conditions arising from faults of moderate frequency (AOOs). Further, it stipulates that assessments of DNB thermal margin should incorporate uncertainty in process variables, instrumentation, critical heat flux (CHF) correlations, core design parameters, and calculation methods, and these should also be evaluated at no less than the 95 percent probability and with 95 percent confidence.

Active intervention in events characterized by an uncontrolled degradation in the DNBR is provided by the Low DNBR Channel LSSS. This function produces a reactor trip when the SAFDL on DNB is approached, and ensures that protection is afforded at a level no less than 95 percent probability and with 95 percent confidence.

3.1 *Design Basis*

The Low DNBR Channel LSSS is designed to protect against normal operation and AOOs which erode DNBR margin due to changes in power, temperature, and pressure. Table 3-1 identifies the AOO events forming the primary basis of the Low DNBR Channel LSSS. The Low DNBR Channel LSSS may also intercede in certain postulated accidents, (for example, the pre-scam main steam line break (MSLB), control rod ejection).

In addition to actively interceding in situations in which the DNBR limit is encroached upon, the Low DNBR Channel will also produce a reactor trip when the calculated hot channel exit quality exceeds a value supported by the CHF correlation used in the online DNBR calculations. The purpose of this functionality is to preserve the quality limit for the CHF correlation.

3.2 *Functional Description*

The following subsections describe the Low DNBR Channel trip. Figure 3-1 depicts the process flow of the Low DNBR Channel LSSS for default (no asymmetric indication) conditions, while Figure 3-2 and Figure 3-3 show the process flow for the asymmetric situation.

3.2.1 *Process Variable Input*

The Low DNBR Channel uses the following process measurement signals:

- Narrow range cold leg temperature (one loop signal per division)
- Narrow range pressurizer pressure (one sensor signal per division)
- Reactor coolant pump (RCP) shaft speed (one loop signal per division)
- Incore self-powered neutron detector (SPND) strings (all divisions see all available calibrated SPND signals)

These signals may be treated with filters prior to being processed by the Low DNBR Channel. These filters will serve to reduce residual signal noise and to accommodate the transport lag times, as applicable.

In order to provide protective capability against asymmetric events characterized by localized peaking increases that erode thermal margin (especially SRP 15.4.3), supplementary inputs are used for the Low DNBR Channel LSSS:

- 89 RCCA position indications (22 RCCA positions per division for three divisions, 23 RCCA positions for the fourth division)
- SPND imbalance signal (sent to all four divisions)
- Three loop operation signals (one global signal indicating three loop operation, and division-specific signals indicating the affected loop)

The control rod position measurement is used to determine whether a rod drop has occurred, while the imbalance is used to determine a core with excessive radial flux tilt. A three loop operation signal is used to indicate that the pump in a particular coolant loop is not operating.

3.2.2 Plant Constant Inputs

The Low DNBR Channel utilizes a number of constants stored in the plant computer. These are shown in Table 3-2.

3.2.3 Algorithm

Details of the online thermal-hydraulic model used in the Low DNBR Channel LSSS are provided in Appendix C.

3.2.4 Setpoints

The Low DNBR Channel LSSS is a composite trip, with several different sequences of setpoints. The default sequence is designed to protect against events in which symmetric core power distributions are present. To accommodate the additional DNB challenge posed by asymmetric core conditions, additional adaptivity is incorporated into the trip through the use of supplementary signals based on radial imbalance and dropped rod indication. The trip will accommodate a limited number of inoperable detectors or detector strings via the use of multiple setpoints.

These features will be discussed within this section. Table 3- summarizes the different sequences of setpoints for the Low DNBR Channel LSSS.

Symmetric Setpoints ($DNBR_{RT}$)

The default operation for the Low DNBR Channel LSSS occurs in the absence of excessive radial core tilt or dropped rod indications. The setpoints used in this condition are $DNBR_{RT}$, which corresponds to a series of six setpoints as a function of the number of inoperable detector strings. The trip in this case always utilizes second min/max logic (i.e., second minimum DNBR signal out of the available signals, and second maximum

exit quality out of the available signals). The motivation for this approach is that the Low DNBR Channel LSSS in each PS division sees the totality of the available SPND signals. If a spuriously high SPND signal were to occur, a reactor trip might be immediately be signaled because all four divisions would see the spurious signal. Figure 3-1 shows a functional diagram for the process leading to a trip based upon a symmetric reactor trip on Low DNBR.

Imbalance/Rod Drop Setpoints ($DNBR_{IMB/RD}$)

The SPND imbalance signal is used to detect radially tilted core power distributions characteristic of the control rod misoperation AOO events (i.e., SRP 15.4.3), or the asymmetric cases in the overcooling AOO events (SRP 15.1). If the calculated imbalance exceeds threshold values, then an excessive SPND imbalance signal is issued to the Low DNBR Channel trip. Section C.2 in Appendix C describes the manner in which the SPND imbalance is calculated.

The RCCA positions are indicated by the safety grade rod position measurement system, and are implemented via coils on the control rod drive mechanism (CRDM) pressure housing. The rod drop signal is formulated by taking sequential rod position measurements over a fixed time period. By design, the period between measurements for the rod drop signal is higher than the total RCCA drop time. The position signals of the 89 RCCAs in the U.S. EPR core are assigned to one of four divisions of 22 sub-banks, with the remaining RCCA being arbitrarily assigned to one of the four divisions. If this rod position derivative exceeds a threshold value, a rod drop signal is sent to the Low DNBR Channel for that division.

Upon receipt of either an excessive SPND imbalance signal or a dropped rod signal from any division, the following changes are initiated automatically by the PS:

- The higher $DNBR_{IMB/RD}$ setpoints are used, based upon a 1st minimum DNBR signal basis

The $DNBR_{IMB/RD}$ setpoints are established such that it protects against DNB for the most limiting transients involving detectable imbalances or detectable dropped rods.

Figure 3-2 shows a functional diagram for the process leading to a trip based upon excessive SPND imbalance or a single rod drop. In this figure, the first maximum quality signal is omitted for clarity, although that signal is used interchangeably with the first minimum DNBR.

If more than one division issues a rod drop signal, then the following additional measure is actuated:

- The $DNBR_{RD}$ setpoints in the DNBR Channel LSSS are used.

Note that the transition from a second to a first minimum DNBR logic is taken with the initial receipt of the first rod drop signal. Figure 3-3 shows a functional diagram for the process leading to a trip based upon rod drops in multiple divisions. In this figure, the first maximum quality signal is omitted for clarity, although that signal is used interchangeably with the first minimum DNBR.

Exit Quality Trips (χ_{RT} and $\chi_{IMB/RD}$)

Violation of the quality trip setpoint in a PS division will cause a trip signal to be issued from that division, unless one has already been issued due to a violation of the DNBR setpoint. The quality and DNBR setpoints are therefore interchangeable.

The exit quality setpoints follow the same signal logic as the DNBR channel. If no SPND imbalance or rod drop signals are present, the χ_{RT} exit quality setpoints are used, and based upon comparison with the second maximum value of hot channel exit quality.

If a SPND imbalance signal or rod drop in one or more divisions is detected, the $\chi_{IMB/RD}$ exit quality setpoints are used based upon comparison to the first maximum signal.

Adjustments for Inoperable SPND Strings

When an SPND becomes inoperable, the system automatically switches to a setpoint designed to accommodate the loss of DNB resolution. There are six setpoints used to support this process. This logic is summarized in Table 3-3. It is also important to note that this process is exercised regardless of what DNBR setpoint is being used. That is, there are six setpoints for each of the Low DNBR Channel LSSS sub-trip functions on DNBR. In summary, there are a total of 30 setpoints that must be established for the Low DNBR Channel LSSS, as follows:

- Six $DNBR_{RT}$ setpoints
- Six $\chi_{IMB/RD}$ setpoints
- Six χ_{RT} setpoints
- Six $DNBR_{IMB/RD}$ setpoints
- Six $DNBR_{RD}$ setpoints

3.2.5 Reactor Trip Signal Scenarios

Because the Low DNBR Channel LSSS is complex, the types of combinations of signals (from a single division) are summarized that would cause a reactor trip signal to be issued by the Low DNBR Channel LSSS from that division. The following scenarios will only occur if the P2 permissive has been enabled (i.e., at power levels greater than around 10 percent RTP).

Symmetric Reactor Trip Signal

This signal is issued in the absence of dropped rod or SPND imbalance indication. If the second minimum DNBR or second maximum exit quality violate the respective reactor trip setpoints in a given division as a function of the number of SPND failures, then a reactor trip signal is issued from that division:

$$\left(\text{MDNBR}^{2^{\text{nd min}}} \leq \text{DNBR}_{\text{RT}|_{\text{N}_{\text{fail}}}} \right) \text{OR} \left(\chi^{2^{\text{nd max}}} \geq \chi_{\text{RT}|_{\text{N}_{\text{fail}}}} \right) \Rightarrow \text{Reactor Trip} \quad (3-1)$$

Dropped Rod Reactor Trip Signal (Single Division) or SPND Imbalance Trip Signal

This trip signal is triggered when either the first minimum DNBR violates the imbalance/rod drop setpoint on DNBR, or the first maximum exit quality violates the quality setpoint. This will happen only when either the SPND imbalance signal, or a dropped rod signal in one of the available PS divisions (shown below on a one out of y division basis) has been issued.

$$\left(\left(\text{MDNBR}^{1^{\text{st min}}} \leq \text{DNBR}_{\text{IMB/RD}|_{\text{N}_{\text{fail}}}} \right) \text{OR} \left(\chi^{1^{\text{st max}}} \geq \chi_{\text{IMB/RD}|_{\text{N}_{\text{fail}}}} \right) \right) \text{AND} \\ \left(\text{IMB}_{\text{SPND}} \text{OR Rod Drop}_{(1/y)} \right) \Rightarrow \text{Reactor Trip} \quad (3-2)$$

Dropped Rod Reactor Trip Signal (Multiple Divisions)

This trip signal is triggered when either the first minimum DNBR violates the dropped rod setpoint on DNBR, or the first maximum exit quality violates the quality setpoint. This will only happen when dropped rod indication was issued by two or more of the available PS divisions.

$$\left(\left(\text{MDNBR}^{1^{\text{st min}}} \leq \text{DNBR}_{\text{rod drop}|_{\text{N}_{\text{fail}}}} \right) \text{OR} \left(\chi^{1^{\text{st max}}} \geq \chi_{\text{IMB/RD}|_{\text{N}_{\text{fail}}}} \right) \right) \\ \text{AND} \left(\text{Rod Drop}_{(2+/y)} \right) \Rightarrow \text{Reactor Trip} \quad (3-3)$$

3.2.6 Function Blocks

There are several functional blocks associated with the Low DNBR Channel algorithm that are stored in the plant computer. These are summarized in Table 3-4.

3.2.7 Inhibition

The Low DNBR Channel LSSS is inhibited at power levels below the P2 permissive setting, which is set to a low power level (generally around 10 percent RTP).

3.3 *Interface with Other Trips*

The Low DNBR Channel LSSS works in conjunction with other trips and protective capabilities in the U.S. EPR to protect against violation of SAFDLs. These other trips and capabilities include:

- High Core Power Level (HCPL)
- Main Steam Safety Valve (MSSV) Actuation
- High LPD Channel Trip

The HCPL LSSS will produce a reactor trip at excessively high power levels and if the coolant conditions at the core exit encroach upon saturation. The MSSVs will restrict the pressure conditions in the steam generators. The High LPD Channel limits the planar peak LPD values in the core. All three effectively restrict the power and primary side coolant temperature conditions that need be considered for the Low DNBR Channel LSSS function.

- Pressurizer Low Pressure Trip

The Pressurizer Low Pressure trip will intercede when the primary system pressure becomes too low. This represents a functional lower bound on the pressure that need be considered in the Low DNBR Channel trip.

- Pressurizer High Pressure Trip
- Pressurizer Relief/Safety Valves

The Pressurizer High Pressure trip and/or actuation of the pressurizer safety or relief valves will restrict the maximum pressure that needs to be considered in the Low DNBR Channel trip.

- Excore Rate of Change Trip

The Excore Rate of Change Trip will intercede in events characterized by rapid power excursions. It effectively puts a restriction on the speed of event the Low DNBR Channel trip is expected to protect.

- Low RCP Speed

This trip will set a bound on the coolant flow rate that needs to be considered in the Low DNBR Channel trip.

Table 3-1 Basis Events for the Low DNBR Channel LSSS

Event	SRP Section	Comments
Decrease in Feedwater Temperature	15.1.1	---
Increase in Feedwater Flow	15.1.2	---
Excess Increase in Steam Flow (Excess Load Increase)	15.1.3	Slower end of event spectrum
Inadvertent Opening of a SG Relief or Safety Valve	15.1.4	---
Uncontrolled Control Rod Assembly Withdrawal at Power	15.4.2	Slower end of event spectrum
Control Rod Misoperation: <i>Dropped Control Rod/Bank</i>	15.4.3	---
Control Rod Misoperation: <i>Single Control Rod Withdrawal</i>	15.4.3	---
Inadvertent Decrease in Boron Concentration in the Reactor Coolant System	15.4.6	---
Inadvertent Opening of a Pressurizer Relief or Safety Valve	15.6.1	---

Table 3-2 Plant Constants Used in the Low DNBR Channel LSSS¹

Constant	Description	Comments
<i>SPND Calibration Arrays</i>		
$C_{i,j}^{DNBR}$	SPND calibration array for DNBR	Periodically updated via SPND calibration
$C_{i,j}^{IMB}$	SPND calibration array for SPND imbalance	Periodically updated via SPND calibration
<i>Filter Time Constants</i>		
τ_{RCP}	Lag time constant in first-order filter for RCP speed, in seconds	---
τ_{lag1}^{Tcold}	Lag time constant in second-order filter for cold leg temperature signal, in seconds	---
τ_{lag2}^{Tcold}	Lag time constant in second-order filter for cold leg temperature signal, in seconds	---
τ_{lead}^{Tcold}	Lead time constant in second-order filter for cold leg temperature signal, in seconds	---
$\tau_{lag1}^{MDNBR\ min1}$	Lag time constant in second-order filter for 1st MDNBR signal, in seconds	---
$\tau_{lag2}^{MDNBR\ min1}$	Lag time constant in second-order filter for 1st MDNBR signal, in seconds	---
$\tau_{lead}^{MDNBR\ min1}$	Lead time constant in second-order filter for 1st MDNBR signal, in seconds	---

¹ For each of these types of setpoints, there are six distinct setpoints, corresponding to zero, one, two, three, four, and five or more failed SPND strings.

Table 3-2 (continued) Plant Constants Used in the Low DNBR Channel LSSS

Constant	Description	Comments
$\tau_{lag1}^{MDNBR\ min2}$	Lag time constant in second-order filter for 2nd MDNBR signal, in seconds	---
$\tau_{lag2}^{MDNBR\ min2}$	Lag time constant in second-order filter for 2nd MDNBR signal, in seconds	---
$\tau_{lead}^{MDNBR\ min2}$	Lead time constant in second-order filter for 2nd MDNBR signal, in seconds	---
$\tau_{lag1}^{\chi\ max1}$	Lag time constant in second-order filter for 1st maximum exit quality signal, in seconds	---
$\tau_{lag2}^{\chi\ max1}$	Lag time constant in second-order filter for 1st maximum exit quality signal, in seconds	---
$\tau_{lead}^{\chi\ max1}$	Lead time constant in second-order filter for 1st maximum exit quality signal, in seconds	---
$\tau_{lag1}^{\chi\ max2}$	Lag time constant in second-order filter for 2nd maximum exit quality signal, in seconds	---
$\tau_{lag2}^{\chi\ max2}$	Lag time constant in second-order filter for 2nd maximum exit quality signal, in seconds	---
$\tau_{lead}^{\chi\ max2}$	Lead time constant in second-order filter for 2nd maximum exit quality signal, in seconds	---

Table 3-2 (continued) Plant Constants Used in the Low DNBR Channel LSSS

Constants	Description	Comment
<i>Plant Constants</i>		
ACORE	Bare rod core flow area, in cm ²	---
ATYPE	Flow area of fuel cell, in cm ²	---
FACT	Units conversion m ³ /hr to cm ³ /s = 277.78	---
Q _{REF}	Reference volumetric flow rate in m ³ /hr, corresponding to Ω _{REF}	Periodically updated via flow calibration
Ω _{REF}	Reference RCP rotational speed flow rate in RPM, corresponding to Q _{REF}	Periodically updated via flow calibration
PCY	Heated perimeter of fuel, in cm	---
FH		
FG		
FRDEB	Mass flow rate adjustment factor, dimensionless.	Used to apply core bypass flow adjustments.

Table 3-2 (continued) Plant Constants Used in the Low DNBR Channel LSSS

Constants	Description	Comment
<i>Setpoints</i>		
$\left(\begin{array}{l} \text{DNBR}_{\text{RT}}^{0 \text{ SPND}} \\ \text{DNBR}_{\text{RT}}^{1 \text{ SPND}} \\ \text{DNBR}_{\text{RT}}^{2 \text{ SPND}} \\ \text{DNBR}_{\text{RT}}^{3 \text{ SPND}} \\ \text{DNBR}_{\text{RT}}^{4 \text{ SPND}} \\ \text{DNBR}_{\text{RT}}^{5+ \text{ SPND}} \end{array} \right)$	Low DNBR Channel LSSS setpoints on low DNBR, as a function of the number of SPND string failures, and in the absence of excessive SPND imbalance or rod drop signals	Setpoints automatically shifted in response to number of inoperable SPND
$\left(\begin{array}{l} \text{DNBR}_{\text{IMB/RD}}^{0 \text{ SPND}} \\ \text{DNBR}_{\text{IMB/RD}}^{1 \text{ SPND}} \\ \text{DNBR}_{\text{IMB/RD}}^{2 \text{ SPND}} \\ \text{DNBR}_{\text{IMB/RD}}^{3 \text{ SPND}} \\ \text{DNBR}_{\text{IMB/RD}}^{4 \text{ SPND}} \\ \text{DNBR}_{\text{IMB/RD}}^{5+ \text{ SPND}} \end{array} \right)$	Low DNBR Channel LSSS setpoints on low DNBR, as a function of the number of SPND string failures, in the presence of an excessive SPND imbalance signal or rod drop signal in one division	Setpoints automatically shifted in response to number of inoperable SPND
$\left(\begin{array}{l} \text{DNBR}_{\text{RD}}^{0 \text{ SPND}} \\ \text{DNBR}_{\text{RD}}^{1 \text{ SPND}} \\ \text{DNBR}_{\text{RD}}^{2 \text{ SPND}} \\ \text{DNBR}_{\text{RD}}^{3 \text{ SPND}} \\ \text{DNBR}_{\text{RD}}^{4 \text{ SPND}} \\ \text{DNBR}_{\text{RD}}^{5+ \text{ SPND}} \end{array} \right)$	Low DNBR Channel LSSS setpoints on low DNBR, as a function of the number of SPND string failures, in the presence of rod drop signals in two or more divisions	Setpoints automatically shifted in response to number of inoperable SPND
$\left(\begin{array}{l} \text{DNBR}_{\text{PT}}^{0 \text{ SPND}} \\ \text{DNBR}_{\text{PT}}^{1 \text{ SPND}} \\ \text{DNBR}_{\text{PT}}^{2 \text{ SPND}} \\ \text{DNBR}_{\text{PT}}^{3 \text{ SPND}} \\ \text{DNBR}_{\text{PT}}^{4 \text{ SPND}} \\ \text{DNBR}_{\text{PT}}^{5+ \text{ SPND}} \end{array} \right)$	Low DNBR limitation setpoints, as a function of the number of SPND string failures	Setpoints automatically shifted in response to number of inoperable SPND

Table 3-2 (continued) Plant Constants Used in the Low DNBR Channel LSSS

Constants	Description	Comment
$\left(\begin{array}{l} \chi_{\text{IMB/RD}}^{0 \text{ SPND}} \\ \chi_{\text{IMB/RD}}^{1 \text{ SPND}} \\ \chi_{\text{IMB/RD}}^{2 \text{ SPND}} \\ \chi_{\text{IMB/RD}}^{3 \text{ SPND}} \\ \chi_{\text{IMB/RD}}^{4 \text{ SPND}} \\ \chi_{\text{IMB/RD}}^{5+ \text{ SPND}} \end{array} \right)$	Low DNBR Channel LSSS setpoint on high exit quality, in the presence of an excessive SPND imbalance signal or rod drop signal in one or more divisions (1 st maximum signal)	---
$\left(\begin{array}{l} \chi_{\text{RT}}^{0 \text{ SPND}} \\ \chi_{\text{RT}}^{1 \text{ SPND}} \\ \chi_{\text{RT}}^{2 \text{ SPND}} \\ \chi_{\text{RT}}^{3 \text{ SPND}} \\ \chi_{\text{RT}}^{4 \text{ SPND}} \\ \chi_{\text{RT}}^{5+ \text{ SPND}} \end{array} \right)$	Low DNBR Channel LSSS setpoint on high exit quality, in the absence of an excessive SPND imbalance signal or rod drop signal (2 nd maximum signal)	---

Table 3-3 Setpoint Logic for the Low DNBR Channel LSSS

Constant	Description
$DNBR_{RT}$	DNBR setpoints in the absence of detected imbalances or dropped rods
$DNBR_{IMB/RD}$	DNBR setpoints for detected SPND imbalance or dropped rods in one division
$DNBR_{RD}$	DNBR setpoints for detected dropped rods in two or more divisions

Table 3-3 Low DNBR Channel Setpoint Adjustments for SPND String Failures

Number of SPND String Failures	Setpoint Adjustment
0	Default Value
1	1 st Modified Value
2	2 nd Modified Value
3	3 rd Modified Value
4	4 th Modified Value
5+	5 th Modified Value

Table 3-4 Function Blocks in the Low DNBR Channel LSSS

Function Block	Description
HFTP	Water property subroutine used to evaluate enthalpy as a function of temperature and pressure
RFHP	Water property subroutine used to evaluate density as a function of enthalpy and pressure
HLV	Water property subroutine used to evaluate liquid and vapor saturated enthalpies as a function of pressure
FHFR	[]
FGFR	[]
FCHF	Subroutine used to evaluate critical heat flux for uniform axial power distributions with an approved CHF correlation, as a function of pressure, local mass velocity, and local quality
FNU	Subroutine used to evaluate the non-uniform critical heat flux adjustment factor from an approved CHF correlation, as a function of local mass velocity, local quality, linear power density, and grid cell type

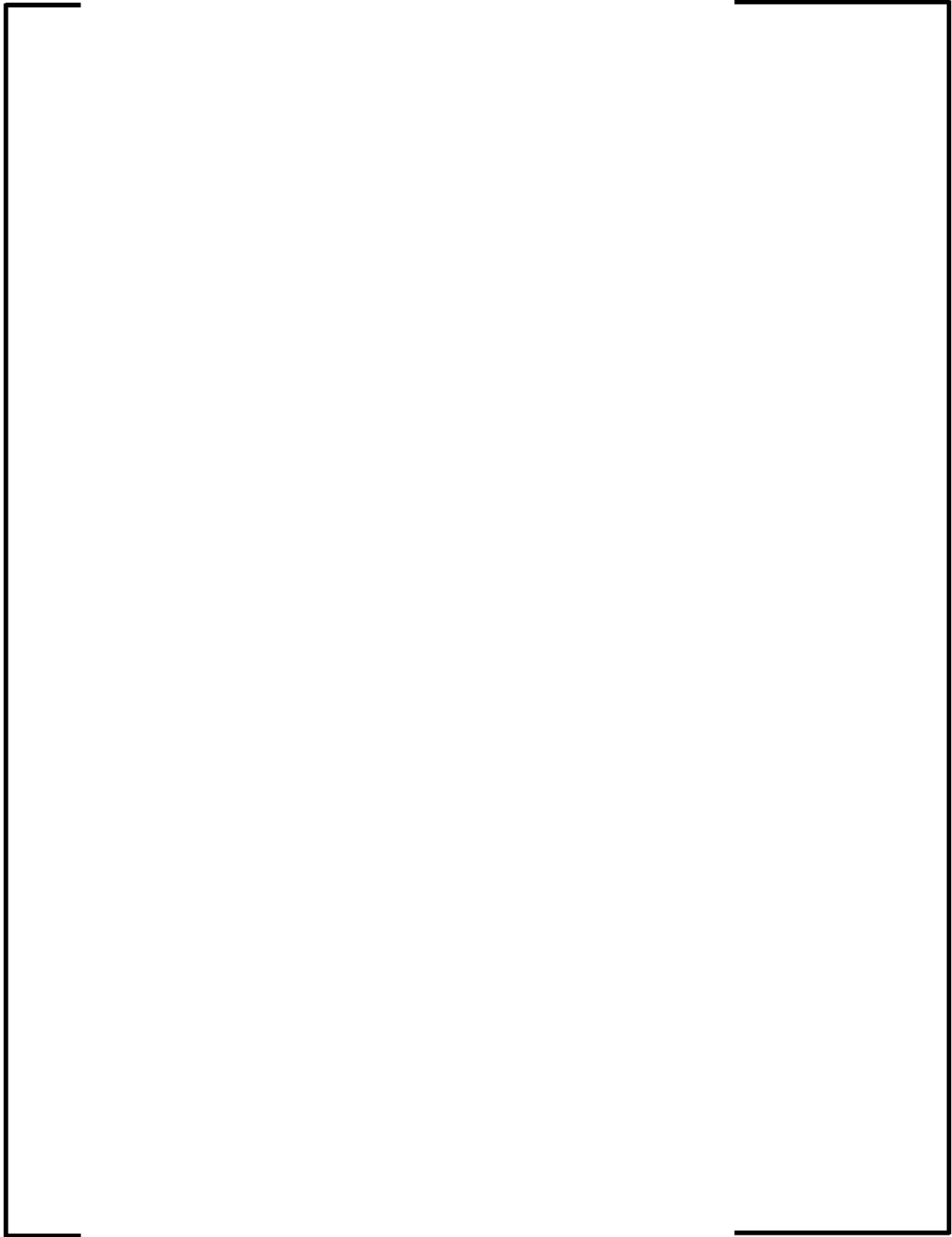


Figure 3-1 Low DNBR Channel Symmetric Trip Scenario

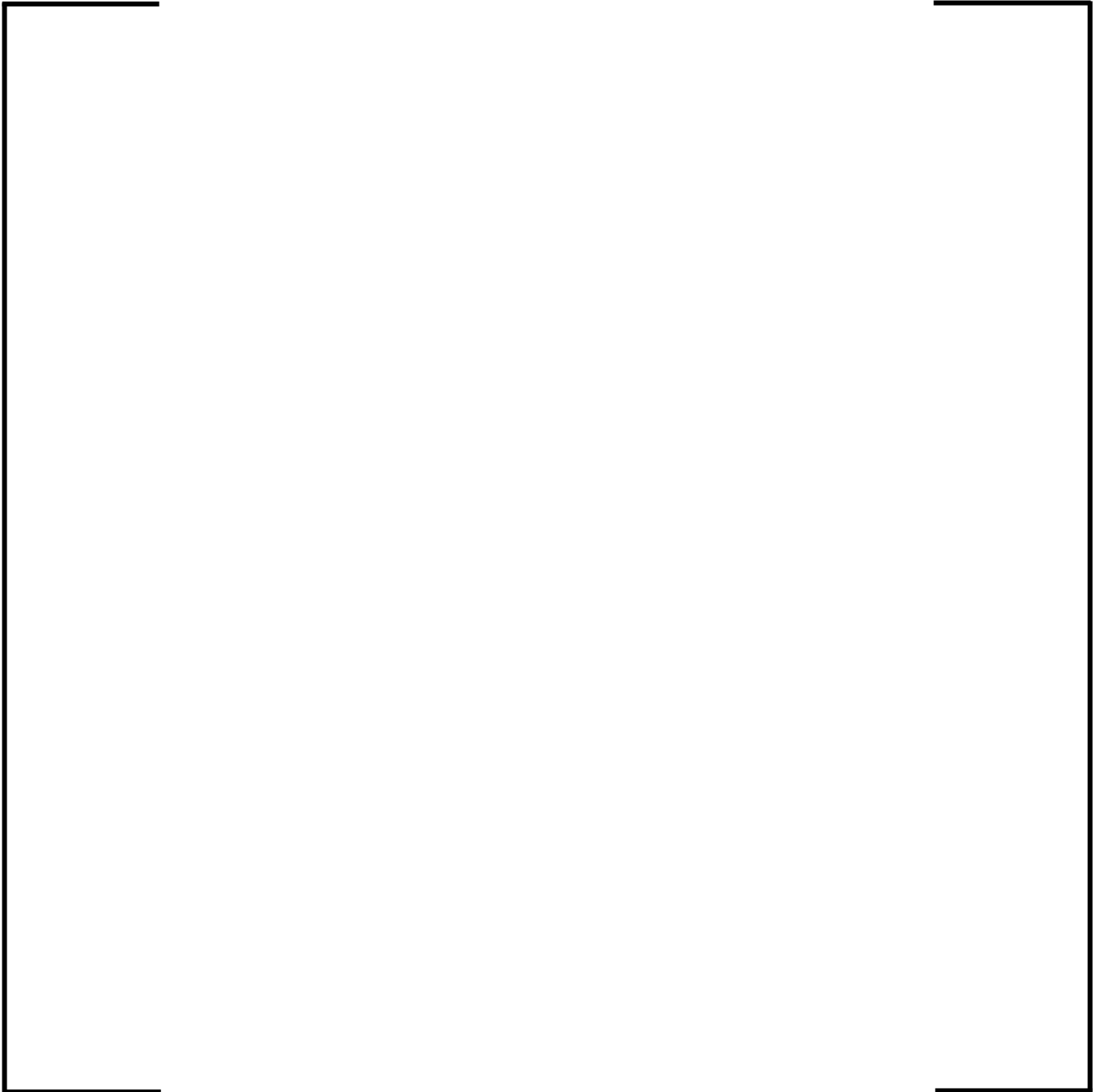


Figure 3-2 Low DNBR Channel Imbalance ($DNBR_{IMB/RD}$) Trip Scenario

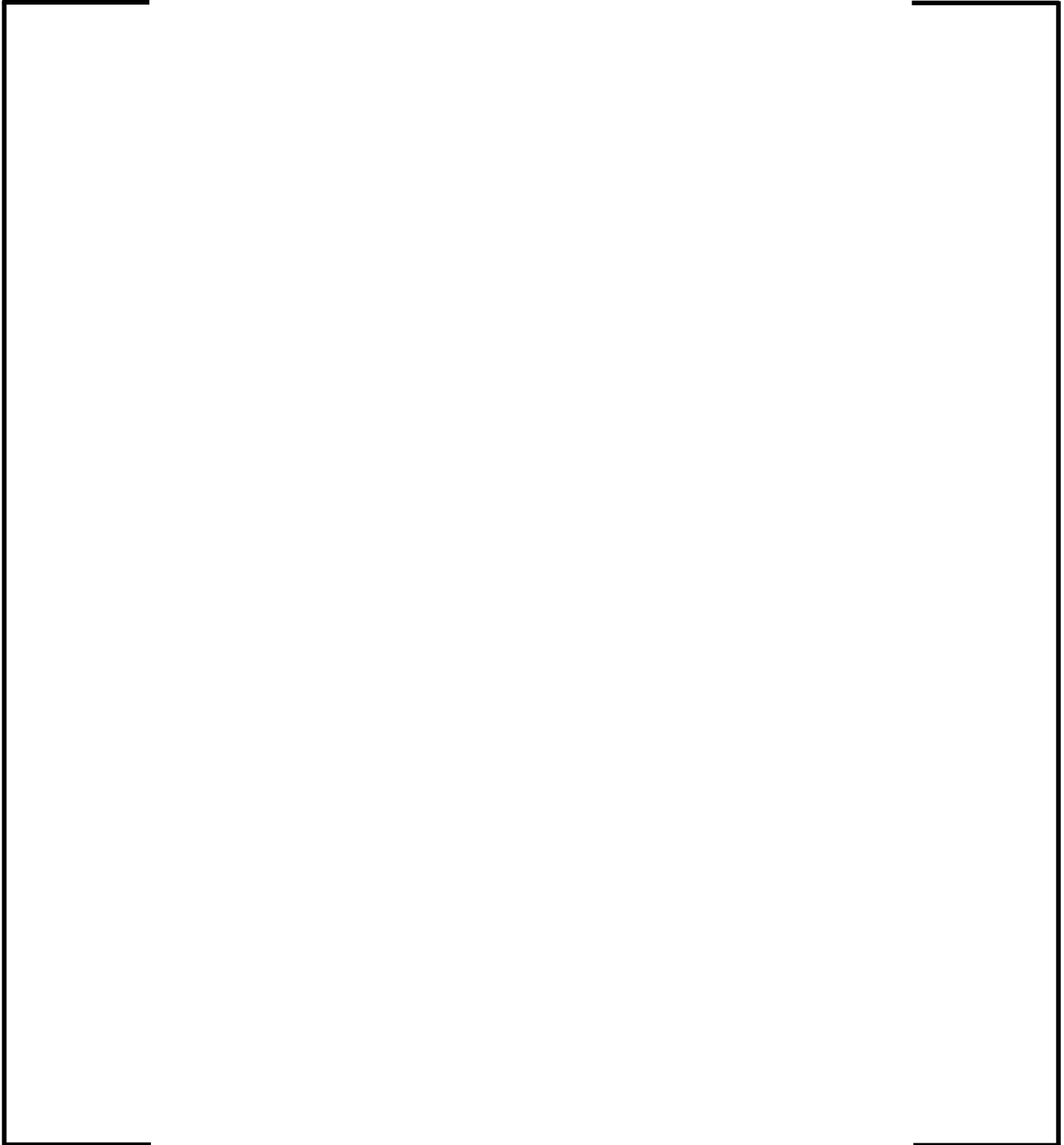


Figure 3-3 Low DNBR Channel Dropped Rod ($DNBR_{RD}$) Trip Scenario

4.0 LIMITING CONDITIONS FOR OPERATION ON DNB

This chapter provides a functional description of the DNB LCO. The methodology used to establish the setpoint for the DNB LCO is essentially identical to that of the Low DNBR Channel LSSS, and is described in Section 5.0.

4.1 *Design Basis*

To ensure that the SAFDL on DNB is not violated for events in which the Low DNBR Channel LSSS cannot intercede, an LCO is established on the synthesized online DNBR. This LCO functionally preserves the initial required DNB margin for the most limiting DNB LCO basis event during steady-state operation, including consideration of applicable measurement errors, operating allowances, and calculation uncertainties, at 95 percent probability, with 95 percent confidence. The term “most limiting” in this context means the event characterized by the maximum DNBR degradation.

DNBR is calculated using the online DNBR model in RCSL and averaged thermal hydraulic conditions, then comparing it against the two sets of graduated setpoints (LCO1 and LCO2). Depending upon which setpoint is violated; progressive actions are taken to return the plant to an acceptable operating state. Violation of the LCO1 setpoint will produce control room alarms and a blocking signal to the RCCA banks. Violation of the LCO2 setpoint will cause RCSL to issue additional signals to reduce generator power and insert control banks.

The specific events against which the DNB LCO is designed to afford protection are summarized in Table 4-1. Although designed to ensure that AOOs not protected by the Low DNBR Channel trip meet the acceptance criteria associated with that class of events, the DNB LCO will also act to mitigate the radiological consequences of postulated accidents.

4.2 *Functional Description*

The following subsections describe the DNB LCO.

4.2.1 Process Variable Input

The DNB LCO utilizes the same process variables (narrow range cold leg temperature, narrow range pressurizer pressure, and RCP speed) as the Low DNBR Channel LSSS (see Section 3.2.1). The DNB LCO does not have the additional control rod position or SPND imbalance measurement inputs.

To reduce the uncertainty in monitored LCO, all signals are averaged prior to use in the DNB LCO algorithm¹. They are also passed through low pass filters for noise reduction and temporal compensation.

RCP Speed

The RCP speed used in the DNB LCO is acquired via the speed sensors on the RCP. As in the Low DNBR Channel LSSS, the individual signals are doubly lag filtered, and averaged:

$$\Omega_{\text{avg}}^{\text{DNBLCO}} = \frac{1}{1 + \tau_{\text{lag2}}^{\Omega} S} \left(\frac{1}{4} \sum_{i=1}^4 \left(\frac{1}{(1 + \tau_{\text{lag1}}^{\Omega} S)} \Omega_{\text{Division } i} \right) \right) \quad (4-1)$$

where $\Omega_{\text{avg}}^{\text{DNBLCO}}$ is the averaged and filtered RCP signal used as input to the DNB LCO, $\Omega_{\text{Division } i}$ is the indicated RCP speed in Division number i , $\tau_{\text{lag1}}^{\Omega}$ and $\tau_{\text{lag2}}^{\Omega}$ are time constants on the two lag functions, and S is the Laplace transform operator.

¹ The averaging of four signals results in the halving of the uncertainty relative to an independent signal.

Pressurizer Pressure

The pressure input to the DNB LCO is the lag filtered average value of the four divisions of narrow range pressurizer pressure measurement:

$$PF_{avg}^{DNBLCO} = \frac{1}{1 + \tau_{lag2}^{PRZ} S} \left(\frac{1}{4} \sum_{i=1}^4 \frac{1}{1 + \tau_{lag1}^{PRZ} S} \cdot P_{Division\ i} \right) \quad (4-2)$$

where PF_{avg}^{DNBLCO} is the filtered averaged pressure input to the DNB LCO, $P_{Division\ i}$ is the narrow range pressure measurement from Division i , and τ_{lag1}^{PRZ} and τ_{lag2}^{PRZ} are the time constants associated with the lag filters.

Cold Leg Temperature

The temperature input to the DNB LCO is the lead-lag filtered average of the four narrow range cold leg temperatures:

$$TF_{avg}^{DNBLCO} = \frac{(1 + \tau_{lead}^{Tcold} S)}{(1 + \tau_{lag2}^{Tcold} S)(1 + \tau_{lag3}^{Tcold} S)} \cdot \left(\frac{1}{4} \sum_{i=1}^4 \frac{1}{1 + \tau_{lag1}^{Tcold} S} \cdot T_{Division\ i} \right) \quad (4-3)$$

where TF_{avg}^{DNBLCO} is the temperature input to the DNB LCO, $T_{Division\ i}$ is the division-specific cold leg temperature, τ_{lag1}^{Tcold} is the time constant on the division-specific T_{cold} signals, and τ_{lag2}^{Tcold} , τ_{lead}^{Tcold} , and τ_{lag3}^{Tcold} are time constants on the second-order filter.

Power Density

The incore power densities are obtained via calibrated SPND signals as described in Appendix B.

4.2.2 Plant Constants

Table 4-2 shows the input constants utilized in the DNB LCO.

4.2.3 *Algorithm*

The online DNB algorithm for the DNB LCO is identical to that used in the Low DNBR Channel LSSS. Since the DNB LCO is evaluated in the RCSL system and the Low DNBR Channel LSSS in the PS, the constants associated with the generic online DNBR model may differ between the two functions.

See Appendix C for a description of the online DNBR algorithm.

4.2.4 *Setpoints*

The DNB LCO has a series of setpoints, reflecting the adaptivity of the function to accommodate a limited number of inoperable SPND detector strings. Table 4-3 shows the setpoint logic for the DNB LCO.

Violation of the LCO1 setpoint will produce control room alarms and a blocking signal to the RCCA banks. Violation of the LCO2 setpoint will cause RCSL to additionally issue a signal to reduce generator power and insert control banks.

4.3 *Inhibition*

The DNB LCO function is inhibited below a low level of power, usually around 10 percent RTP.

Table 4-1 Basis Events for the DNB LCO

Constant	Description	Comments
<i>Design Basis AOO Events</i>		
Excess Increase in Steam Flow (Excess Load Increase)	15.1.3	Fast end of event spectrum
Partial and Complete Loss of Forced Reactor Coolant Flow	SRP 15.3.1 SRP 15.3.2	Primary limiting AOO
Uncontrolled Control Rod Assembly Withdrawal from a Subcritical or Low Power Startup Condition	15.4.1	---
Uncontrolled Control Rod Assembly Withdrawal at Power	15.4.2	Fast end of event spectrum
<i>Additional Events (Postulated Accidents)</i>		
Steam System Piping Failures Inside and Outside of Containment	15.1.5	---
Reactor Coolant Pump Rotor Seizure	15.3.3	---
Reactor Coolant Pump Shaft Break	15.3.4	---
Spectrum of Rod Ejection Accidents	15.4.8	---

Table 4-2 Plant Constants for the DNB LCO¹

Constant	Description
<i>Calibration Factors</i>	
$C_{i,j}^{\text{DNBR}}$	SPND calibration array for DNBR
<i>Filter Time Constants</i>	
$\tau_{\text{lag1}}^{\Omega}$	Lag filter time constant for division-specific RCP speed signals, in seconds
$\tau_{\text{lag2}}^{\Omega}$	Lag filter time constant for averaged RCP speed signal, in seconds
$\tau_{\text{lag1}}^{\text{PRZ}}$	Lag filter time constant for division-specific pressurizer pressure signals, in seconds
$\tau_{\text{lag2}}^{\text{PRZ}}$	Lag filter time constant for averaged pressurizer pressure signal, in seconds
$\tau_{\text{lag1}}^{\text{Tcold}}$	Lag filter time constant for division-specific cold leg temperature signals, in seconds
$\tau_{\text{lag2}}^{\text{Tcold}}$	Second-order filter lag time constant for averaged Tcold signal, in seconds
$\tau_{\text{lag3}}^{\text{Tcold}}$	Second-order filter lag time constant for averaged Tcold signal, in seconds
$\tau_{\text{lead}}^{\text{Tcold}}$	Second-order filter lead time constant for averaged Tcold signal, in seconds

¹ Other time constants associated with the generic online DNBR algorithm are shown in Table 3-2, and will not be repeated in the interest of brevity.

Table 4-2 (continued) Plant Constants for the DNB LCO

Constant	Description
<i>Setpoints</i>	
$\left(\begin{array}{l} \text{DNBR}_{\text{LCO1}}^{0 \text{ SPND}} \\ \text{DNBR}_{\text{LCO1}}^{1 \text{ SPND}} \\ \text{DNBR}_{\text{LCO1}}^{2 \text{ SPND}} \\ \text{DNBR}_{\text{LCO1}}^{3 \text{ SPND}} \\ \text{DNBR}_{\text{LCO1}}^{4 \text{ SPND}} \\ \text{DNBR}_{\text{LCO1}}^{5+ \text{ SPND}} \end{array} \right)$	DNB LCO setpoints for LCO1 threshold, as a function of the number of SPND failures
$\left(\begin{array}{l} \text{DNBR}_{\text{LCO2}}^{0 \text{ SPND}} \\ \text{DNBR}_{\text{LCO2}}^{1 \text{ SPND}} \\ \text{DNBR}_{\text{LCO2}}^{2 \text{ SPND}} \\ \text{DNBR}_{\text{LCO2}}^{3 \text{ SPND}} \\ \text{DNBR}_{\text{LCO2}}^{4 \text{ SPND}} \\ \text{DNBR}_{\text{LCO2}}^{5+ \text{ SPND}} \end{array} \right)$	DNB LCO setpoints for LCO2 threshold, as a function of the number of SPND failures

Table 4-3 DNB LCO Setpoint Adjustments for SPND Failures

Number of Inoperable SPND Strings	Setpoint
0	Default Value
1	1 st Modified Value
2	2 nd Modified Value
3	3 rd Modified Value
4	4 th Modified Value
5+	5 th Modified Value

5.0 STATIC DNBR SETPOINT METHODOLOGY

As noted in SRP Section 4.4, the acceptance criterion for fuel design limits on DNB is based upon the assurance that the DNBR-limiting fuel pin in the reactor core will not experience a DNB or transition condition during normal operation or during AOOs, at 95 percent or greater probability, and with 95 percent or greater confidence. This section describes of the methodology used to fulfill this design goal. As the Low DNBR Channel reactor trip on quality is part of the overall trip channel and formulated in a similar manner, the quality trip methodology will also be integrated into this section.

For a more detailed discussion on the [] refer to Appendix A.

The DNBR limitation setpoints are established via operational considerations, not via a static statistical methodology. For a discussion of the methodology used to establish these setpoints, see Section 9.6.

5.1 *Statement of Problem*

The approach used for meeting this acceptance criterion for the U.S. EPR Low DNBR Channel LSSS and DNB LCO functions is to establish a setpoint equal to the one-sided 95/95 [] on the calculated online MDNBR. This [] is established based upon the following criterion:

[] *then the DNBR setpoint will be established such that a reactor trip would occur no less than 95 percent of the time, with 95 percent confidence, considering all relevant uncertainties.*

Mathematically, this can be expressed for the Low DNBR Channel LSSS as a conditional probability of the form:

$$[\quad] \quad (5-1)$$

where [] is the []

Since the reactor trip (RT) needs to be actuated by the Low DNBR Channel LSSS, it is required that [] where [] is the []

[] and [] is the []

[] Therefore, Equation (5-1) can be rewritten as:

$$[\quad] \quad (5-2)$$

where [] is the [] is the []
[] and [] is the []

[] In this expression, the interior brackets refer to the [], while the outer brackets refer to the []. A graphical depiction of this process is shown in Figure 5-1.

An analogous problem statement holds for the calculated hot channel exit quality:

[]
[] *then the exit quality setpoint will be established such that a reactor trip would occur no less than 95 percent of the time, with 95 percent confidence, considering all relevant uncertainties.*

Mathematically, this can be expressed as a conditional probability of the form:

$$[\quad] \quad (5-3)$$

where [] is the [] is the []

]

] and [

] A graphical

depiction of this process is shown in Figure 5-2.

The DNB LCO is offset, relative to the Low DNBR Channel LSSS, by the transient $\Delta(\text{DNBR})$ allowance. Therefore, for the DNB LCO, Equation (5-2) becomes:

$$[\quad \quad \quad] \quad (5-4)$$

A graphical depiction of this process is shown in Figure 5-3.

5.2 Clarification of Terminology

In the balance of this chapter (for Section 8.0 similar definitions will hold), certain terminology will be used. The definitions of these terms are as follows:

Systemic vs. Non-Systemic Uncertainties

The term “systemic uncertainties” will be used to refer to those uncertainties that affect the underlying DNBR or exit quality phenomena, but are not related to either the measurement process or to the particular algorithm used to synthesize those process parameters into DNBR or exit quality. In particular, it covers perturbations to the design geometry, such as rod bow, assembly bow, and engineering (hot channel factor) uncertainties.

All other uncertainties related to process measurement, algorithmic, and epistemic uncertainties are applied to the sensed DNBR or exit quality, and will be referred to as “non-systemic” uncertainties.

Reference DNBR or Exit Quality

The reference DNBR or exit quality refers to the underlying DNBR or hot channel exit quality that exists due to the best estimate thermal hydraulic conditions, but perturbed geometry relative to design. The uncertainties that are systemic (i.e., unrelated to the

measurement process) are [] and applied to this calculation. The power distribution is [

]

Sensed (or Online) DNBR or Exit Quality

The sensed DNBR or exit quality are the values sensed by the online Low DNBR Channel LSSS or LCO functions, [

] and subject

to measurement uncertainty adjustments to the best estimate thermal hydraulic conditions. All non-systemic uncertainties are applied to this calculation.

[

]

Statepoint

The term “statepoint” or “reactor statepoint” will be used to refer to a unique “snapshot” set of conditions in terms of core inlet temperature, core inlet flow (RCP speed and calibrated flow rate), pressurizer pressure, and power distribution.

5.3 *Uncertainties Affecting DNBR Monitoring and Protection*

As the computation of the online DNBR is rather complex, it is subject to a large number of uncertainties. The following subsections describe the uncertainties used as inputs to the DNBR setpoint calculation.

The uncertainties used in the setpoints can be characterized by both random and non-random (bias) components. More complicated situations, such as distributions with non-symmetrical uncertainty intervals, can be supported by directly using the cumulative distribution function (rather than a density function), and sampling via the methods described in Appendix D.

Uncertainties may be expressed in either multiplicative form or absolute form. Absolute errors are differences, in which the uncertainty is expressed in terms of a difference (in the same units) from a nominal value. These take the general form $x \pm \delta x$, where x is the nominal value, and δx is the uncertainty. In the multiplicative form, it is $x \cdot (1 + \delta x)$.

The following subsections present the derivation of the [

] in terms of a mixture of relative and absolute forms.

However, the alternate form of the uncertainties may be used, depending upon the nature of the uncertainty and how to most appropriately characterize it. If the behavior of an uncertainty suggests that the alternative form of the uncertainty is more appropriate, the transition to the other form will change the algebraic expressions slightly, but does not change the basic methodology being presented in this topical report.

5.3.1 Cold Leg Temperature Measurement

The core inlet temperature measurement input to the Low DNBR Channel and DNB LCO is provided by the narrow range cold leg resistance temperature detector (RTD) sensors in each of the coolant loops. For the Low DNBR Channel LSSS, the signal from each loop is reserved for a separate protection system division, while for the DNB LCO the available temperature signals are averaged prior to use in the online DNBR algorithm. The individual sensor uncertainties are assumed to be independent of each other.

The cold leg temperature uncertainty input is evaluated using the Reference 5 or an equivalent methodology, and contains the uncertainty components associated with the temperature signal acquisition, conditioning, and digitization. It is assumed to take the following form:

$$\begin{aligned}
 T_{\text{cold}}^{\text{sensed}} &= T_{\text{cold}} \pm \delta_{T_{\text{cold}}} + B_{T_{\text{cold}}} \\
 &= T_{\text{cold}} + \varepsilon_{T_{\text{cold}}}
 \end{aligned}
 \tag{5-5}$$

where δ_T is the random portion of the cold leg temperature measurement uncertainty, $B_{T_{\text{cold}}}$ is a non-random bias term, and $\varepsilon_{T_{\text{cold}}}$ is the random variable containing both uncertainty components.

5.3.2 Pressurizer Pressure Measurement

The pressure measurement input to the Low DNBR Channel and DNB LCO is provided by the narrow range pressure sensors in the pressurizer steam dome. For the Low DNBR Channel LSSS, the signal from each sensor is reserved for a separate protection system division, while for the DNB LCO the available pressure signals are averaged prior to use in the online DNBR algorithm. The individual sensor uncertainties are assumed to be independent of each other.

The pressure measurement uncertainty input is evaluated using Reference 5 or an equivalent methodology, and contains the uncertainty components associated with the pressure signal acquisition, conditioning, and digitization. It is assumed to take the following form:

$$\begin{aligned}
 P_{\text{prz}}^{\text{sensed}} &= P_{\text{prz}} \pm \delta_{P_{\text{prz}}} + B_{P_{\text{prz}}} \\
 &= P_{\text{prz}} + \varepsilon_{P_{\text{prz}}}
 \end{aligned}
 \tag{5-6}$$

where $\delta_{P_{\text{prz}}}$ is the random portion of the pressurizer pressure measurement uncertainty, $B_{P_{\text{prz}}}$ is the non-random bias term, and $\varepsilon_{P_{\text{prz}}}$ is the random variable containing both uncertainty components.

5.3.3 Inlet Flow Rate

The rotational speed of the pump shaft is provided by tachymetric measurement. During periodic surveillance measurements, the RCP speed and volumetric flow rate are measured and the results stored in the plant computer until the next surveillance

measurement. These results provide an estimate of the flow at different speeds, per the affinity relationship:

$$\dot{G}_{\text{indicated}} = \frac{\Omega_{\text{indication}}}{\Omega_{\text{calibration}}} \cdot \dot{G}_{\text{calibration}} \quad (5-7)$$

There are two uncertainties associated with this process. First, the RCP speed signal acquisition process has uncertainties associated with it, which affect $\Omega_{\text{indicated}}$.

Additionally, the flow calibration process is uncertain, which affects $\dot{G}_{\text{calibration}}$. Both uncertainties can be accounted for distinctly, or the calculation can be evaluated at minimum design flow, in which case the flow calibration uncertainty is deterministically accounted for.

The flow uncertainty inputs are evaluated using the Reference 5 or an equivalent methodology, and assume the following form:

$$1 + \varepsilon_{\dot{G}} = \frac{1 \pm \delta_{\Omega} + B_{\Omega}}{1 \pm \delta_{\dot{G}_{\text{calibration}}} + B_{\dot{G}_{\text{calibration}}}} \quad (5-8)$$

where $\delta_{\dot{G}_{\text{calibration}}}$ is the random variable describing the flow calibration process, δ_{Ω} is the random uncertainty in RCP speed indication, and $B_{\dot{G}_{\text{calibration}}}$ and B_{Ω} are the non-random bias factor terms associated with the two uncertainties. $\varepsilon_{\dot{G}}$ is the random variable containing both components.

5.3.4 *SPND Measurement*

The currents delivered by the SPNDs are affected by process measurement uncertainty. This uncertainty only accounts for the instrumentation, signal processing, and TELEPERM™ related components affecting the SPND currents $I_{i,j}$. SPND calibration effects, which influence the conversion of detector currents into effective LPD at the detector location, are addressed separately per the discussion in Section 5.3.9 and Appendix B. The individual SPND sensor uncertainties are assumed to be independent of each other.

The SPND current uncertainty input to the DNBR-related setpoint calculations is evaluated using the Reference 5 or an equivalent methodology. It contains the uncertainty components associated with the SPND current signal acquisition, conditioning, and digitization, and assumes the following form:

$$\begin{aligned} I_{i,j}^{\text{sensed}} &= I_{i,j} \cdot (1 \pm \delta_{\text{SPND}} + B_{\text{SPND}})_{i,j} \\ &= I_{i,j} \cdot (1 + \varepsilon_{i,j}^{\text{SPND}}) \end{aligned} \quad (5-9)$$

where δ_{SPND} is the random component of SPND measurement uncertainty, B_{SPND} is the non-random (bias) component, and $\varepsilon_{i,j}^{\text{SPND}}$ is the random variable containing both uncertainty components.

In this expression, it is stipulated that different [] uncertainties (from the same probability distribution or density) are applied to individual SPND, rather than a single sampled uncertainty to all SPND collectively. It should be noted that this is the only SPND-related uncertainty in the methodology that is applied in this manner.

5.3.5 CHF Correlation

By definition, the DNBR is the ratio between the critical heat flux (Φ_{critical}) and the local heat flux (φ_{local}):

$$\begin{aligned} \text{DNBR} &= \frac{\Phi_{\text{critical}}}{\varphi_{\text{local}}} \\ &= \frac{\Phi_{\text{critical}}^{\text{predicted}}}{\varphi_{\text{local}}} \cdot \frac{\Phi_{\text{critical}}}{\Phi_{\text{critical}}^{\text{predicted}}} \\ &= \text{DNBR}_{\text{predicted}} \cdot \frac{\Phi_{\text{critical}}}{\Phi_{\text{critical}}^{\text{predicted}}} \end{aligned} \quad (5-10)$$

where the ratio $\frac{\Phi_{\text{critical}}}{\Phi_{\text{critical}}^{\text{predicted}}}$ is the uncertainty in the CHF correlation.

This uncertainty is evaluated using the measurement of CHF in the experimental test, and the CHF predicted by the design subchannel analysis code using the same thermal hydraulic conditions. This may be expressed as:

$$\frac{\Phi_{\text{critical}}^{\text{predicted}}}{\Phi_{\text{critical}}^{\text{measured}}} = \frac{\Phi_{\text{critical}}^{\text{predicted}}}{\Phi_{\text{critical}}^{\text{predicted}}} \Bigg|_{\text{CHF test}} \quad (5-11)$$

$$= \frac{M}{P}$$

When reducing the CHF correlation, the uncertainty in the differences between the predicted CHF from the correlation fit and the measured CHF (generally denoted as the P/M ratio) is the uncertainty in the measured DNBR:

$$\text{DNBR} = \text{DNBR}_{\text{predicted}} \cdot \frac{\Phi_{\text{critical}}^{\text{measured}}}{\Phi_{\text{critical}}^{\text{predicted}}} \quad (5-12)$$

$$= \text{DNBR}_{\text{predicted}} \cdot \frac{M}{P}$$

Per the definition of the critical heat flux, DNB occurs when the DNBR is equal to 1.0. Therefore the uncertainty distribution of the predicted DNBR at DNB corresponds to the P/M statistics. Assuming this uncertainty can be expressed in terms of a random and bias component, it may be expressed as:

$$\text{DNBR}_{\text{predicted}} \Big|_{\text{DNB}} = \pm \delta_{P/M} + B_{P/M} \quad (5-13)$$

$$= \varepsilon_{P/M}$$

5.3.6 Online Algorithm

Due to the complexity and limited performance characteristics of the design subchannel analysis code, it is not directly implemented within a protection or monitoring system algorithm. Rather, a simplified, higher-performance online algorithm is used as a surrogate for the design code. This substitution process introduces an additional uncertainty that must be accounted for in the establishment of setpoints for the online

algorithm. Because the online algorithm has both DNBR and hot channel exit quality trip functionality, two distinct uncertainties are required.

The P/M statistics for the CHF correlation are based upon local thermal hydraulic parameters evaluated within the design subchannel analysis code. As such, the P/M distribution can be applied only to DNBR analyses performed with that code. For this reason, substitution of the online algorithm for the design subchannel analysis code makes it necessary to incorporate an additional uncertainty component. This uncertainty is due to differences in DNBR predictions arising from deviations in calculated local conditions from the online algorithm.

The random variable describing the differences between the DNBR predictions of the online algorithm is designated as $\epsilon_{\text{online}}^{\text{DNBR}}$, and that for hot channel exit quality predictions as $\epsilon_{\text{online}}^{\chi}$. By definition, the relationship between the DNBR and exit quality predictions from the simplified online algorithm and the design code in the methodology is defined as:

$$\begin{aligned} \text{DNBR}_{\text{online}} &= \text{DNBR}_{\text{design}} \cdot (1 \pm \delta_{\text{online}}^{\text{DNBR}} + B_{\text{online}}^{\text{DNBR}}) \\ &= \text{DNBR}_{\text{design}} \cdot (1 + \epsilon_{\text{online}}^{\text{DNBR}}) \end{aligned} \quad (5-14)$$

and

$$\begin{aligned} \chi_{\text{online}} &= \chi_{\text{design}} \pm \delta_{\text{online}}^{\chi} + B_{\text{online}}^{\chi} \\ &= \chi_{\text{design}} + \epsilon_{\text{online}}^{\chi} \end{aligned} \quad (5-15)$$

where $\delta_{\text{online}}^{\text{DNBR}}$ and $B_{\text{online}}^{\text{DNBR}}$ are the random and non-random components of the uncertainty in DNBR predictions between the design code and the online algorithm, $\delta_{\text{online}}^{\chi}$ and B_{online}^{χ} are random and non-random components of the uncertainty in hot channel exit quality predictions between the design code and the online algorithm, and $\epsilon_{\text{online}}^{\text{DNBR}}$ and $\epsilon_{\text{online}}^{\chi}$ are the random variables containing both uncertainty components.

5.3.7 Power Calorimetric

The absolute core power is periodically determined via a calorimetric heat balance. The calorimetric uncertainty is then applied to the SPND calibration process when the absolute power density is determined. The SPND calibration arrays for DNBR and exit quality must incorporate this uncertainty. The uncertainty in the calorimetric calibration is assumed to take the following form:

$$\begin{aligned} Q_{\text{measured}} &= Q \cdot (1 \pm \delta_Q + B_Q) \\ &= Q \cdot (1 + \varepsilon_Q) \end{aligned} \quad (5-16)$$

where δ_Q and B_Q are the random and non-random components of the calorimetric measurement uncertainty, and ε_Q is the random variable containing both uncertainty components.

5.3.8 Transient SPND Decalibration

At the time of SPND calibration, the hot rod conditions are known to within the calibration method uncertainty. At this time, the SPND calibration array is established, which correlates the sensed currents in the SPND with the calculated powers based upon the reconstructed power distribution:

$$C_{i,j}^{\text{CAL}} = \frac{P_{i,j}^{\text{AMS}}}{I_{i,j}^{\text{CAL}}} \quad (5-17)$$

where $P_{i,j}^{\text{AMS}}$ is the calibrated SPND power obtained from the reconstructed power distribution of the DNBR-limiting rod based upon Aeroball Measurement System (AMS) measurements, $I_{i,j}^{\text{CAL}}$ are the sensed SPND currents at the time of calibration, and $C_{i,j}^{\text{CAL}}$ is the SPND calibration array establishing the proportionality between detector current and calibrated SPND power for DNBR.

Between SPND calibrations in the plant, the same SPND calibration proportionality from Equation (5-17) is used to predict the SPND powers, based upon the sensed SPND currents:

$$P_{i,j} = C_{i,j}^{CAL} \cdot I_{i,j} \quad (5-18)$$

However, the SPND powers inferred in this fashion are not exact, because away from the point of calibration, the core has a different power distribution. This will produce a change in the relationship between SPND power and detector current, and/or a change in the power distribution or location of the DNBR-limiting rod. This effect is referred to as transient SPND decalibration.

In order to characterize the complex effects of transient decalibration, it is necessary to perform calculations with the design neutronics code. In neutronics design calculations, the SPND calibration process is directly simulated as:

$$\left[\quad \quad \right] \quad (5-19)$$

where [

]

A large number of postulated power distributions are generated by the neutronics design code, considering various normal and off-normal conditions. At various exposure points throughout the cycle, an SPND calibration is conducted, establishing $C_{i,j}^{DCAL}$. Following this, an off-normal transient event or uncontrolled xenon swing is initiated, which produces a power distribution that differs significantly from the one at the

point of calibration. [

]

[

]

(5-20)

where [

]

Equation (5-20) expresses [

] To get the

actual transient power distribution, a distinct SPND calibration array is defined at the transient condition:

$$[\quad]$$

(5-21)

[

]

[

]

(5-22)

To convert between [

] the following expression holds:

[]

(5-23)

To summarize, the following SPND calibration (for DNBR) data are available, based upon neutronics design code calculations:

- []
- []
- []
- []

This provides all the information necessary to determine [] and also provides a means for [].

For other uncertainty parameters, the uncertainty is [] and propagated through the formulations discussed in Section 5.4. The effect of this transient SPND decalibration on the trip or LCO function response will be handled by []

There are two other uncertainty components related to SPND transient calibration that are considered distinctly in the setpoint methodology. []

]

This is discussed in Section 5.3.11.

The other component is the variability in the relationship between SPND power and detector current due to changes in the thermal-hydraulic conditions considered in the neutronics design code. This is described in Section 5.3.9 and in Appendix E.

5.3.9 Reconstructed Power Distribution (AMS)

As noted in Appendix B, the SPND calibration process is used to periodically determine the power density profile on the DNBR-limiting pin in the core, as well as the peak planar LPDs. This calibration process utilizes the AMS for the discrete flux measurements in the core, followed by a reconstruction algorithm that produces a fine resolution flux map in the core. As a consequence of the use of the AMS and the reconstruction algorithm, the reconstructed power distribution is subject to uncertainties. These represent the capability of the AMS and incore monitoring software to resolve the DNBR-limiting pin and the axial offset.

These uncertainties are assumed to have the following forms:

$$\begin{aligned} F\Delta H_{\text{measured}} &= F\Delta H_{\text{design}} \cdot (1 \pm \delta_{F\Delta H}^{\text{AMS}} + B_{F\Delta H}^{\text{AMS}}) \\ &= F\Delta H_{\text{design}} \cdot (1 + \epsilon_{F\Delta H}^{\text{AMS}}) \end{aligned} \quad (5-24)$$

and

$$\begin{aligned} AO_{\text{measured}} &= AO \pm \delta_{AO}^{\text{AMS}} + B_{AO}^{\text{AMS}} \\ &= AO + \epsilon_{AO}^{\text{AMS}} \end{aligned} \quad (5-25)$$

The axial offset variable represents a second-order effect in calculated results from the methodology, and will heretofore be neglected.

Appendix E describes the methodology used to reduce neutronics uncertainties.

5.3.10 Thermal Hydraulic Conditions for SPND Data

The licensing neutronics methodology used to generate the SPND data considers sets of thermal hydraulic conditions that may differ from those used in the static setpoint calculation. This is due the use of expansive scans over the postulated operating statepoints (including accident conditions) in the setpoint methodology and the necessity of generating neutronics data for a limited subset of these conditions.

A sensitivity analysis is conducted to assess the changes in the SPND calibration array that occur when the thermal hydraulic conditions are modified. [

] One can expand the

relationship between SPND calibrations at the reference and modified conditions as:

$$[\quad \quad \quad] \quad (5-26)$$

where [

] Equation (5-26) [

]

- The thermal hydraulic parameters
- The SPND position (both axial and radial)
- The cycle and exposure point

The sensitivity factors are obtained via a broad range of neutronics design calculations. SPND calibrations are [

]

5.3.11 SPND Calibration Frequency

The SPNDs must be periodically calibrated against the AMS at least once within a maximum EFPD window (typically around 15 EFPD). However, SPND calibrations may be conducted at any time, and may even be conducted multiple times within this window. Due to evolution of power distributions and detector burnout effects, the SPND calibration matrix generated in the plant $C_{i,j}^{CAL}$ will be variable, and a function of the time in cycle.

In the neutronics design code calculations used to generate the numerous power distribution inputs to the setpoint analysis, a limited number of SPND calibrations are simulated at several points in cycle, [

] The process of [

] gives rise to [

] The magnitude of this uncertainty is dependent on the length of the burnup window. This uncertainty is obtained by simulating numerous SPND calibrations through a given cycle (albeit without the subsequent generation of expansive numbers of transient power distribution shapes), [

] over a specified EFPD window.

The uncertainty is expressed in terms of the available SPND calibration arrays for DNBR, with the form:

$$\begin{aligned} C'_{i,j} &= C_{i,j} \cdot (1 \pm \delta_{burnup} + B_{burnup}) \\ &= C_{i,j} \cdot (1 + \epsilon_{burnup}) \end{aligned} \quad (5-27)$$

where $C_{i,j}$ is the available SPND calibration, $C'_{i,j}$ is the SPND calibration array with burnup uncertainties applied, δ_{burnup} is the random component of the uncertainty in SPND calibration factors with respect to burnup effects, B_{burnup} is the non-random (bias)

component of the uncertainty, and $\varepsilon_{\text{burnup}}$ is the random variable containing both uncertainty components.

5.3.12 Assembly Geometry Deviations

Intrinsic variability of the assembly manufacturing process may result in a subsequent variability of the hot channel flow channel area. This affects the enthalpy rise in the hot channel, which in turn impacts DNBR and the hot channel exit quality. The assembly manufacturing tolerances are accounted by an uncertainty on the radial peaking power factor:

$$\begin{aligned} F\Delta H_{\text{actual}} &= F\Delta H_{\text{design}} \cdot \left(1 \pm \delta_{F\Delta H}^{\text{ENG}} + B_{F\Delta H}^{\text{ENG}}\right) \\ &= F\Delta H_{\text{design}} \cdot \left(1 + \varepsilon_{F\Delta H}^{\text{ENG}}\right) \end{aligned} \quad (5-28)$$

where $F\Delta H_{\text{actual}}$ is the $F\Delta H$ present when manufacturing deviations result in a different radial peaking than the design value $F\Delta H_{\text{design}}$, $\delta_{F\Delta H}^{\text{ENG}}$ is the random component of uncertainty in $F\Delta H$ due to manufacturing deviations (i.e. engineering $F\Delta H$ uncertainty), $B_{F\Delta H}^{\text{ENG}}$ is the non-random component of the uncertainty, and $\varepsilon_{F\Delta H}^{\text{ENG}}$ is the random variable containing both uncertainty components.

5.3.13 Rod Bow

Rod bow is a phenomenon in which the design pitch dimensions between adjacent fuel rods are altered due to burnup effects. The major concerns with fuel rod bowing are a localized reduction in the fuel cell flow area and an increase in adjacent fuel rod-to-rod spacing leading to increased moderation and an increase in power peaking.

[

]

• [

]

• [

]

5.3.14 *Assembly Bow*

Assembly bow is analogous to the rod bow phenomenon, except that it affects the assembly as a whole, rather than individual pins. The concern with assembly bow is that the increased moderation associated with the wider inter-assembly gap will increase the peaking, particularly of the peripheral pins in the hot assembly.

[

] Fresh fuel assemblies can be affected by adjacent burned assemblies that are bowed, and the flow area effects are not addressed in the engineering hot channel factor. Therefore, assembly bow penalties must be applied to both DNBR and LPD calculations.

The assembly bow penalties assume the following form:

$$\begin{aligned} F\Delta H_{\text{actual}} &= F\Delta H_{\text{design}} \cdot \left(1.0 \pm \delta_{F\Delta H}^{\text{ass'y bow}} + B_{F\Delta H}^{\text{ass'y bow}} \right) \\ &= F\Delta H_{\text{design}} \cdot \left(1 + \epsilon_{F\Delta H}^{\text{ass'y bow}} \right) \end{aligned} \quad (5-29)$$

where $\delta_{FQ}^{\text{ass'y bow}}$ is the random component of the penalty due to assembly bow, $B_{FQ}^{\text{ass'y bow}}$ is the non-random component, and $\epsilon_{FQ}^{\text{ass'y bow}}$ is the random variable containing both uncertainty components.

5.3.15 *Epistemic*

The epistemic uncertainty is designed to accommodate applicable epistemic uncertainties that are not already addressed via other uncertainties. It may also be used as a mechanism for incorporating operational margin allowances in the statistical process.

When applied to DNBR calculations, the epistemic uncertainty component assumes the form:

$$\begin{aligned} \left(\frac{P}{M}\right)_{\text{adjusted}} &= \left(\frac{P}{M}\right) \pm \delta_{\text{epistemic}}^{\text{DNBR}} + B_{\text{epistemic}}^{\text{DNBR}} \\ &= \left(\frac{P}{M}\right) + \epsilon_{\text{epistemic}}^{\text{DNBR}} \end{aligned} \tag{5-30}$$

In the case where it is applied to the quality trip, it takes the form:

$$\begin{aligned} \chi_{\text{adjusted}} &= \chi_{\text{limit}} \pm \delta_{\text{epistemic}}^{\chi} + B_{\text{epistemic}}^{\chi} \\ &= \chi_{\text{limit}} + \epsilon_{\text{epistemic}}^{\chi} \end{aligned} \tag{5-31}$$

In these expressions $\delta_{\text{epistemic}}^{\text{DNBR}}$ and $\delta_{\text{epistemic}}^{\chi}$ are the random epistemic components of DNBR and hot channel exit quality uncertainty, $B_{\text{epistemic}}^{\text{DNBR}}$ and $B_{\text{epistemic}}^{\chi}$ are the non-random (bias) components, and $\epsilon_{\text{epistemic}}^{\text{DNBR}}$ and $\epsilon_{\text{epistemic}}^{\chi}$ are the random variables incorporating both components.

5.4 Coverage Method for Establishing DNBR/Quality Setpoints

There are three alternative methods that may be used to statically establish (unknown) setpoints for the Low DNBR Channel LSSS and DNB LCO setpoints, as follows:

[]
 []
 []

The coverage and testing methodologies are described in Appendix A.

The coverage method may be used when there are no predetermined setpoints, while the testing method requires that setpoints be known (although they may be estimated).

]

Once the trip setpoints are established, [

]

The following trips or sub-trips are [

]

- Reactor trip on low DNBR for no detected asymmetries
- Reactor trip on low DNBR with dropped rod indication in one division or SPND imbalance indication
- Reactor trip on low DNBR with dropped rod indication in more than one division
- Reactor trip on high exit quality with 2nd maximum signal
- Reactor trip on high exit quality with 1st maximum signal (regardless of imbalance or rod drop signals)

[

]

[] and is established independently using the coverage method (see Section 8.3). It may, however, [] as will be discussed in Section 5.5.

The coverage process for DNBR or exit quality flows as follows:

- []

This is based upon 95 percent probability and 95 percent confidence and utilizes the relationships provided in Appendix A []

]

- []

At each statepoint protected by a given DNBR function (LSSS or LCO), [] At each combination of thermal-hydraulic conditions and power distribution, the following process is used:

- []

Each of the random variables describing a DNB- or exit quality-related uncertainty variable (see Section 5.3) is []

]

- []

[

]

[] Details on the process [] is described in Section 5.4.6.

- []

This process is described in more detail in Sections 5.4.2 and 5.4.3.

- []

This process is described in more detail in Section 5.4.4 and 5.4.5. []

]

- []

]

- []

]

- []

The setpoint is set to the []

5.4.2 Calculation of Reference DNBR

As noted earlier, the term “reference DNBR” is used to refer to the DNBR that arises when a set of assumed process parameter values in the core are used in conjunction with systemic uncertainties (unrelated to the measurement process), [

] This also [

]

The systemic uncertainty factors considered in this stage of the calculation are:

- Statistics of the CHF correlation, $\epsilon_{P/M}$
- Assembly bow penalty, $\epsilon_{F\Delta H}^{ass'y\ bow}$
- Online DNBR algorithm uncertainty with respect to DNBR¹, ϵ_{online}^{DNBR}
- Assembly geometry variations (engineering uncertainty), $\epsilon_{F\Delta H}^{ENG}$
- Sensitivities in the SPND calibration arrays, due to changes in the thermal hydraulic conditions used in neutronics analysis, δ_{sens}
- SPND calibration frequency (also known as burnup decalibration), ϵ_{burnup}
- Epistemic allowance in the DNBR and hot channel exit quality calculations, $\epsilon_{epistemic}^{DNBR}$ and $\epsilon_{epistemic}^X$.

¹ This uncertainty, although not a systemic uncertainty, is applied here because the online DNBR algorithm is used in lieu of the design subchannel analysis code. The substitution of the online algorithm for the design subchannel analysis code in the calculation of the reference DNBR was motivated by the substantial performance improvements the online algorithm affords, and the huge number of power distributions used as input to the analysis.

The relationship between the DNBR calculated via the design subchannel analysis code at a given set of thermal hydraulic calculations, and the reference underlying DNBR satisfies the relationship:

$$[\quad] \quad (5-32)$$

where the form takes into account Equations (5-13) and (5-30). If the online DNBR algorithm is used in lieu of the design subchannel analysis code, the algorithm uncertainty must be additionally introduced:

$$[\quad] \quad (5-33)$$

The DNBR calculation must account for systematic perturbations to the fuel geometry, in particular hot channel factor (engineering) and assembly bow uncertainty.

Additionally, the power distribution used in the online DNBR calculation must account for the changes [

] in SPND calibration frequency and the thermal-hydraulic conditions.

Therefore, Equation (5-33) becomes:

$$[\quad] \quad (5-34)$$

In this expression, the power distribution [

] corresponding to an off-normal power distribution. It is obtained by generating an off-normal power distribution in the neutronics design code, then calculating the SPND response for DNBR that corresponds to that flux distribution exactly.

Per the definition of the DNBR setpoint problem, [

] Therefore, the power distribution is [

] the CHF correlation mean. This

is equivalent to [

]. Therefore, the [] takes the form:

$$[\hspace{15em}]$$

(5-35)

In this expression, it is explicitly noted that the form is applicable to the DNBR trip function only. The formulation for the DNB LCO is identical to Equation (5-35), with the sole exception that [

] Therefore, it takes the slightly modified form:

$$[\hspace{15em}]$$

(5-36)

5.4.3 Calculation of Reference Exit Quality

The reference exit quality is the exit quality that arises when a set of assumed process parameter values in the core are used in conjunction with systemic uncertainties

(unrelated to the measurement process), and calculated [

].

$$[\hspace{15em}]$$

The systemic uncertainty factors considered in this stage of the calculation are:

- Assembly bow penalty, $\varepsilon_{F_{\Delta H}}^{\text{ass'y bow}}$
- Online DNBR algorithm uncertainty with respect to quality, $\varepsilon_{\text{online}}^x$
- Engineering uncertainty on $F_{\Delta H}$, $\varepsilon_{F_{\Delta H}}^{\text{ENG}}$
- SPND calibration frequency (also known as burnup decalibration), $\varepsilon_{\text{burnup}}$
- Sensitivities in the SPND calibration arrays, due to changes in the thermal hydraulic conditions used in neutronics analysis, δ_{sens}
- Epistemic allowance in the exit quality calculations, $\varepsilon_{\text{epistemic}}^x$

The reference exit quality is dependent upon the enthalpy rise in the hot channel, and as such is dependent upon systemic effects impacting the $F_{\Delta H}$. Therefore, based upon the discussion presented in Section 5.4.2, the reference exit quality may be written in the same form, without the uncertainties related to the CHF correlation and using the additive form of the algorithm uncertainty:

$$[\quad \quad \quad] \quad (5-37)$$

where all terms were defined previously.

Per the definition of the exit quality setpoint problem, [

] Therefore, the power

distribution is [

] shown in Equation (5-35), even though the [

]

[

(5-38)

5.4.4 Calculation of Sensed DNBR

The sensed DNBR is the value that the online system calculates, based upon sensed conditions, [] The sensed DNBR is subject to process measurement uncertainties, including those on temperature, pressure, RCP speed, and power. Power distribution effects are also an important effect on the sensed DNBR. This arises from uncertainties introduced when the SPND calibration process is conducted, drift from the calibrated state (i.e., transient SPND decalibration), and SPND instrument uncertainties. The sensed DNBR in the plant is expressed as:

[] (5-39)

where all the values inside the parentheses on the RHS of Equation (5-39) are sensed values.

The SPND sensor and calibration related uncertainties, which enter the sensed DNBR through the online DNBR calculation, incorporate the following components:

- SPND (instrumentation) current uncertainties, $\epsilon_{I\&C}^{SPND}$
- Calorimetric uncertainty, ϵ_Q
- The power distribution acquired by the AMS and reconstructed by the incore monitoring software, $\epsilon_{F\Delta H}^{AMS}$

Incorporating the process measurement uncertainties and power distribution uncertainties, Equation (5-39) can be expressed as:

$$[\hspace{15em}] \tag{5-40}$$

where the sensed power distribution is modified by the same scaling factor F_{scale}^{DNBR} that was used to drive the reference exit quality (with the true power distribution) to the exit quality limit, per Equation (5-35). This form is applicable both for the Low DNBR Channel LSSS and the DNB LCO.

5.4.5 Calculation of Sensed Exit Quality

The sensed exit quality, as noted previously, is the exit quality that the online system calculates, based upon sensed conditions. The sensed exit quality is subject to process measurement uncertainties, including those on temperature, pressure, RCP speed, and power distributions. The sensed exit quality is expressed in an essentially identical form to that for the sensed DNBR:

$$[\hspace{15em}] \tag{5-41}$$

where the sensed power distribution is modified by the same scaling factor F_{scale}^X that was used to drive the reference exit quality (with the true power distribution) to the exit quality limit, per Equation (5-38).

5.4.6 Treatment of Inoperable SPNDs

As noted earlier, both the Low DNBR Channel LSSS and DNB LCO are adaptive with respect to a limited number of inoperable SPNDs. The methodology supports this functionality.

Sampling Process for Inoperable SPNDs

[

]

[

]

[

] This has the effect of

adding a conservative effect, relative to a purely random process.

5.5 Testing Method for Confirming Existing Setpoints

The testing method can be used to confirm existing setpoints for either LCO or LSSS functions. Additionally, it can be used for establishing setpoints, provided that initial estimates of the setpoints are available. The setpoints can either be based upon engineering judgment¹, or derived in a previous coverage analysis. This section will

¹ An postulated situation where setpoints are established via an initial guess, followed by an iterative application of the testing method, is applied where setpoints are being established for a core similar to one previously analyzed in detail.

discuss the testing method for confirming existing setpoints, including setpoints other than those related to DNBR.

[

]

It should be noted that the testing process described herein is intended as a method of confirming static setpoints for the incore trip and LCO functions within the scope of this topical report, rather than for system trips or other LCOs.

5.5.1 General Flow of Testing Process

The general testing process is shown in Figure 5-5. The steps in applying the testing process are as follows:

[

]

This is identical to that discussed for the coverage method documented in Section 5.4.

[

]

[

]

- []

This method is identical to that used in the coverage method.

- []

[

] The trips are not necessarily limited

to incore trip functions, and may include other trips such as the High LPD Channel LSSS or High Core Power Level. If the function is treated statistically, the nominal value is used. If treated deterministically, then the deterministic value is used.

- []

[

] but may require additional variables if

additional trips are treated statistically, rather than deterministically.

- []

¹ This term is meant to describe trip functions encompassing more than one setpoint or series of setpoints. For example, the Low DNBR Channel has several setpoints to protect against various type of asymmetric events, and the High Core Power Level trip has both a power setpoint and a core exit saturation setpoint.

[

]

[

] based

upon the sampled uncertainties.

• [

]

[

]

[

]

[

]

[

]

[

] Unlike the coverage

method, [

]

5.5.2 Testing Method for LSSS versus LCO Functions

Application of the testing method for LSSS versus LCO functions is conducted separately, although the calculations are quite similar in structure. This is due to the

separation of functions between the safety-grade PS and the non-safety grade RCSL. Additionally, non-safety grade functions or protective capabilities are not credited in the LSSS testing analysis.

For example, an LSSS testing analysis might consider the High LPD Channel LSSS, the Low DNBR Channel LSSS, the MSSV actuation, and the High Core Power Level LSSS, but could not incorporate the DNB LCO or LPD LCO, or the HLPD or DNBR limitation functions.

For the LCO testing analysis, one could conceivably credit safety grade trip or protective functions, as well as non-safety grade limitation functions, although it is not necessary since they will not intercede in the operating range. For example, a LCO testing analysis might consider the DNB LCO, the LPD LCO (both top and bottom halves), the reactor thermal power LCO.

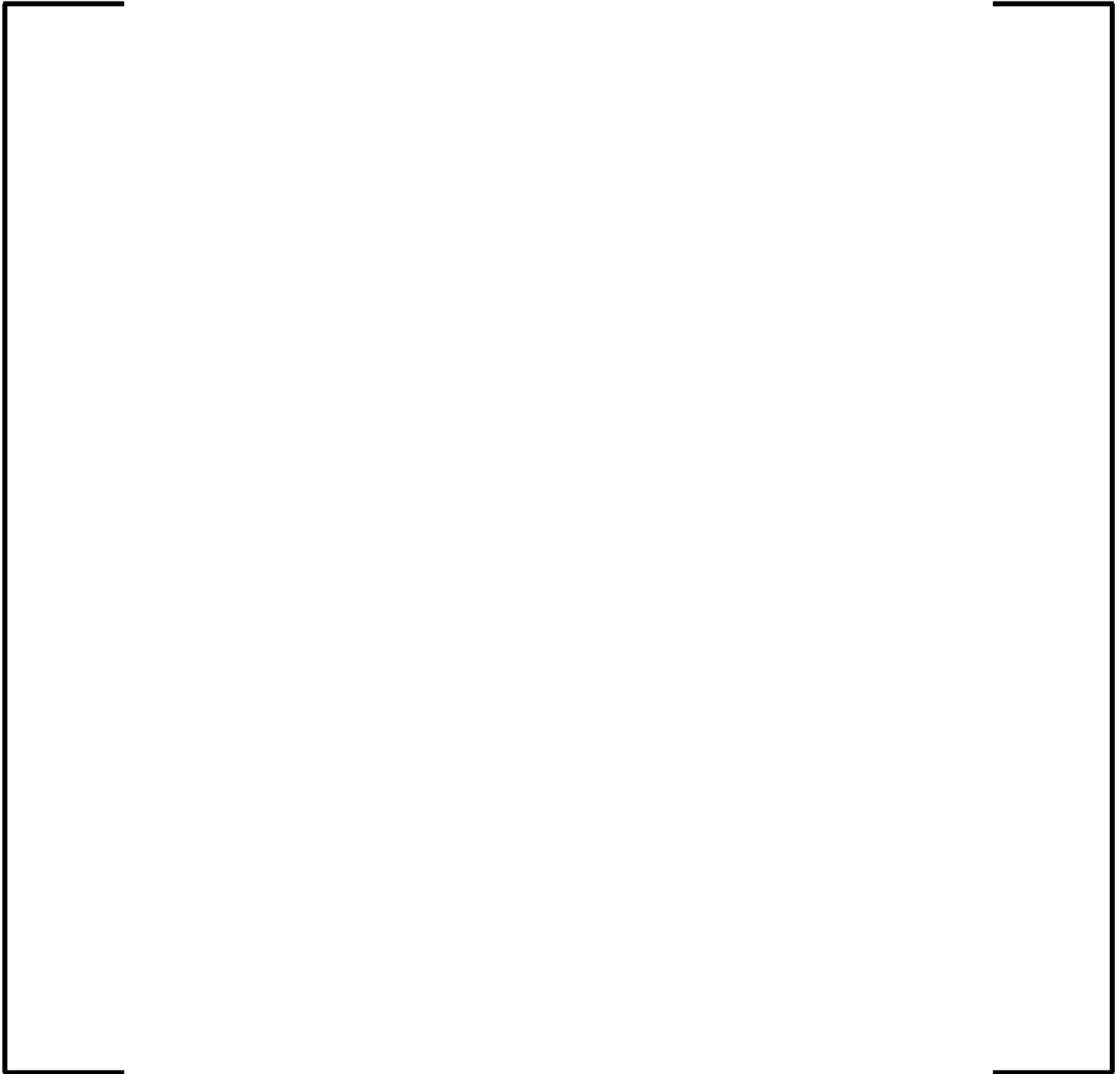


Figure 5-1 Establishing the DNBR Trip Setpoint

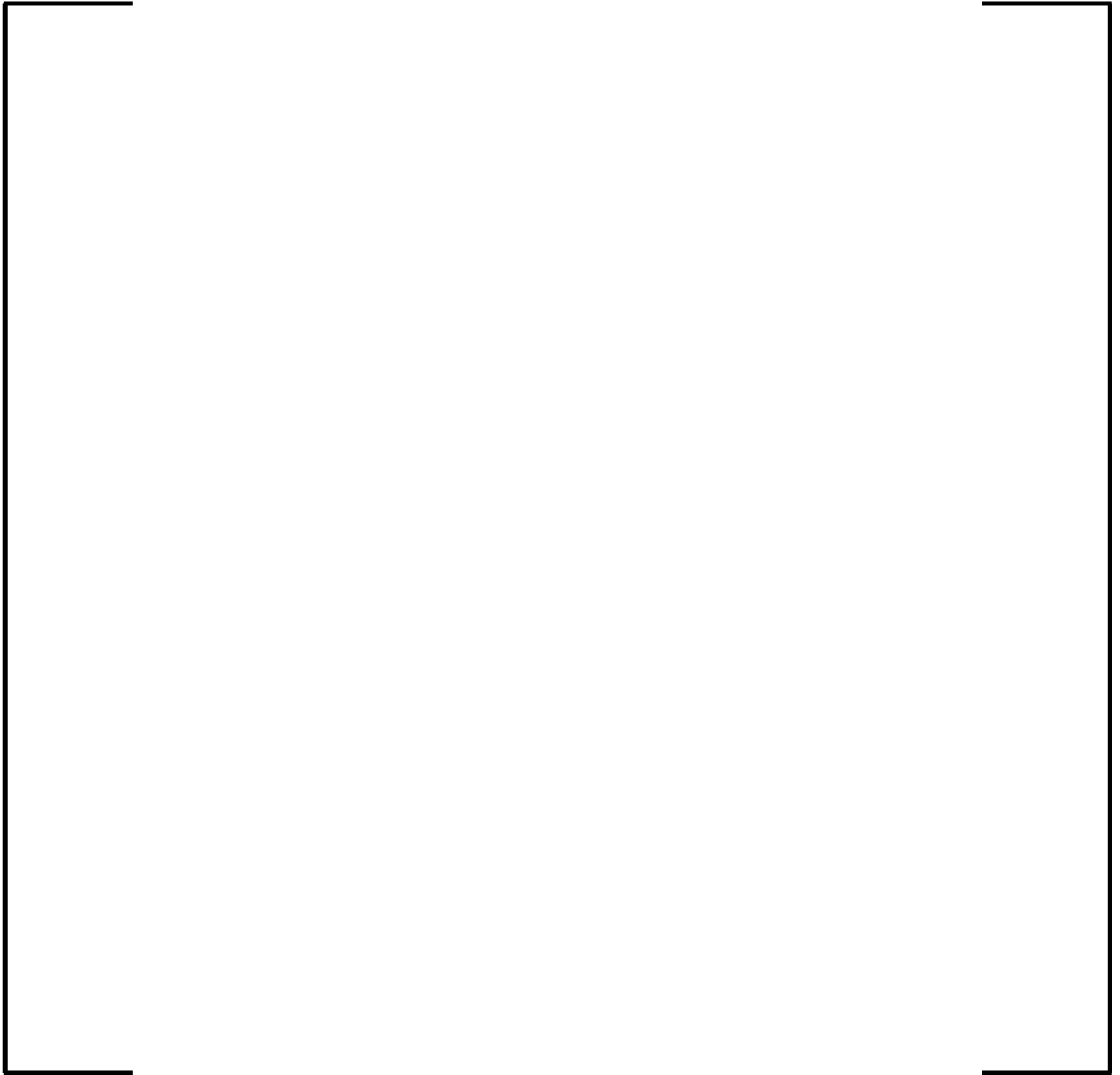


Figure 5-2 Establishing the Exit Quality Trip Setpoint

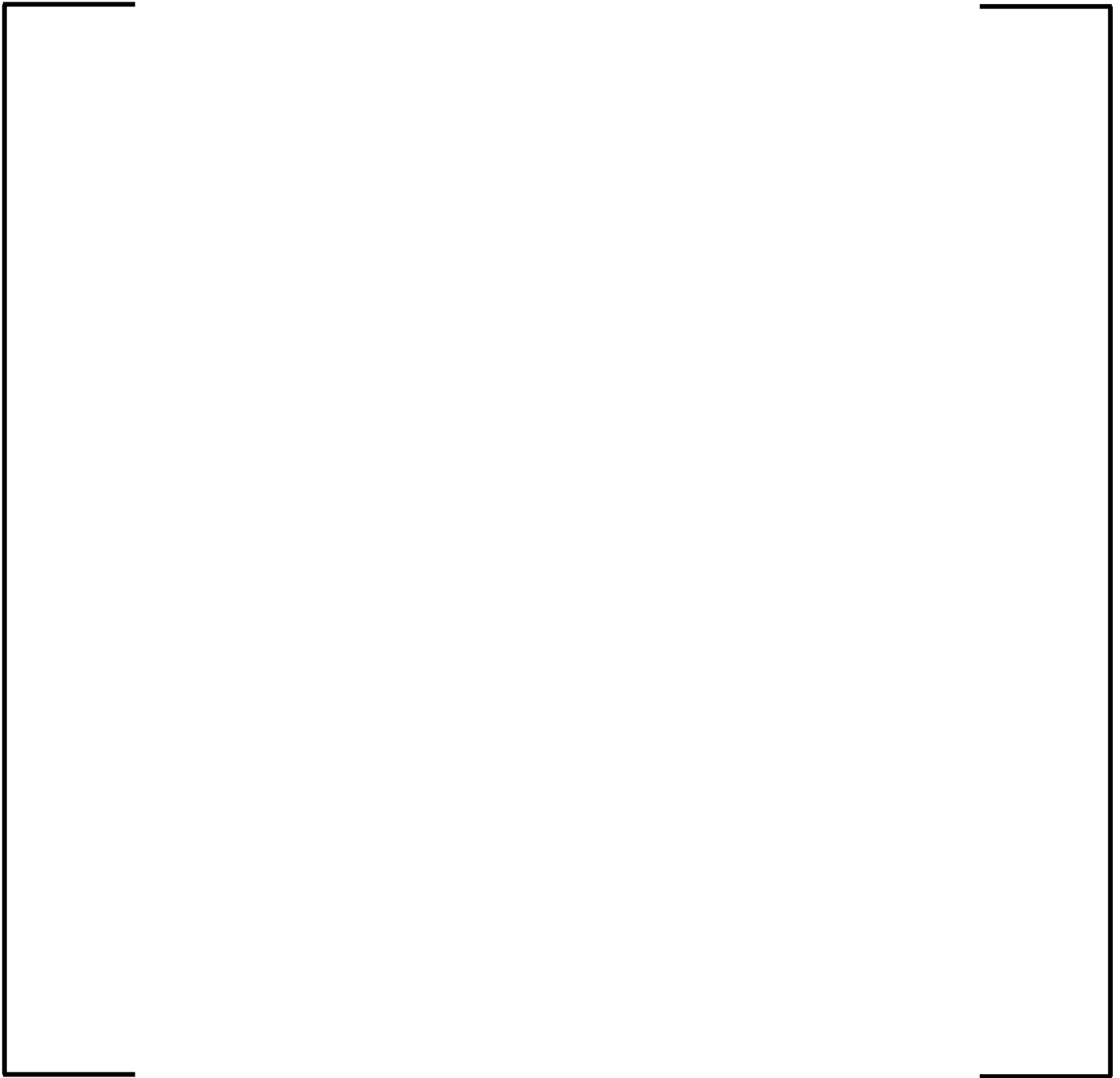


Figure 5-3 Establishing the DNB LCO Setpoint

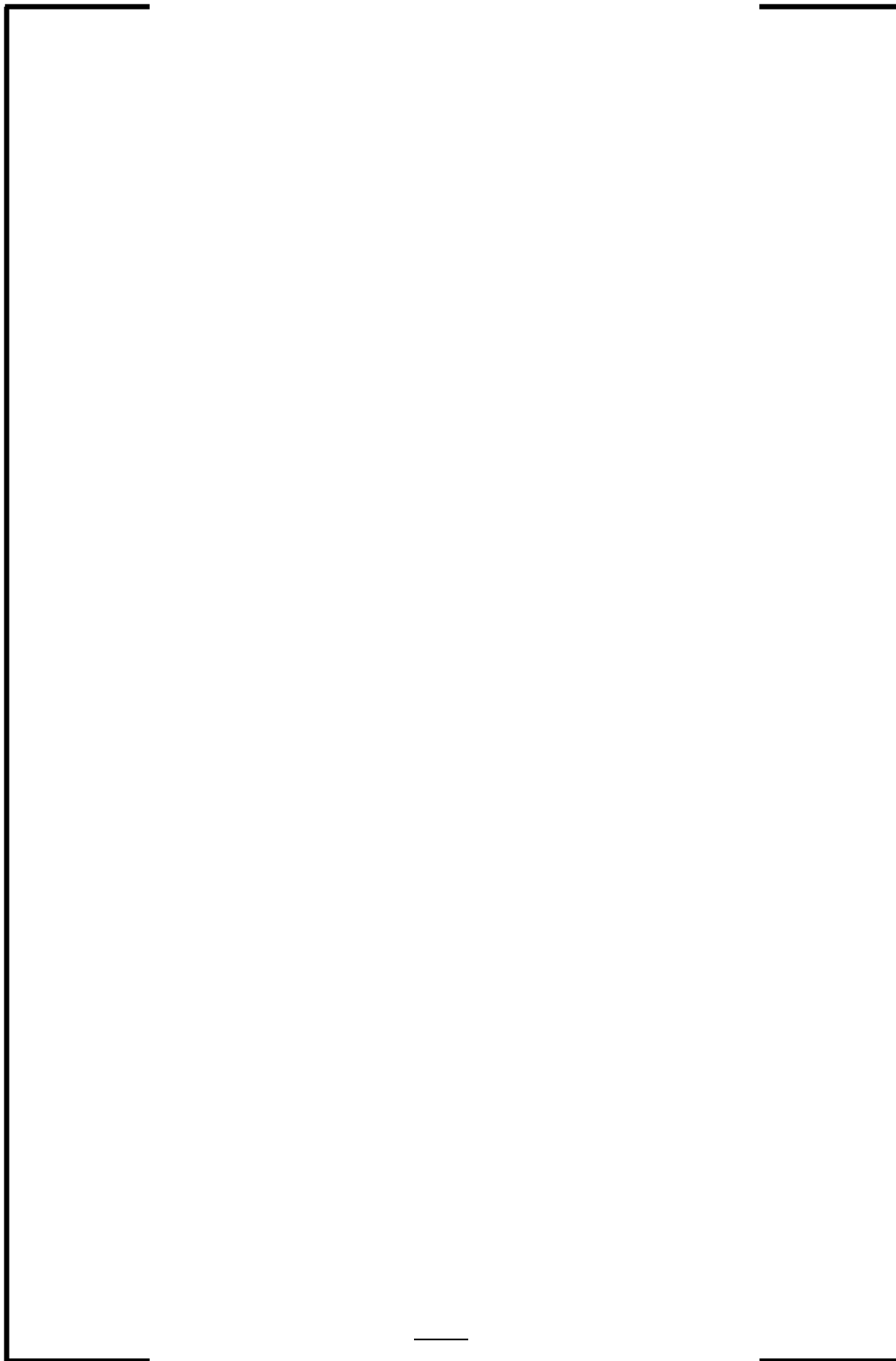


Figure 5-4 DNBR and Exit Quality Coverage Method

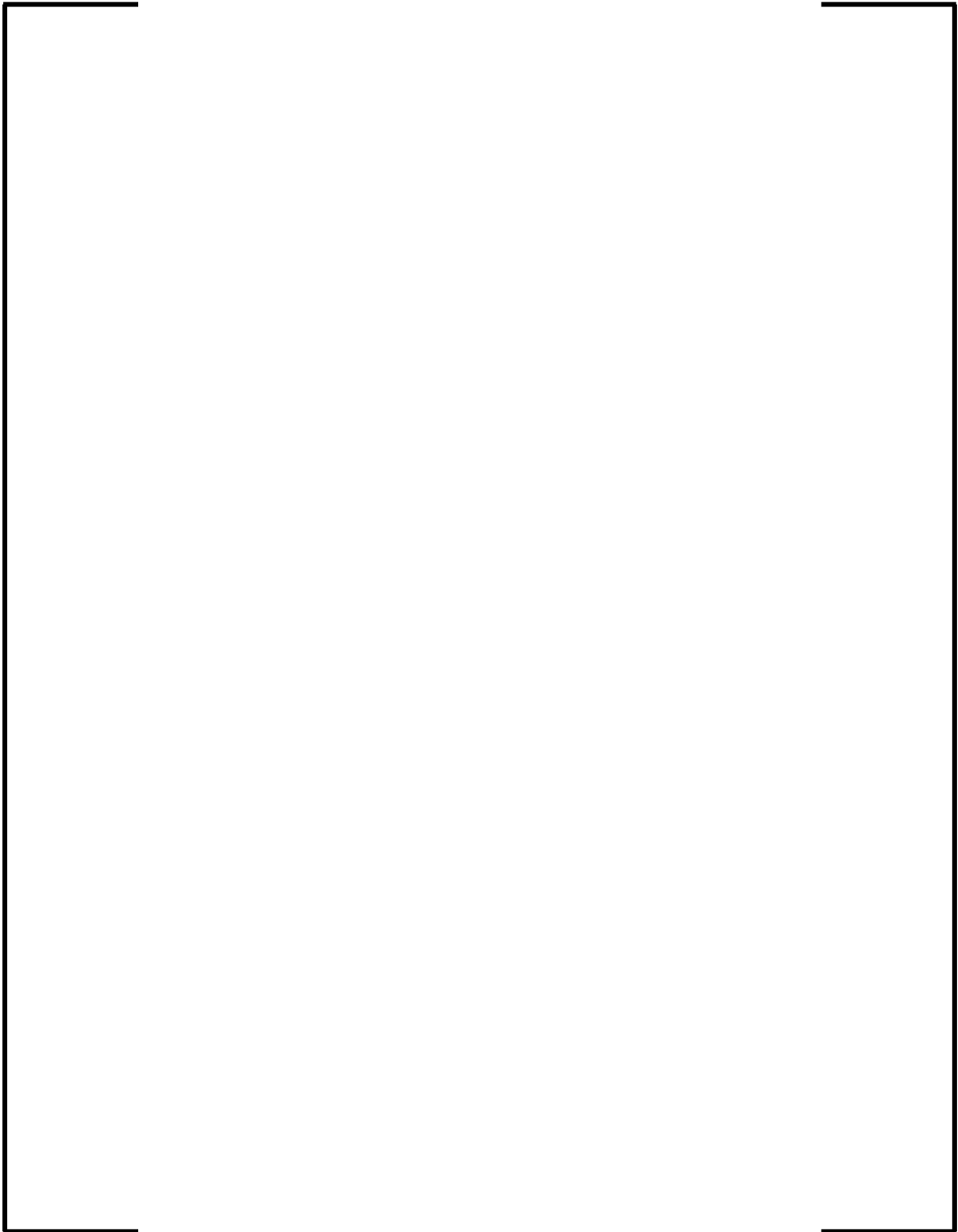


Figure 5-5 Testing Method for Confirming Setpoints

6.0 HIGH LPD CHANNEL LIMITING SYSTEM SAFETY SETTING

Per the Standard Review Plan (Reference 2), Section 4.2, the SAFDL on the overheating of fuel pellets requires that, for the core location with the maximum linear heat generation rate, including all hot spots, hot channel factors, compositional, and burnup effects, centerline melting is not permitted in normal operation and for AOOs. As stipulated in Sections 4.3 and 4.4 of the SRP, the assessments should incorporate uncertainty in process variables, instrumentation, core design parameters, and calculation methods, and should be evaluated at no less than 95 percent probability and with 95 percent confidence.

Active intervention in events characterized by an uncontrolled degradation in the peak LPD and in which the evolution of the local power in time can be resolved is provided by the High LPD Channel LSSS. This function produces a reactor trip when the SAFDL on fuel centerline melt or clad strain is approached, and ensures that protection is afforded at a level no less than 95 percent probability with 95 percent confidence.

6.1 *Design Basis*

The High LPD Channel LSSS is designed to protect against normal operation and AOOs in which the SAFDL on LPD¹ is approached due to changes in gross reactor power and/or core power distributions. Protective capability is accomplished by monitoring the maximum linear power density in the reactor core with the SPNDs, and comparing it against a maximum allowable linear power density. Violation of this setpoint will result in the issuance of a reactor trip signal.

Depending upon the characteristic speed of evolution of particular cases within each event, the High LPD Channel LSSS may or may not be able to intercede. Events which evolve too quickly to be protected by the trip must be protected by the initial LPD margin afforded by the LPD LCO settings, or by a combination of the LPD LCO and system trips (in particular, the Excore Rate of Change trip).

Potential occurrences of a High LPD Channel LSSS reactor trip are minimized via the use of the High LPD limitation function. This function, which is also implemented in the PS, uses common signals with the reactor trip, but with distinct setpoints. Upon the issuance of a partial trip signal to RCSL by the High LPD limitation function, a series of automatic actions are undertaken to bring the plant to an acceptable operating state. Ultimately, the High LPD Limitation is designed to increase plant availability by preventing the reactor from reaching a full trip setpoint.

Table 6-1 shows the AOO events forming the primary basis of the High LPD Channel LSSS. The High LPD Channel LSSS may also intercede in certain postulated accidents (e.g. pre-scrum MSLB, control rod ejection), but is not specifically designed to do so.

6.2 *Functional Description*

The following subsections provide a functional description of the High LPD Channel LSSS. Figure 6-1 illustrates of the online High LPD Channel LSSS calculation.

6.2.1 *Process Variable Input*

The High LPD Channel LSSS uses calibrated signals from all available SPND. [

] per the methods discussed in Appendix B.

Figure 6-2 shows the assignment of the SPNDs to the High LPD Channel LSSS.

6.2.2 *Plant Constant Inputs*

The High LPD Channel LSSS utilizes a number of constants stored in the plant computer. These are shown in Table 6-2.

¹ This may be due to either fuel centerline melt, or clad strain limits, whichever is more limiting.

6.2.3 Algorithm

The High LPD Channel LSSS directly estimates power densities in the core using calibrated SPND readings. The readings are then compared against maximum allowable setpoint values. The particulars of the algorithm are as follows:

Acquisition and Conditioning of the LPD Signal

[For each of the six SPND currents arising from each of the twelve detector strings, a conversion from current to power density is accomplished via the use of a SPND calibration array for LPD ($C_{i,j}^{LPD}$):

$$P_{i,j}^{LPD} = C_{i,j}^{LPD} \cdot I_{i,j} \quad (6-1)$$

where:

$P_{i,j}^{LPD}$ \equiv Linear power density in W/cm, as determined by SPND i on detector string j .

$C_{i,j}^{LPD}$ \equiv Conversion array between detector current and [established at the time of SPND calibration.]

$I_{i,j}$ \equiv Current indicated by the SPNDs

Appendix B provides a description of the SPND calibration process for LPD, which is used to generate the $C_{i,j}^{LPD}$ array.

To preclude spurious actuation of the High LPD Channel LSSS, the highest LPD measurement in the core (as a whole) is discarded¹ and the remaining SPND signals used as a basis for the LSSS computation:

[]

$$P_{\max 2}^{\text{LPD}} = \text{MAX2}(P_{i,j}^{\text{LPD}}) \quad (6-2)$$

where $P_{\max 2}^{\text{LPD}}$ is the second maximum LPD of the available SPND signals, and MAX2 is used to indicate a function that extracts the second maximum value.

A second-order low pass filter function is used on the second maximum LPD signal to filter signal noise and to compensate for the algorithm processing time:

$$PF_{\max 2}^{\text{LPD}} = \left[\frac{1 + \tau_2 S}{(1 + \tau_1 S)(1 + \tau_3 S)} \right] \cdot P_{\max 2}^{\text{LPD}} \quad (6-3)$$

In Equation (6-3), $PF_{\max 2}^{\text{LPD}}$ is used to indicate the filtered second maximum LPD signal, and the τ values are filter time constants.

Comparison Against Reactor Trip Setpoints

The second maximum LPD signal obtained in this manner is then evaluated against the reactor trip setpoints. If the signal from a particular division exceeds the reactor trip setpoint, then a reactor trip signal is issued from that division:

$$\left(PF_{\max 2}^{\text{LPD}} \geq HLPD_{RT} \right) \Rightarrow \text{reactor trip signal} \quad (6-4)$$

where the $HLPD_{RT}$ indicates the applicable reactor trip setpoint.

Comparison Against PT Setpoints

The same signals used for comparison against the RT setpoints are also compared against the partial trip (PT) setpoints. These PT comparisons take similar form to the RT comparisons above, and result in a PT signal being sent to the RCSL system:

$$\left(PF_{\max 2}^{\text{LPD}} \geq HLPD_{PT} \right) \rightarrow \text{partial trip signal (RCSL)} \quad (6-5)$$

6.2.4 Setpoints

The High LPD Channel LSSS has multiple setpoints designed to accommodate a limited number of inoperable SPNDs, both for the full reactor trip and the partial trip. Inoperable SPNDs are eliminated from the LPD calculation, and the setpoints are modified according to the logic shown in Table 6-3. The switch to these setpoints is automatic when SPNDs are declared inoperable. The same logic is used both for the full reactor trip and the partial trip setpoints.

6.2.5 Inhibition

The High LPD Channel LSSS and its associated partial trip are inhibited at power levels below the P2 permissive setting, which is set to a low power level (generally around 10 percent RTP).

6.3 Interface with Other Trips

The High LPD Channel LSSS will afford protection against events in conjunction with other trips and protective capabilities in the U.S. EPR to provide protection against violation of the SAFDLs. These other trips and capabilities include:

Low DNBR Channel

The Low DNBR Channel LSSS will trip when sensed DNBR conditions in the core encroach upon the DNB SAFDL. As it is generally difficult to reach high power densities without simultaneously causing DNBR problems, the Low DNBR Channel will frequently intercede prior to the High LPD Channel.

High Core Power Level, MSSV Actuation

The HCPL trip will produce a reactor trip at excessively high power levels and if the coolant conditions at the core exit encroach upon saturation. The MSSVs will serve to restrict the pressure conditions in the steam generators. Both can be expected to intercede in overpower events, in conjunction with the High LPD Channel.

Excure Rate of Change Trip

The Excure Rate of Change Trip will serve to intercede in events characterized by rapid power excursions. It effectively puts a restriction on the speed of event the High LPD Channel trips are expected to protect against.

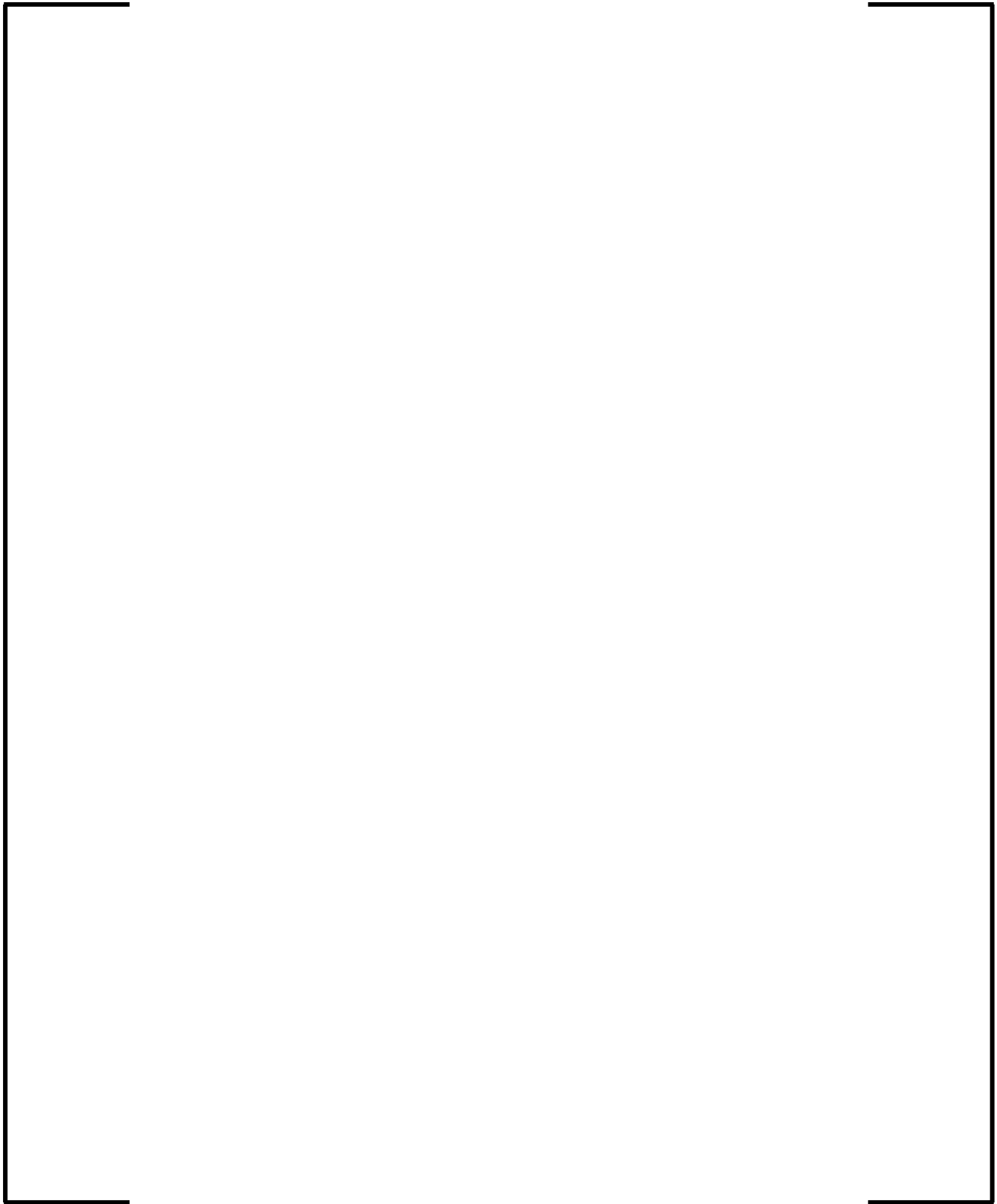


Figure 6-1 High LPD Channel LSSS Functional Diagram

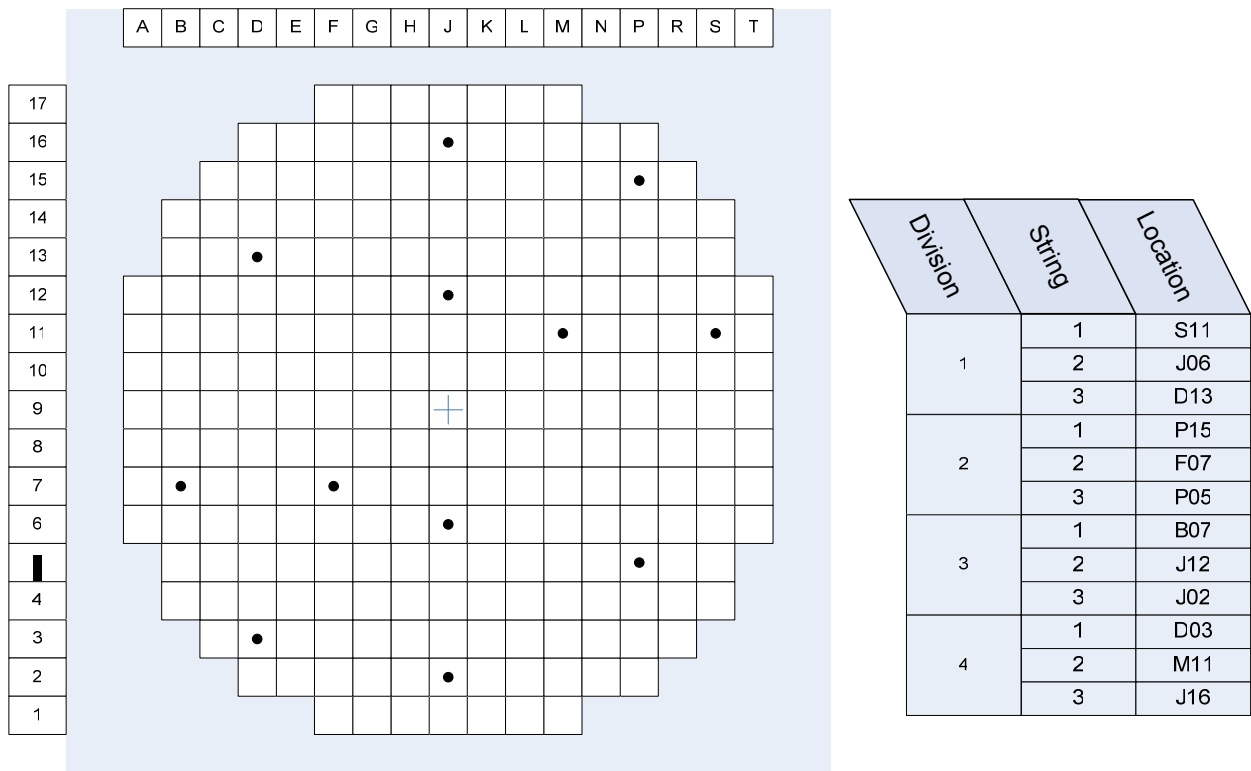


Figure 6-2 Core Layout for the High LPD Channel LSSS

Table 6-1 Basis Events for the High LPD Channel LSSS

Event	SRP Section	Comments
Excess Increase in Steam Flow (Excess Load Increase)	15.1.3	Slower end of event spectrum
Uncontrolled Control Rod Assembly Withdrawal at Power	15.4.2	Slower end of event spectrum
Control Rod Misoperation: <i>Dropped Control Rod/Bank</i>	15.4.3	---
Control Rod Misoperation: <i>Single Control Rod Withdrawal</i>	15.4.3	---
Inadvertent Decrease in Boron Concentration in the Reactor Coolant System	15.4.6	---

Table 6-2 High LPD Channel LSSS Constants

Constant	Description
Calibration Factors	
$C_{i,j}^{LPD}$	SPND calibration array for LPD
Filter Time Constants	
τ_1	Lag time constant in second-order filter for 2 nd maximum LPD signal, in seconds
τ_2	Lead time constant in second-order filter for 2 nd maximum LPD signal, in seconds
τ_3	Lag time constant in second-order filter for 2 nd maximum LPD signal, in seconds
Setpoints	
$\begin{pmatrix} HLPD_{RT}^{0\ SPND} \\ HLPD_{RT}^{1\ SPND} \\ HLPD_{RT}^{2\ SPND} \\ HLPD_{RT}^{3\ SPND} \\ HLPD_{RT}^{4\ SPND} \\ HLPD_{RT}^{5+\ SPND} \end{pmatrix}$	High LPD LSSS reactor trip setpoints, in W/cm, as a function of the number of SPND failures
$\begin{pmatrix} HLPD_{PT}^{0\ SPND} \\ HLPD_{PT}^{1\ SPND} \\ HLPD_{PT}^{2\ SPND} \\ HLPD_{PT}^{3\ SPND} \\ HLPD_{PT}^{4\ SPND} \\ HLPD_{PT}^{5+\ SPND} \end{pmatrix}$	High LPD limitation partial trip setpoint, in W/cm, as a function of the number of SPND failures

Table 6-3 High LPD Channel LSSS Logic for Failed SPNDs

Number of Inoperable SPNDs	LPD Setpoint Adjustments
1	No adjustment
2	1 st modified value
3	2 nd modified value
4	3 rd modified value
5+	4 th modified value

7.0 LIMITING CONDITIONS FOR OPERATION ON LPD

To ensure that the SAFDL on fuel centerline melting is not violated for events in which the High LPD Channel LSSS cannot intercede, an LCO is established on peak LPD.

7.1 *Design Basis*

The LPD LCO functionally preserves the initial required LPD margin for the most limiting LPD LCO basis event is preserved during steady-state operation, including all applicable measurement errors, operating allowances, and calculation uncertainties.

The term “most limiting” in this context means the event characterized by the maximum LPD degradation.

Protective capability is accomplished by monitoring the maximum LPD in the bottom and top halves of the reactor core with the SPNDs, and comparing each to sets of graduated setpoints (LCO1 and LCO2). Depending upon which setpoint is violated, a series of graduated actions are taken to return the plant to an acceptable operating state.

The specific events against which the LPD LCO is designed to afford specific protection are summarized in Table 7-1. Typically the upper core half setpoints are established based upon LOCA considerations. Separate lower core half setpoints are used to provide flexibility in establishing LPD limits for events that characteristically challenge that part of the core (in contrast to LOCA).

7.2 *Functional Description*

The following subsections provide a functional description of the High LPD Channel LSSS. Figure 7-1 illustrates the online LPD LCO calculation.

7.2.1 *Process Variable Input*

The LPD LCO is based upon measurements by the SPND. [

]. This is functionally similar to the High LPD Channel LSSS, with the distinction that the SPND calibration matrix $C_{i,j}^{LPD}$ may differ from that used by the trip.

The methodology for establishing these calibration factors is discussed in Appendix B.

7.2.2 Plant Constant Inputs

The LPD LCO utilizes a number of constants stored in the plant computer. These are shown in Table 7-2.

7.2.3 Algorithm

The LPD LCO directly estimates power densities in the core using calibrated SPND readings. The readings are then compared against maximum allowable setpoint values, less an offset value. The particulars of the algorithm are as follows:

Acquisition and Conditioning of the Power Density Signals

The LPD LCO utilizes the currents from all available SPND. A conversion from current to power density (in W/cm) is accomplished via the use of a SPND calibration array for LPD ($C_{i,j}^{LPD}$):

$$P_{i,j}^{LPD} = C_{i,j}^{LPD} \cdot I_{i,j} \quad (7-1)$$

where:

$P_{i,j}^{LPD}$ ≡ Linear power density in W/cm, as determined by SPND i on detector string j .

$C_{i,j}^{LPD}$ ≡ Conversion array between detector current [] established at the time of SPND calibration.

$I_{i,j}$ ≡ Current indicated by the SPNDs

Appendix B describes the method for establishing $C_{i,j}^{LPD}$.

To preclude spurious actuation of the LPD LCO, the highest LPD measurements in the top and bottom halves of the core are discarded, and the next highest values retained:

$$P_{i,j}^{\max2\ lower} = \text{MAX2} \left(P_{i,j}^{LPD} \Big|_{\substack{i=1..12 \\ j=1..3}} \right) \quad (7-2)$$

$$P_{i,j}^{\max2\ upper} = \text{MAX2} \left(P_{i,j}^{LPD} \Big|_{\substack{i=1..12 \\ j=4..6}} \right) \quad (7-3)$$

where $P_{i,j}^{\max2\ lower}$ is the second maximum LPD in the lower core half, and $P_{i,j}^{\max2\ upper}$ is the second maximum LPD in the upper core half.

A first-order low pass filter is then used on both of the second maximum LPD signals, in order to remove high frequency signal noise:

$$PF_{i,j}^{\max2\ upper} = \left(\frac{1}{1 + \tau_{LPD\ LCO} S} \right) \cdot P_{i,j}^{\max2\ upper} \quad (7-4)$$

$$PF_{i,j}^{\max2\ lower} = \left(\frac{1}{1 + \tau_{LPD\ LCO} S} \right) \cdot P_{i,j}^{\max2\ lower} \quad (7-5)$$

where $PF_{i,j}^{\max2\ lower}$ and $PF_{i,j}^{\max2\ upper}$ are the filtered second-maximum signals in the lower and upper halves of the core (respectively), $\tau_{LPD\ LCO}$ is the time constant for the filter, and S is used to indicate a Laplace transform operator.

Comparison Against LCO1 and LCO2 Setpoints

The filtered second maximum LPDs from Equation (7-4) and (7-5) are then compared against the offset-corrected setpoints¹ for the upper and lower core halves. Any signals from designated inoperable SPNDs are omitted from the calculations, and the setpoint selected according to the total number of failed detectors. As will be discussed in Section 7.2.4, two thresholds are present, reflecting the graduated setpoints LCO1 and LCO2. Signals indicating an LCO setpoint violation are issued if the following relationships are detected:

$$\begin{aligned} (PF_{i,j}^{\max 2 \text{ lower}} - \text{HLPD_LLCO}) &\geq \text{HLPD_LLCO1}_{x \text{ SPND}} \Rightarrow \text{Lower LCO1 violation signal} \\ (PF_{i,j}^{\max 2 \text{ upper}} - \text{HLPD_ULCO}) &\geq \text{HLPD_ULCO1}_{x \text{ SPND}} \Rightarrow \text{Upper LCO1 violation signal} \end{aligned} \quad (7-6)$$

$$\begin{aligned} (PF_{i,j}^{\max 2 \text{ lower}} - \text{HLPD_LLCO}) &\geq \text{HLPD_LLCO2}_{x \text{ SPND}} \Rightarrow \text{Lower LCO2 violation signal} \\ (PF_{i,j}^{\max 2 \text{ upper}} - \text{HLPD_ULCO}) &\geq \text{HLPD_ULCO2}_{x \text{ SPND}} \Rightarrow \text{Upper LCO2 violation signal} \end{aligned} \quad (7-7)$$

Here the subscript “x SPND” refers to the particular setpoint applicable to ‘x’ number of failed SPNDs, and other terms were previously defined.

7.2.4 Setpoints

The LPD LCO has multiple setpoints designed to accommodate a limited number of inoperable SPNDs, as well as distinct setpoints for the upper and lower half of the core. Inoperable SPNDs are eliminated from the LPD calculation, and the setpoints are modified according to the same logic as the High LPD Channel LSSS (see Table 6-3).

¹ The reason the offsets are used is related to the use of the PCI limitation, which shares certain design requirements with the LPD LCO.

The LCO1 and LCO2 setpoints represent thresholds for a graduated series of actions. Violation of the LCO1 setpoints will result in RCSL issuing the following automatic signals:

- Control room alarm
- Block dilution signal (for lower core half LCO1 violation only)
- RCCA bank withdrawal blocking signal
- Generator power increase blocking signal
- Block lead control bank insertion (for lower core half LCO1 violation only)

Violation of the LCO2 setpoints will result in the additional actions:

- Reduce generator power signal
- Insert lead control bank (for upper core half LCO1 violation only)

7.2.5 Inhibition

The LPD LCO is inhibited below a low level of power (~10 percent RTP).

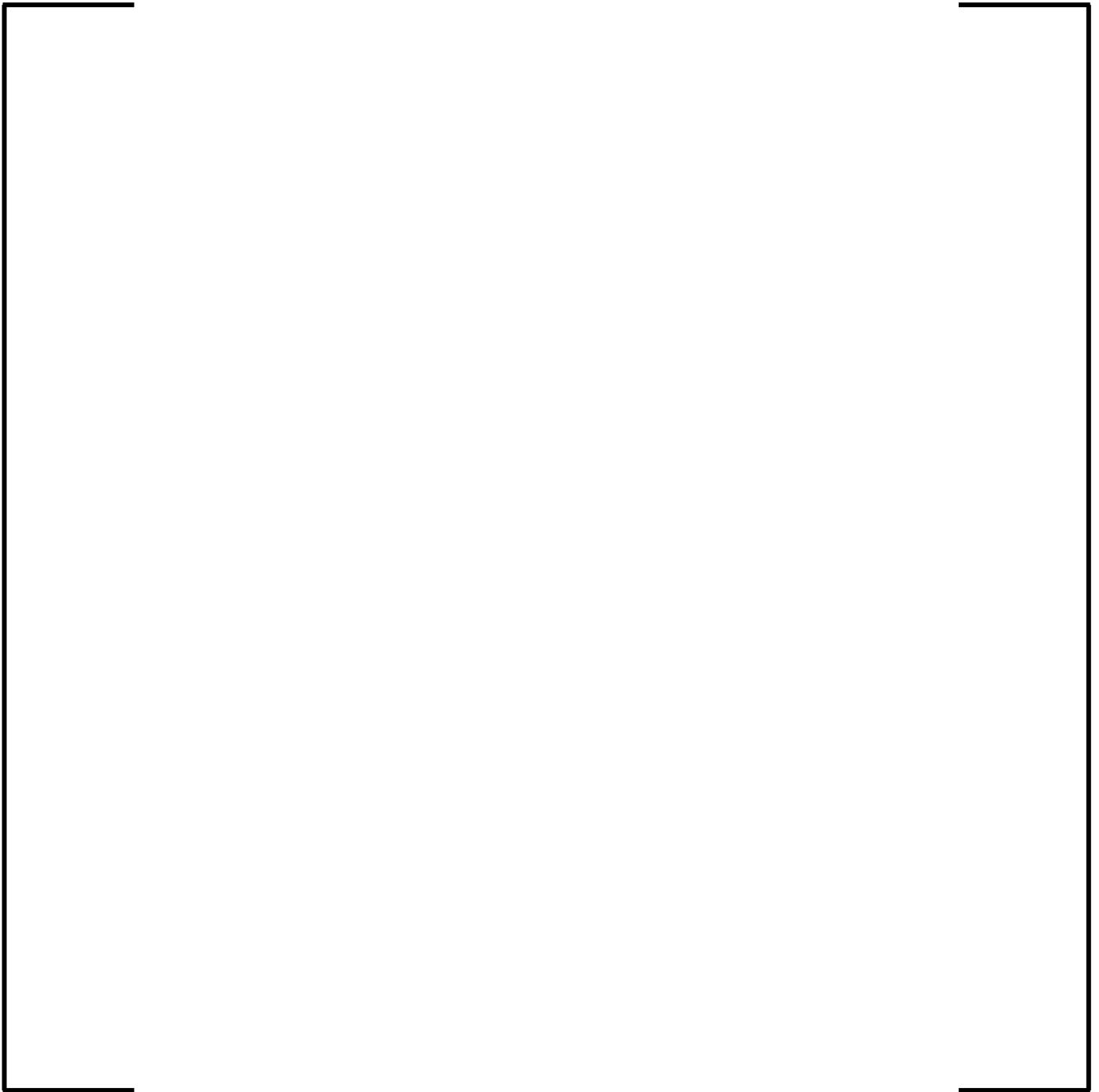


Figure 7-1 LPD LCO Functional Diagram

Table 7-1 Basis Events for the LPD LCO

Event	SRP Section	Comments
Spectrum of Rod Ejection Accidents	15.4.8	---
Excess Increase in Steam Flow (Excess Load Increase)	15.1.3	Fast end of event spectrum
Uncontrolled Control Rod Assembly Withdrawal from a Subcritical or Low Power Startup Condition	15.4.1	---
Uncontrolled Control Rod Assembly Withdrawal at Power	15.4.2	Fast end of event spectrum
Spectrum of Rod Ejection Accidents	15.4.8	---
Loss-of-Coolant Accidents Resulting From Spectrum of Postulated Piping Breaks Within the Reactor Coolant Pressure Boundary	15.6.5	---

Table 7-2 LPD LCO Constants

Constant	Description
Calibration Factors	
C_{ij}^{LPD}	SPND calibration array for LPD
Filter Time Constants	
$\tau_{LPD LCO}$	Lag time constant in second-order filter for 2 nd maximum LPD signal in top and bottom core halves, in seconds
Setpoints	
$\left(\begin{array}{l} HLPD_ULCO1_{0\ SPND} \\ HLPD_ULCO1_{1\ SPND} \\ HLPD_ULCO1_{2\ SPND} \\ HLPD_ULCO1_{3\ SPND} \\ HLPD_ULCO1_{4\ SPND} \\ HLPD_ULCO1_{5+\ SPND} \end{array} \right)$	LCO1 setpoints for the upper core half, in W/cm, as a function of the number of SPND failures
$\left(\begin{array}{l} HLPD_LLCO1_{0\ SPND} \\ HLPD_LLCO1_{1\ SPND} \\ HLPD_LLCO1_{2\ SPND} \\ HLPD_LLCO1_{3\ SPND} \\ HLPD_LLCO1_{4\ SPND} \\ HLPD_LLCO1_{5+\ SPND} \end{array} \right)$	LCO1 setpoints for the lower core half, in W/cm, as a function of the number of SPND failures
$\left(\begin{array}{l} HLPD_ULCO2_{0\ SPND} \\ HLPD_ULCO2_{1\ SPND} \\ HLPD_ULCO2_{2\ SPND} \\ HLPD_ULCO2_{3\ SPND} \\ HLPD_ULCO2_{4\ SPND} \\ HLPD_ULCO2_{5+\ SPND} \end{array} \right)$	LCO2 setpoints for the upper core half, in W/cm, as a function of the number of SPND failures

Constant	Description
$\left(\begin{array}{l} \text{HLPD_LLCO2}_{0\text{ SPND}} \\ \text{HLPD_LLCO2}_{1\text{ SPND}} \\ \text{HLPD_LLCO2}_{2\text{ SPND}} \\ \text{HLPD_LLCO2}_{3\text{ SPND}} \\ \text{HLPD_LLCO2}_{4\text{ SPND}} \\ \text{HLPD_LLCO2}_{5+\text{ SPND}} \end{array} \right)$	LCO2 setpoints for the lower core half, in W/cm, as a function of the number of SPND failures
HLPD_LLCO	Setpoint offset for the lower core half LCO setpoints, in W/cm
HLPD_ULCO	Setpoint offset for the upper core half LCO setpoints, in W/cm

8.0 STATIC LPD SETPOINT METHODOLOGY

The static methodology used to establish LPD setpoints is based upon a [] on calculated online LPD. In the case of the High LPD Channel LSSS, the LPD limit is the safety limit for fuel centerline melt or clad strain (whichever is more limiting). In the case of the LPD LCO, the limits are the LPD limits established for the upper and lower core halves.

8.1 Statement of Problem

The approach used for meeting this acceptance criterion for the U.S. EPR High LPD Channel LSSS and LPD LCO functions is to establish a setpoint equal to [] on the calculated online LPD. This tolerance limit is established based upon the following criterion:

[] *then the LPD setpoint is established such that a reactor trip would occur no less than 95 percent of the time, with 95 percent confidence, considering all relevant uncertainties.*

Mathematically, this can be expressed for the High LPD Channel LSSS as a conditional probability of the form:

$$[] \quad (8-1)$$

Where [] Since the reactor trip (RT) needs to be actuated by the High LPD Channel LSSS, we required that [] where [] and []

[] Therefore, Equation (8-1) can be rewritten as:

$$[] \quad (8-2)$$

where [

] In this expression, [

]. This process is illustrated in Figure

8-1.

The LPD LCO is offset, relative to the High LPD Channel LSSS, by either the transient $\Delta(\text{LPD})$ allowance, or (for the top half of the core) the difference between the LOCA limit and the transient LPD limit. Therefore, for the LPD LCO, Equation (8-2) becomes:

$$[\quad \quad \quad] \quad (8-3)$$

and

$$[\quad \quad \quad] \quad (8-4)$$

This process is illustrated in Figure 8-2.

8.2 *Uncertainties Impacting LPD Monitoring and Protection*

The following subsections describe the uncertainties used as inputs to the LPD setpoint calculation. Since the High LPD Channel LSSS and LPD LCO only rely on power, the set of applicable uncertainties is much reduced relative to that for the Low DNBR Channel LSSS and DNB LCO.

The discussion presented in Section 5.3 regarding absolute and relative errors also applies to the LPD-related setpoint calculations.

8.2.1 *SPND Measurement*

This uncertainty is identical to that discussed in Section 5.3.4.

8.2.2 *Power Calorimetric*

This uncertainty is identical to that discussed in Section 5.3.7.

8.2.3 *Transient SPND Decalibration*

This uncertainty is analogous to that discussed in Section 5.3.8, but pertains to the calibrated SPND signals for LPD, rather than DNBR. The uncertainty is addressed by

[

].

8.2.4 *Reconstructed Power Distribution (AMS)*

This uncertainty is analogous to that discussed in Section 5.3.9, but pertains to the ability to reconstruct the correct FQ values. It assumes the following form:

$$\begin{aligned} FQ_{\text{measured}} &= FQ_{\text{design}} \cdot \left(1 \pm \delta_{FQ}^{\text{AMS}} + B_{FQ}^{\text{AMS}} \right) \\ &= FQ_{\text{design}} \cdot \left(1 + \varepsilon_{FQ}^{\text{AMS}} \right) \end{aligned} \quad (8-5)$$

Appendix E describes the methodology used to reduce neutronics uncertainties.

8.2.5 *Thermal Hydraulic Conditions for SPND Data*

These uncertainties are analogous to those discussed in Section 5.3.10, and take the same form. However, the sensitivity coefficients are different, as they are based upon changes in $C_{i,j}^{\text{LPD}}$ rather than $C_{i,j}^{\text{DNBR}}$. They are derived in the same manner as the sensitivity coefficients for $C_{i,j}^{\text{DNBR}}$.

8.2.6 *SPND Calibration Frequency*

This uncertainty is analogous to that described in Section 5.3.11, and takes the same basic form. Since the uncertainty is tied to $C_{i,j}^{\text{LPD}}$ calibration rather than $C_{i,j}^{\text{DNBR}}$, however, the value will be different.

8.2.7 Pellet Manufacturing Deviations

Intrinsic variability of the pellet manufacturing process may result in an increase in peaking. The manufacturing tolerances are accounted by an uncertainty on the total peaking power factor:

$$\begin{aligned} FQ_{\text{actual}} &= FQ_{\text{design}} \cdot \left(1 \pm \delta_{FQ}^{\text{ENG}} + B_{FQ}^{\text{ENG}}\right) \\ &= FQ_{\text{design}} \cdot \left(1 + \varepsilon_{FQ}^{\text{ENG}}\right) \end{aligned} \quad (8-6)$$

where FQ_{actual} is the FQ present when manufacturing deviations result in a different peaking than the design value FQ_{design} , δ_{FQ}^{ENG} is the uncertainty in FQ due to manufacturing deviations (i.e., engineering FQ uncertainty), B_{FQ}^{ENG} is the non-random (bias) component of the uncertainty, and $\varepsilon_{\text{burnup}}$ is the random variable containing both uncertainty components.

8.2.8 Rod Bow

The rod bow effect on the planar LPD peak is assumed to take the following form:

$$\begin{aligned} FQ_{\text{actual}} &= FQ_{\text{design}} \cdot \left(1 \pm \delta_{FQ}^{\text{rod bow}} + B_{FQ}^{\text{rod bow}}\right) \\ &= FQ_{\text{design}} \cdot \left(1 + \varepsilon_{FQ}^{\text{rod bow}}\right) \end{aligned} \quad (8-7)$$

where FQ_{actual} is the FQ in the presence of an existing rod bow, $B_{FQ}^{\text{rod bow}}$ is the non-random component of the rod bow FQ uncertainty, and $\varepsilon_{FQ}^{\text{rod bow}}$ is the random variable containing both uncertainty components.

8.2.9 Assembly Bow

Assembly bow is an analogy to the rod bow phenomenon, except that it affects the assembly as a whole, rather than individual pins. The concern with assembly bow is that the increased moderation associated with the wider inter-assembly gap will increase the peaking, particularly of the peripheral pins.

The assembly bow penalties are assumed to take the following form:

$$\begin{aligned} FQ_{\text{actual}} &= FQ_{\text{design}} \cdot \left(1 \pm \delta_{FQ}^{\text{ass'y bow}} + B_{FQ}^{\text{ass'y bow}} \right) \\ &= FQ_{\text{design}} \cdot \left(1 + \varepsilon_{FQ}^{\text{ass'y bow}} \right) \end{aligned} \quad (8-8)$$

where $\delta_{FQ}^{\text{ass'y bow}}$ is the random component of the penalty due to assembly bow, $B_{FQ}^{\text{ass'y bow}}$ is the non-random component, and $\varepsilon_{FQ}^{\text{ass'y bow}}$ is the random variable containing both uncertainty components.

8.2.10 *Epistemic*

The epistemic uncertainty is designed to accommodate any epistemic uncertainties not already addressed via other uncertainties. It may also be used as a mechanism for incorporating operational margin in the statistical process.

When applied to LPD calculations, the epistemic uncertainty is applied to the LPD limit as:

$$\begin{aligned} LPD'_{\text{limit}} &= LPD_{\text{limit}} \cdot \left(1 \pm \delta_{\text{epistemic}}^{\text{LPD}} + B_{\text{epistemic}}^{\text{LPD}} \right) \\ &= LPD_{\text{limit}} \cdot \left(1 + \varepsilon_{\text{epistemic}}^{\text{LPD}} \right) \end{aligned} \quad (8-9)$$

where LPD'_{limit} is the LPD limit adjusted for epistemic uncertainties, $\delta_{\text{epistemic}}^{\text{LPD}}$ and $B_{\text{epistemic}}^{\text{LPD}}$ are the random and non-random components of the LPD epistemic uncertainty, and $\varepsilon_{\text{epistemic}}^{\text{LPD}}$ is the random variable encompassing both uncertainty components.

8.3 *Coverage Method for Establishing LPD Setpoints*

The same methods described in Section 5.4 also apply to the static analysis of the High LPD Channel LSSS and LPD LCO, under the same constraints with regards to whether setpoints are known or not.

The coverage and testing methodology basis is described in Appendix A. Figure 8-3 shows a process flowchart for the LPD coverage calculation that applies to both the High LPD Channel LSSS and the LPD LCO.

The following assumptions apply to the coverage method for establishing the LPD setpoints:

- []
-]
- The setpoints for the functions are unknown.

The coverage process has the following steps:

[]

This is based upon 95 percent probability and 95 percent confidence, and utilizes the relationships provided in Appendix A []

]

[]

[] At each combination of thermal-hydraulic conditions and power distribution, the following process is used:

- []

[]

[(see
Section 8.2) [

]

- []

[

]

- []

This process is described in more detail in Sections 8.3.1.

- []

This process is described in more detail in Section 8.3.2.

- []

[

]

[]

[

]

[]

[]

8.3.1 Calculation of Reference LPD

Analogous to the definition of the reference DNBR given in Section 5.4.2, the reference LPD is the LPD that arises when an [] is used in conjunction with systemic uncertainties unrelated to process measurement, such that the LPD []]. This is the [] that the High LPD Channel LSSS or LPD LCO function must defend against at a 95 percent probability, with 95 percent confidence.

The systemic uncertainty factors considered in this stage of the calculation are:

- Rod bow penalty on FQ, $\epsilon_{FQ}^{\text{rod bow}}$
- Assembly bow penalty on FQ, $\epsilon_{FQ}^{\text{ass'y bow}}$
- Sensitivity factors on SPND data due to T/H conditions, δ_{sens}
- SPND calibration frequency (also known as burnup decalibration), ϵ_{burnup}
- Engineering uncertainty on FQ, $\epsilon_{FQ}^{\text{ENG}}$
- Epistemic allowance in the LPD calculation, $\epsilon_{\text{epistemic}}^{\text{LPD}}$

These all act in a multiplicative manner due to the manner in which they are defined.

Thus, for a given SPND response $P_{i,j}^D$ (the SPND responses are calibrated for LPD, although the LPD superscript is suppressed for clarity), the reference LPD for the LSSS is:

[] (8-10)

[] The rod
bow FQ uncertainty, assembly bow FQ uncertainty, and engineering FQ factors are all removed from the MAX function because they affect all detectors uniformly. The SPND data sensitivity to thermal-hydraulic conditions and burnup decalibration uncertainties are []. The maximum value is used because it represents the value that the trip is protecting against, even though the High LPD LSSS utilizes the second maximum signal.

Per the definition of the problem, [

] Therefore, Equation (8-10) becomes:

[]

(8-11)

Similar expressions hold for the LPD LCO. The differences between the LPD LCO and the High LPD Channel LSSS reference LPDs are as follows:

- Separate expressions hold for the upper and lower core halves.

• [

]

• [

]

- The power distributions $P_{i,j}^D$ correspond to operational conditions, rather than transient conditions.
- The epistemic uncertainty associated with the LPD LCO may be different than that for the High LPD Channel LSSS.

Therefore, the equivalent expressions to Equation (8-11) for the LPD LCO are:

$$[\hspace{15em}] \tag{8-12}$$

and

¹ As noted in Section 5.3.4, different draws from a single cumulative distribution or density are used for each individual SPND. The burnup uncertainty is a single draw from a single cumulative distribution or density, and applied to each individual SPND.



(8-13)

8.3.2 Calculation of Sensed LPD

The sensed LPD is what the online system potentially perceives, considering non-systemic uncertainties. The applicable uncertainties to the sensing process are:

- Uncertainty in the SPND currents, $\epsilon_{i,j}^{SPND}$
- Uncertainty in the resolution of planar peak LPD by the AMS/incore monitoring system at calibration, ϵ_{FQ}^{AMS}
- Calorimetric uncertainty, ϵ_Q

The High LPD Channel and LPD LCO both select the second maximum LPD signal of the available SPND signals, the latter using the second maximum from the top half of the core for the upper LCO comparison, the former the second maximum from the lower half of the core. As noted earlier, the sampled uncertainties affect the SPNDs as a whole except for the SPND measurement uncertainty, where each detector is affected by a different uncertainty. Therefore, the sensed LPD for the LSSS is:

$$[\hspace{15em}] \tag{8-14}$$

where the[

]

The expressions for the LPD LCO are similar, and may be written as:

$$\left[\begin{array}{l} \text{ } \\ \text{ } \\ \text{ } \end{array} \right] \quad (8-15)$$

and

$$\left[\begin{array}{l} \text{ } \\ \text{ } \\ \text{ } \end{array} \right] \quad (8-16)$$

8.3.3 Treatment of Inoperable SPNDs

The [] of inoperable SPNDs in the LPD calculations is identical to that used in the DNBR calculations.

8.4 Methodology for Confirming Existing LPD Setpoints

As with the DNBR setpoints, confirming existing LPD setpoints can be accomplished by:

- []
- []

The latter method is the most practical approach for confirming existing setpoints, and []

Section 5.5 documented the application of the testing method for one or more trip functions (for LSSS testing analysis) or one or more LCO functions (for LCO testing

analysis). This method was generally described, and either applies to multiple LSSS functions (including the High LPD Channel LSSS) or LCO functions (including the LPD LCO).

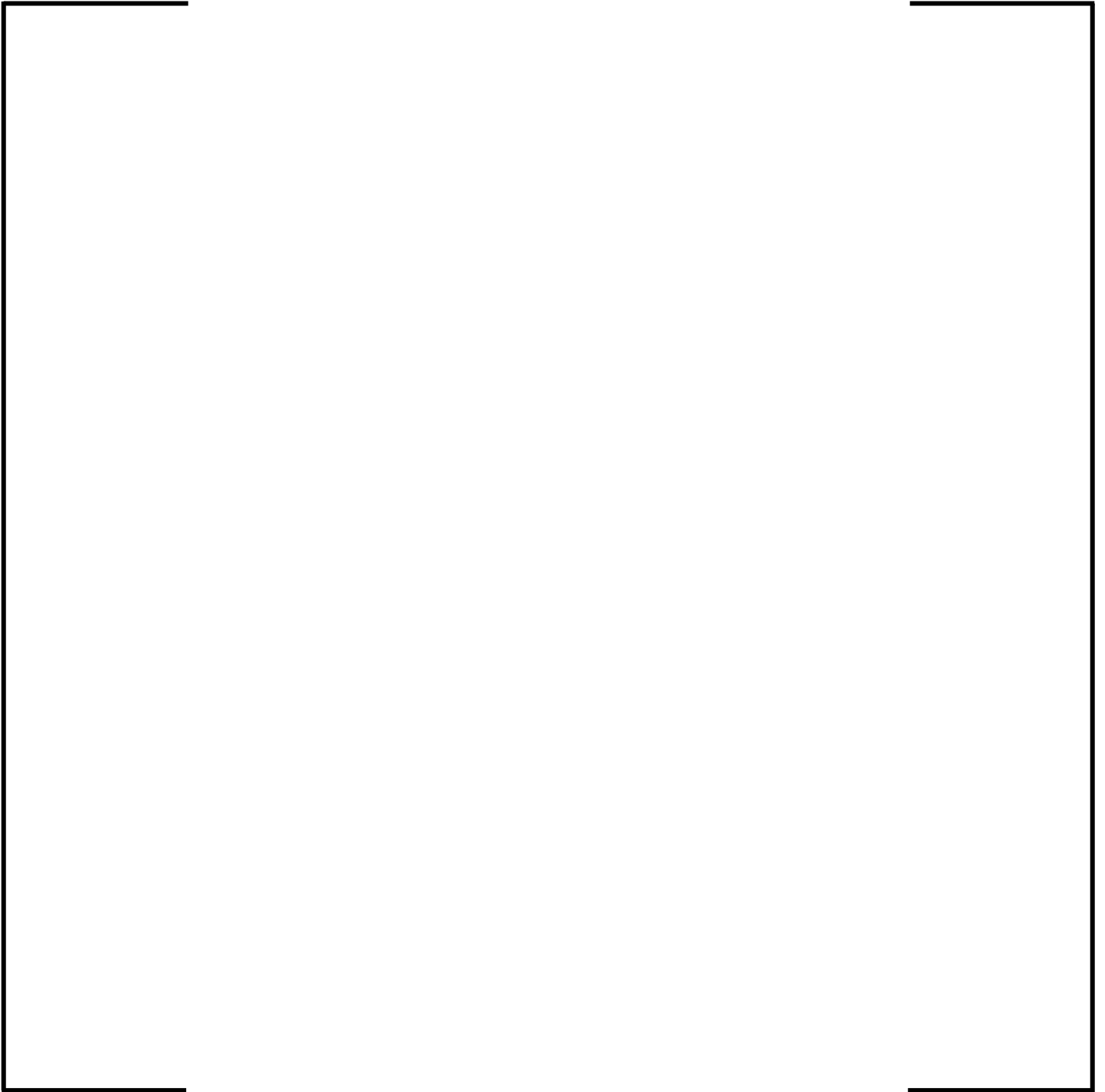


Figure 8-1 Establishing the LPD Trip Setpoint

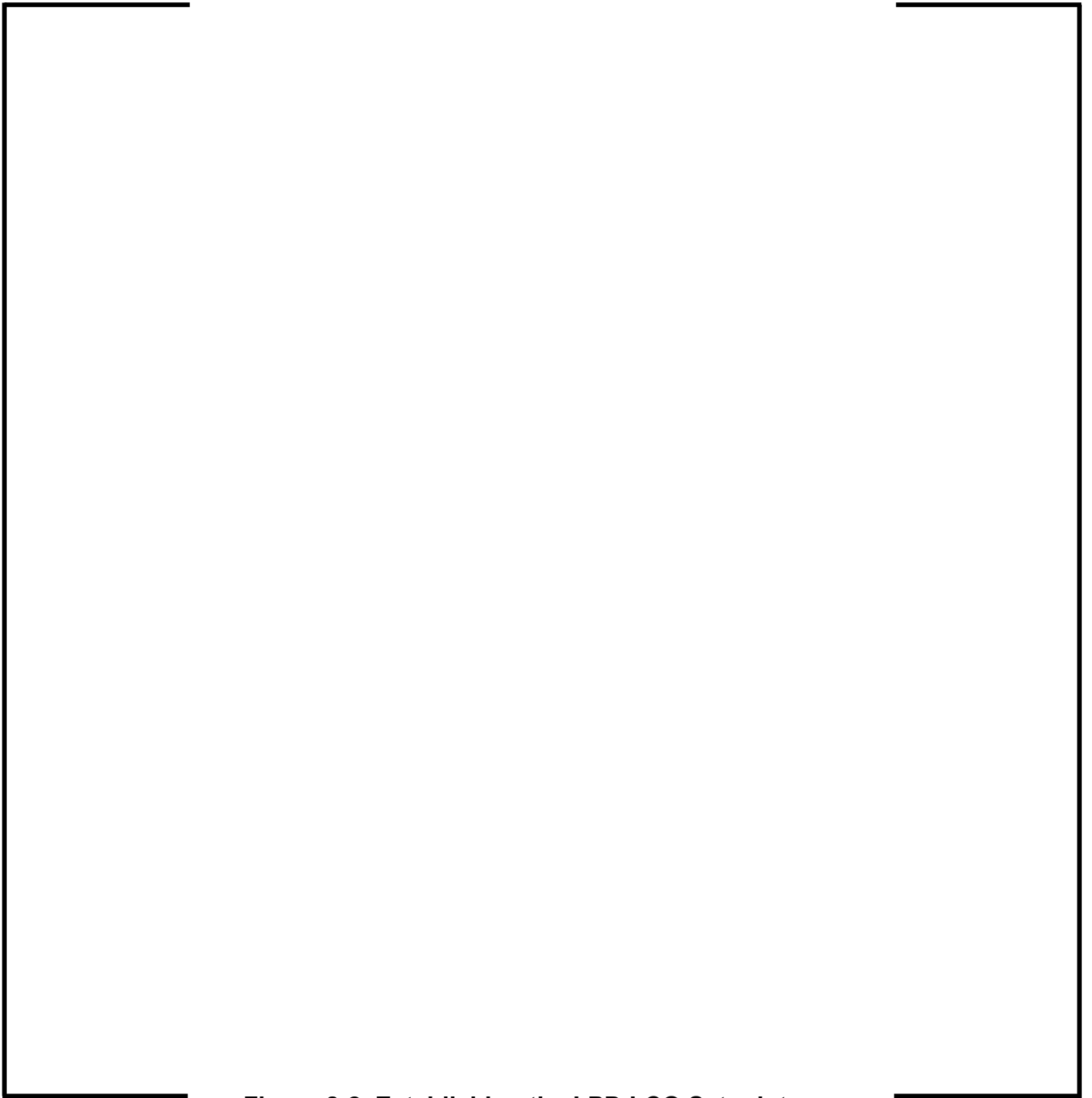


Figure 8-2 Establishing the LPD LCO Setpoint

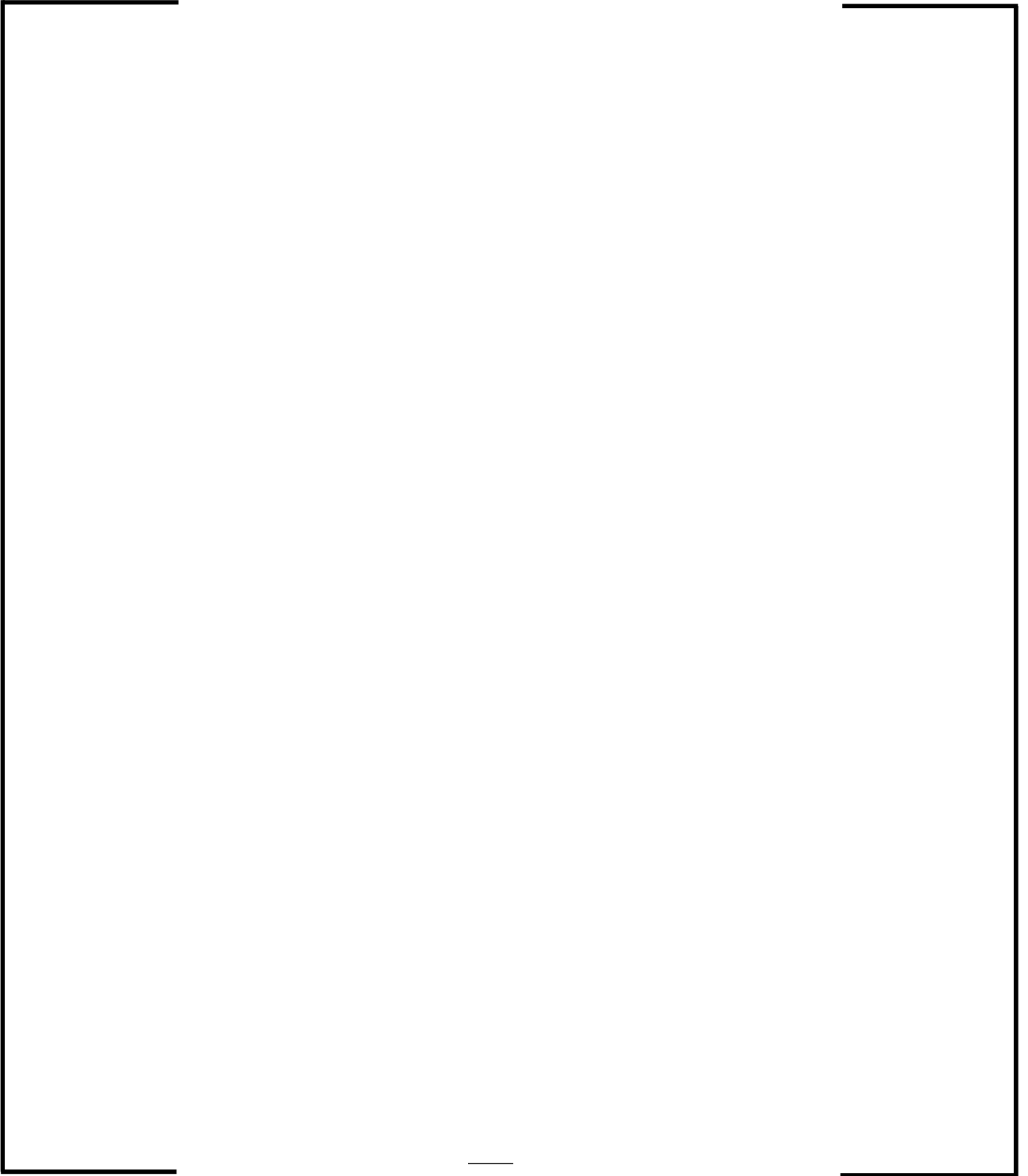


Figure 8-3 LPD Coverage Method for Establishing Setpoints

9.0 TRANSIENT ANALYSIS FOR INCORE TRIPS

The U.S. EPR plant design protects against the occurrence of DNB via a combination of the Low DNBR Channel trip, reservation of initial DNBR margin per the DNB LCO, and the ensemble of other system trips and LCOs. Analogously, it protects against the occurrence of LPD via a combination of the Low DNBR Channel trip, reservation of initial LPD margin per the LPD LCO, and the ensemble of other system trips and LCOs.

Up to this point in the methodological discussion, setpoints have been established for both the Low DNBR Channel trip (both on high exit quality and low DNBR), the DNB LCO, the High LPD Channel LSSS, and the LPD LCO. However, these are based upon evaluation of the static functions for “snapshot” power distributions/thermal-hydraulic conditions.

Once the static incore trip setpoints have been established to meet their design criterion of protecting the SAFDLs with 95% probability and 95% confidence, it is necessary to confirm that dynamic effects do not result in these setpoints being violated. This is accomplished in safety analysis calculations.

The Low DNBR and High LPD limitation function settings are also based upon transient analysis. They are established based upon (1) the timing of events approaching the Low DNBR Channel and High LPD Channel trip setpoints, and (2) operational considerations.

9.1 Overview

As stipulated previously, DNBR and LPD protection in the U.S. EPR can be split into two categories, (1) events and cases protected by either of the incore trips, and (2) events and cases protected by a combination of initial steady-state DNB or LPD margin, and/or a system trip. For a given case, the categories into which it falls has implications for the safety analysis process used to ensure that the SAFDL are protected.

For events in which the Low DNBR Channel or High LPD Channel trips intercede, it is necessary to demonstrate that the setpoint value is not violated by the underlying DNBR or HLPD in the event. As described earlier, the static setpoint methodology establishes thresholds for the online DNBR and LPD algorithms. If these thresholds are not violated, then there is a 95 percent probability with 95 percent confidence that the safety limit will not be violated, considering all uncertainties. Therefore, the purpose of the dynamic portion of the setpoint analysis is to demonstrate that these thresholds are not violated due to setpoint undershoot (for DNBR) or overshoot (for exit quality or LPD). The methodology for conducting overshoot and undershoot analysis will be documented in Section 9.4.

For events in which the Low DNBR Channel LSSS or High LPD Channel LSSS do not afford primary protection, protection is afforded by the DNB or LPD LCO functions prior to transient initiation, and by system trips at the end of the transient. System trips are generally designed to protect process parameters and variables other than DNBR or LPD (although they protect the SAFDLs indirectly). For this reason, it is necessary to demonstrate that the LCO functions reserve sufficient thermal margin so that when the system trip intercedes, the SAFDL is protected. The methodology for accomplishing this is discussed in Section 9.5.

Figure 9-2 shows the overall flow for the transient analysis as related to incore trip and LCO functions.

9.2 Initial Conditions Credited in the Transient Analysis

There are a number of limiting conditions for operation which define an acceptable initial operating envelope during normal operation. Several of these are credited when evaluating the transient response of the Low DNBR Channel or High LPD Channel trip, as follows:

DNB LCO

The DNB LCO restricts the sensed MDNBR during normal operation to a minimum allowable value. If the most adverse DNB LCO basis event is initiated from this minimum DNBR value, it will preclude DNB from being experienced during the event, at 95 percent probability, with 95 percent confidence. The plant cannot operate in violation of the DNB LCO without countermeasures being taken to return the plant to an acceptable operating state. Therefore, the DNB LCO is credited as an initial condition in the transient analysis.

[

]

LPD LCO

The LPD LCO serves to restrict the maximum allowable LPD in the upper and lower halves of the core during normal operation. This LPD is limited to a value consistent with the initial conditions from the LOCA analysis, or to a value that prevents (for AOO events) or mitigates (for postulated accident (PA) events) violations of the SAFDL on LPD.

If a given power distribution is characterized by a peak LPD value that exceeds the setpoint for either the bottom or top core halves, then the power distribution [

]. This is only done if the LPD LCO is more

limiting than the DNB LCO.

F Δ H LCO

The maximum allowable radial peaking value during normal operation is limited as a consequence of the LOCA analysis (and other potentially limiting safety analysis events). If a given power distribution is characterized by an F Δ H value that exceeds the deterministic limit at transient initiation, then the shape is not credible at transient initiation and is discarded.

APS LCO

The axial power shape LCO restricts the allowable axial offset during normal operation, as a function of power level. A representative example is shown in Figure 9-1. The APS LCO is credited by considering the APS LCO “barn” and the measurement uncertainties in the APS LCO. If the shift in axial offset is not being directly modeled (see the discussion in Section 9.3), then an additional allowance corresponding to the maximum anticipated axial offset shift experienced during the transient is also incorporated on the deterministic APS LCO barn.

If a given initial power distribution is characterized by an axial offset and power level that violates the APS LCO bounds described above, then the shape is not considered credible at transient initiation and is discarded.

Thermal Hydraulic Conditions

The thermal hydraulic core boundary conditions for Chapter 15 SRP events are generated in safety analysis calculations, using the Reference 4 or another approved transient methodology.

[

]

9.3 Treatment of Power Distributions

SPND responses are pre-generated using one or more “snapshot” values corresponding to off-normal core conditions. The same bounding set of power distributions generated for the purpose of the static setpoint methodology is also used in the transient analysis. The temporal evolution of these distributions can be accommodated by one of several means:

[]

[

] This approach is valid for transients which are not characterized by power redistribution during the transient.

[]

[

] This approach may be used for all classes of transient events regardless of whether they are characterized by power redistribution.

[]

[

]

9.4 Method for Performing Undershoot/Overshoot Assessments

The following signals associated with the Low DNBR Channel LSSS are dynamically compensated:

- RCP speed (first order filter)
- Narrow range cold leg temperature (second order filter)
- First and second maximum calculated exit quality (second order filter)
- First and second minimum calculated MDNBR (second order filter)

Analogously, the following signals associated with the High LPD Channel LSSS are also dynamically compensated:

- Second minimum LPD (second order filter)

These filters are designed both to reduce signal noise and compensate for coolant transport delays (in the case of the T_{cold} filter on the Low DNBR Channel) and accommodate finite algorithm evaluation times (for the calculated exit quality, MDNBR, and LPD). However, they have the effect of temporally perturbing the output signal given an input signal, and if the time constants on the filters are improperly tuned, may dynamically cause the statically established setpoints to be violated. For example, this may happen if the Low DNBR Channel trips the plant due to sensed DNBR, but does not do so in time to prevent the real DNBR from penetrating the SAFDL. If it does, then

either additional allowances must be incorporated into the trip setpoints, or modification of the time constants in the filters must occur.

[

].

For the Low DNBR Channel LSSS, the uncompensated trip model has the following differences relative to the compensated trip:

- The cold leg temperature input is the physical value from the core inlet, rather than the sensed value from the cold leg RTDs
- The pressure input is the physical value from the core exit, rather than the sensed value from the pressurizer steam dome
- The power input is the clad surface heat flux power, rather than the neutron power
- The flow input is the physical core inlet mass flux, rather than the core inlet mass flux inferred from the indicated RCP speed, reference RCP speed, and reference volumetric flow rate.
- All filters are removed from the trip.

For the High LPD Channel, the only difference between the compensated and uncompensated trip models is the removal of filters.

Based upon these the compensated and uncompensated trip models, the statement of the problem may be expressed as follows:

[

]

Figure 9-3 shows a diagram clarifying this process for the Low DNBR Channel LSSS (for a trip on DNBR). At point ①, the compensated Low DNBR Channel trip model reaches the DNBR setpoint. Once this point is reached, there will be delays due to trip signal processing ②, the time for the CRDM clutch coil magnetic field to decay ③, time for the dropping control rods to terminate the DNBR degradation ④, and the time to completion of scram (rod bottom) ⑤. At some point between ① and ⑤, the MDNBR will be experienced, at which time it will start to rise due to the effects of the scram. []

[] (as depicted in Figure 9-3), [

]

[

]

]

- []

- [

]

- [

]

9.5 *Method for $\Delta(DNBR)$ and $\Delta(LPD)$ Allowances*

Two methods may be used to either establish new $\Delta(DNBR)$ or $\Delta(LPD)$ allowances, or confirm existing values. These are discussed in subsequent subsections.

9.5.1 *Establishing New $\Delta(DNBR)$ and $\Delta(LPD)$ Allowances*

[

]

The analogous is true with the LPD LCO. [

]

[

Based upon the relative severity of the event, it may be possible to disposition one or more of the calculations as non-limiting.

Figure 9-5 illustrates the Δ (DNBR) evaluation process. The transient response indicated by ① is the MDNBR trace from the event. [

] (the latter is shown in Figure 9-5). The event is then evaluated past the point ②, where the system trip intercedes and terminates the DNBR degradation.

[

] The final Δ (DNBR) from this process

[

]. A similar process can be used for the LPD LCO, as well.

Typically the most limiting event in the DNB LCO design basis (with respect to delta-DNBR) is the loss of forced reactor coolant flow event (SRP 15.3.1 and 15.3.2). However, when establishing a safety analysis baseline for a plant, a systematic examination of all transient events not protected by the incore trips is made to ensure that a conservative delta-DNBR value is selected.

The specific calculation flow for analyzing delta-DNBR or delta-LPD allowances is as follows:

- []

- []

- [

]

[

]

- [

]

- [

]

- [

]

[

]

9.5.2 Confirming $\Delta(DNBR)$ and $\Delta(LPD)$ Allowances

If a DNB LCO or LPD LCO already exists, then confirmation can be done one of two ways. [

]

The confirmatory approach is similar to the process described in Section 9.5.1, and proceeds as follows (the DNB LCO is used as an example):

- []
- []
- []

]

[

]

- [

]

- [

]

- [

]

[

]

9.6 Method for Establishing Limitation Function Setpoints

These DNBR and LPD limitation functions are designed to avoid the actuation of a full reactor trip on DNBR or LPD. More specifically, they are designed to intercede and complete the partial trip process prior to the point where the setpoints for the Low DNBR Channel LSSS or High LPD Channel LSSS are reached.

The treatment of limitation function setpoints is associated with the dynamic analysis.

[

]

Consider the following example for the Low DNBR Channel trip. The criterion for the time at which a limitation function must intercede is:

$$[\quad] \quad (9-3)$$

where:

$t_{trip} \equiv$ Time at which the full trip setpoint is reached

$t_{limitation} \equiv$ Time at which the limitation setpoint is reached

$$[\quad] \equiv [\quad]$$

$$[\quad] \equiv [\quad]$$

$$[\quad] \equiv [\quad]$$

The value for the trip time is known from safety analysis cases, and [

]

Once a required intercession time is calculated based upon Equation (9-3), the DNBR or LPD limitation setpoint is then calculated as:

[

]

(9-4)

(9-5)

As the limitation functions are not required to protect every single case from reaching a full reactor trip, the approach described above can be tempered by operational considerations.

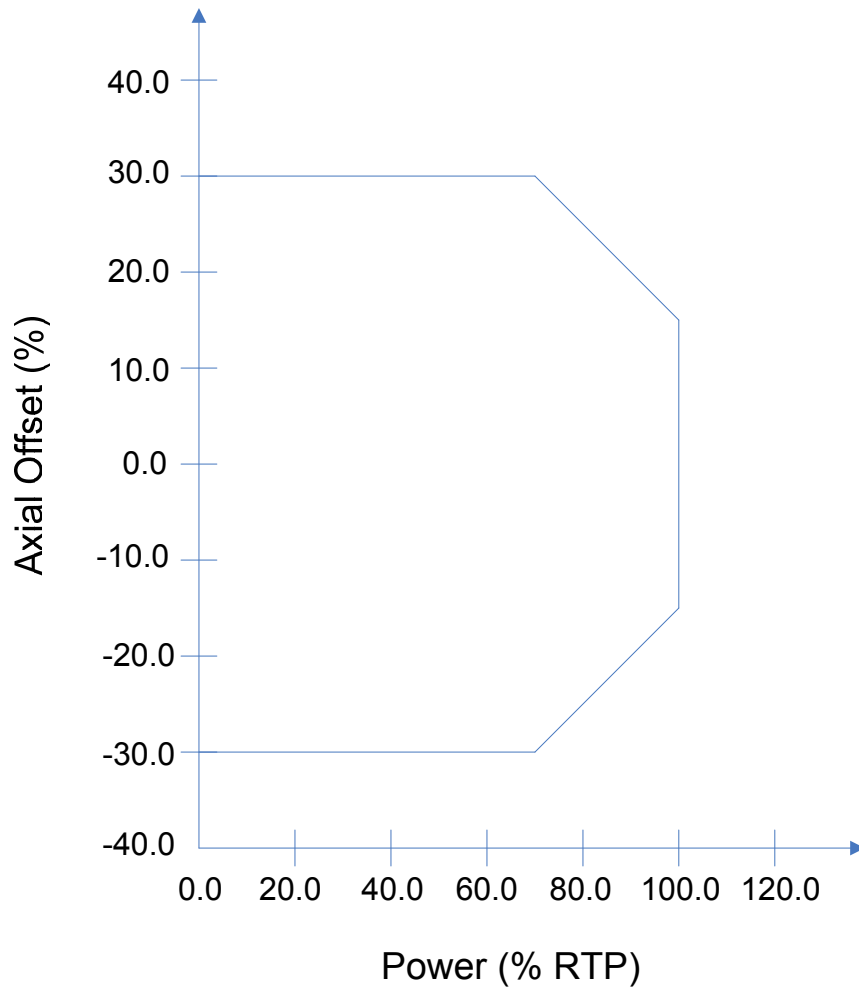


Figure 9-1 Example of APS LCO “Barn¹”

¹ This figure is for demonstration purposes only. The actual LCO settings will be determined as a consequence of design calculations.

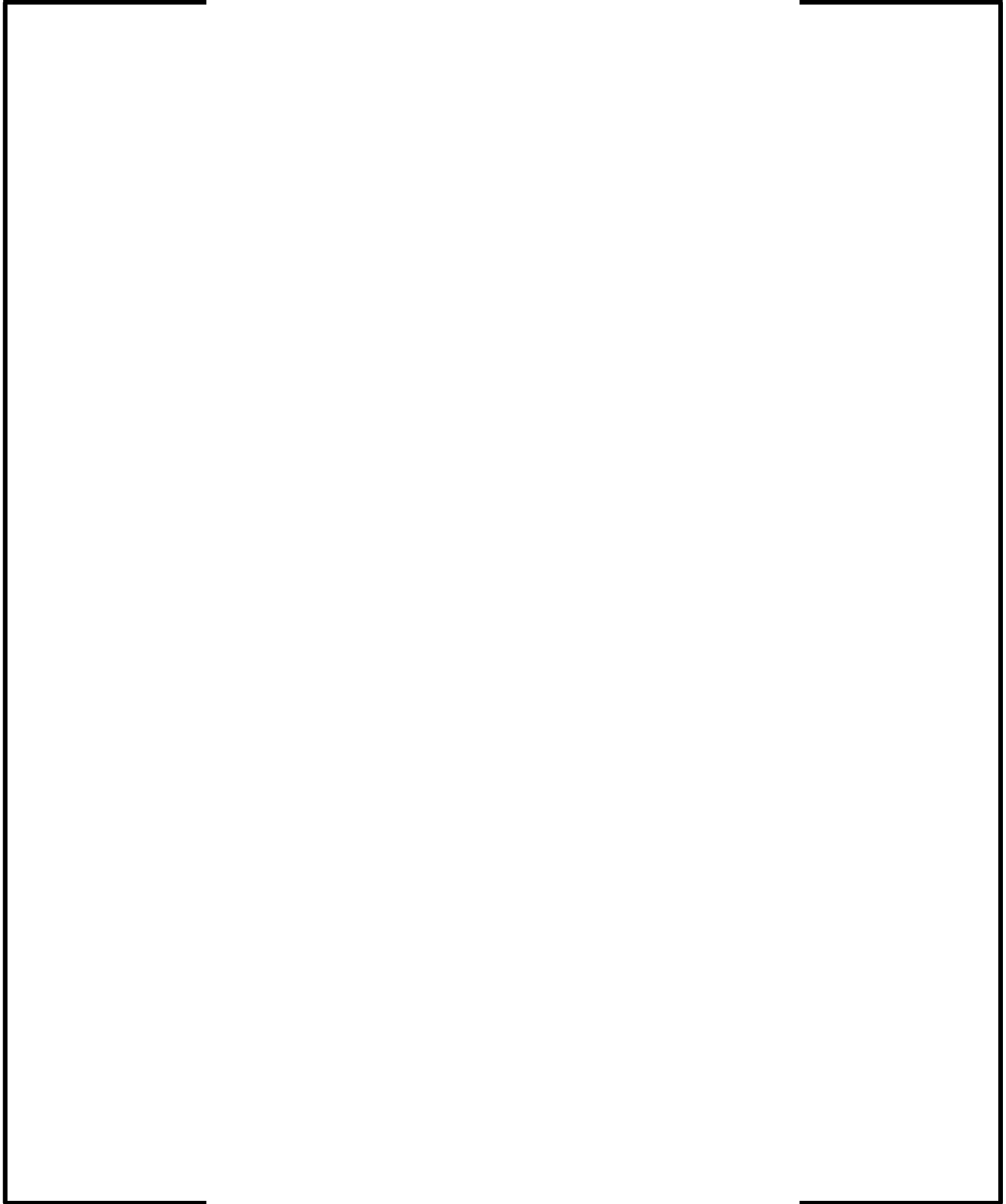


Figure 9-2 Transient Analysis Process Flow

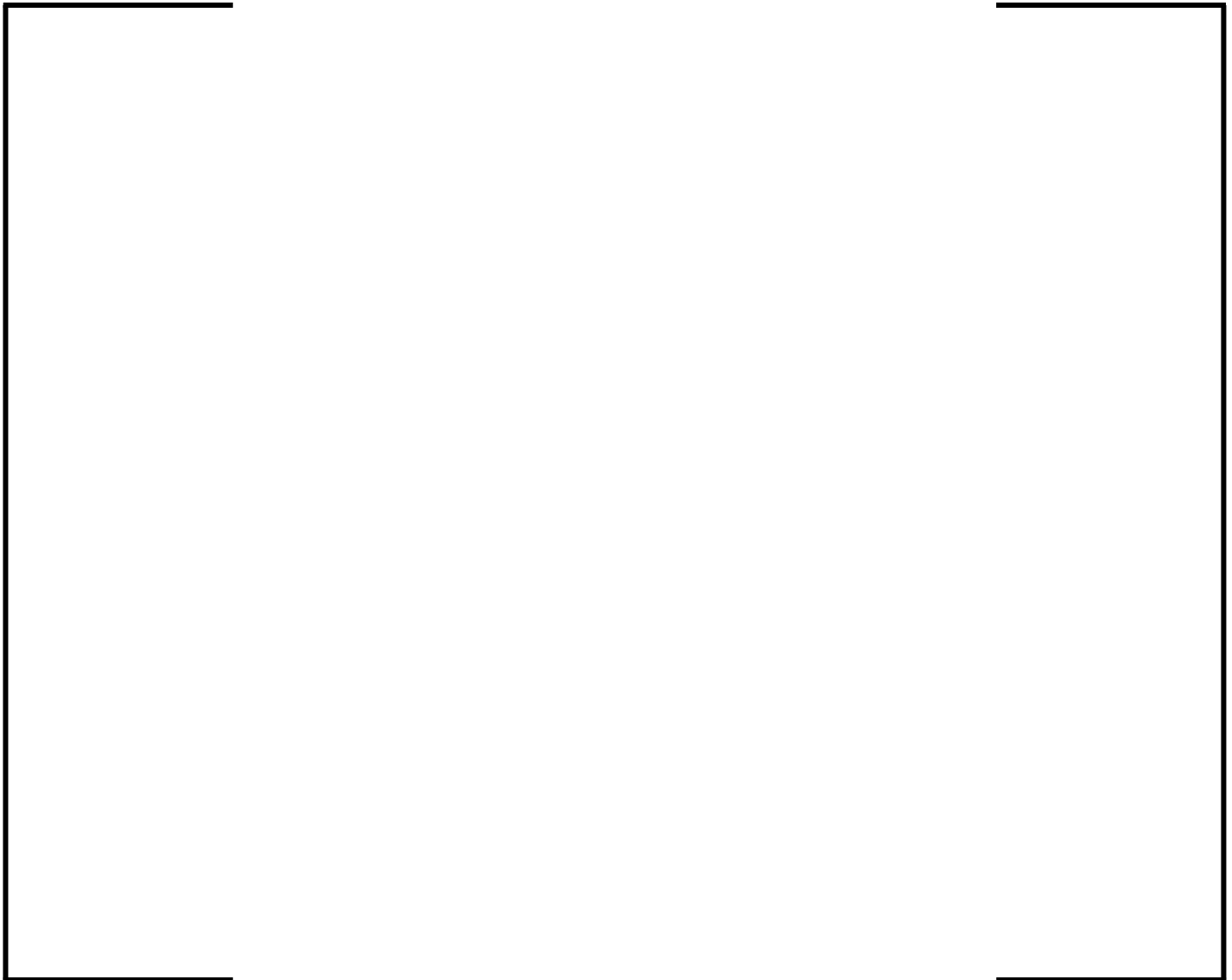


Figure 9-3 DNBR Undershoot Assessment

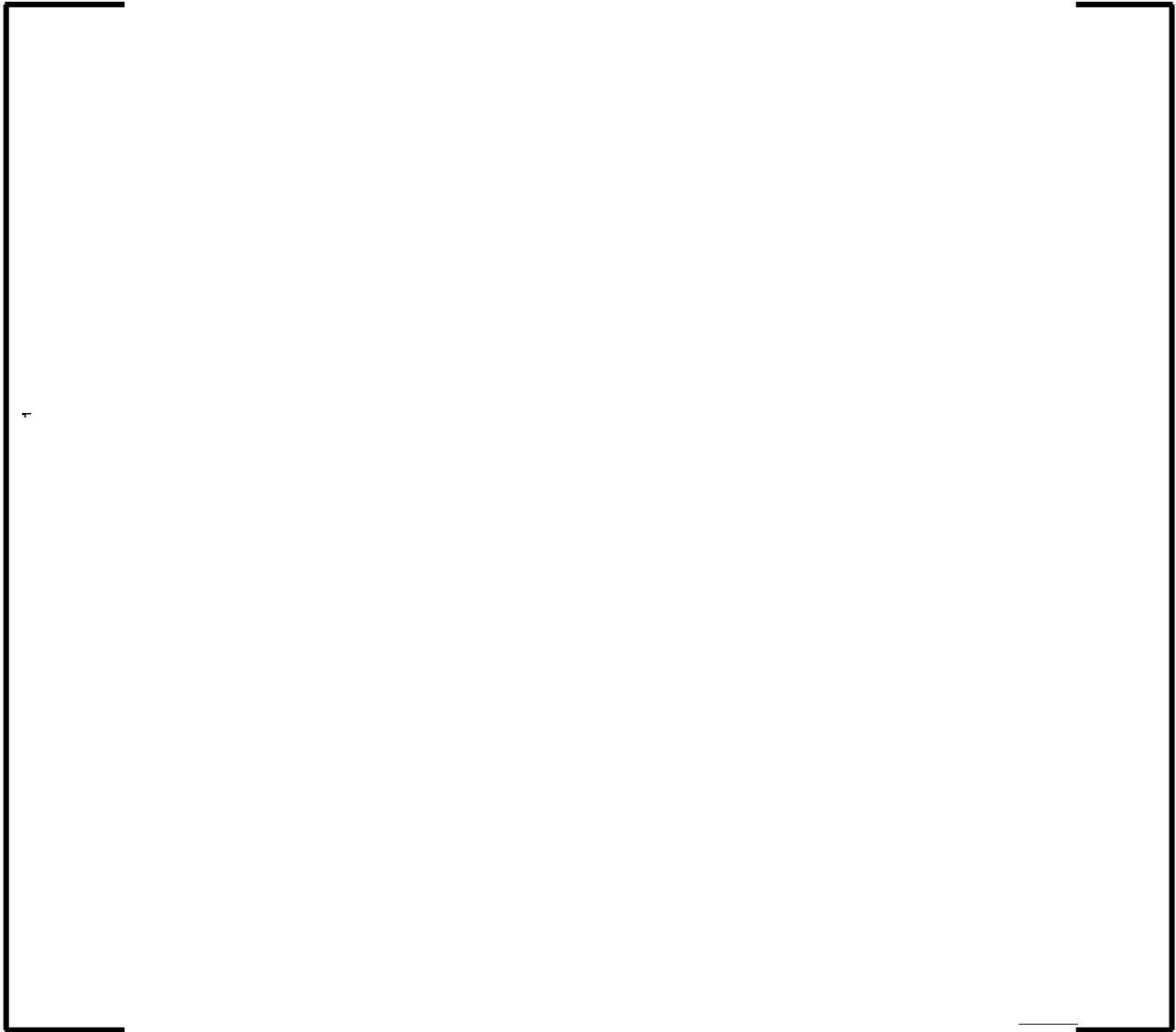


Figure 9-4 LPD Overshoot Assessment

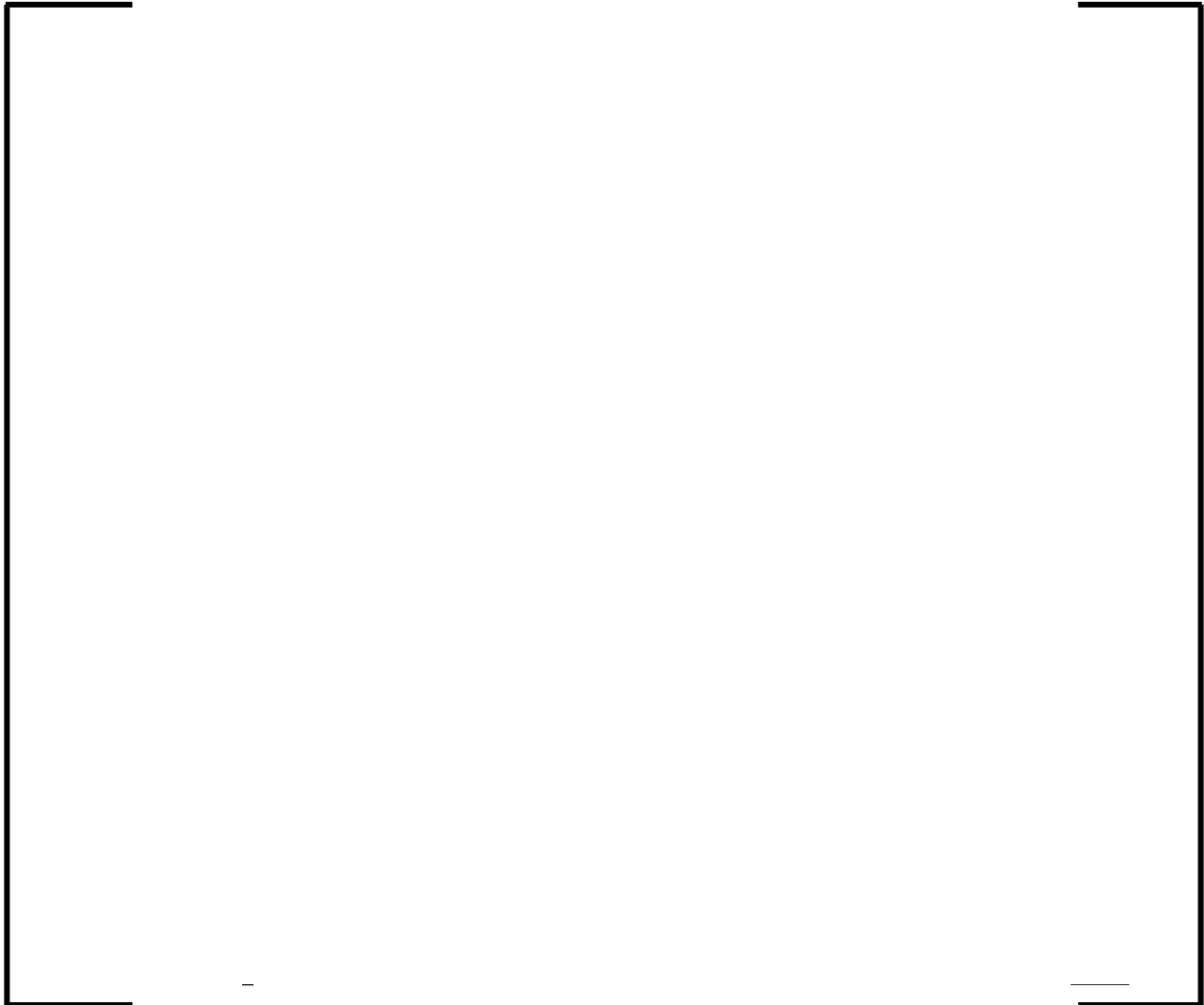


Figure 9-5 Method for Establishing New Δ (DNBR) Allowances

10.0 SAMPLE CALCULATIONS

10.1 *Static Setpoint Sample Calculation – LSSS Functions*

The following sample calculations exercise the coverage method for establishing new setpoints. Separate calculations are conducted for the following setpoints:

- Low DNBR Channel LSSS (DNBR_{RT} setpoints)
- Low DNBR Channel LSSS ($\text{DNBR}_{\text{IMB/RD}}$ setpoints)
- Low DNBR Channel LSSS (DNBR_{RD} setpoints)
- Low DNBR Channel LSSS (χ_{RT} for 2nd maximum exit quality)
- Low DNBR Channel LSSS ($\chi_{\text{IMB/RD}}$ for 1st maximum exit quality)
- High LPD Channel LSSS

10.1.1 *Trip Configuration Inputs*

The Low DNBR Channel LSSS configuration inputs (plant constants) are shown in Table 10-1. To expedite the calculation, only the setpoints corresponding to zero and five SPND (or SPND string) failures were considered.

An LPD limit of [] was used as a basis for the High LPD Channel LSSS calculation.

The exit quality limit used as a basis for the χ_{RT} trip setpoint calculations was []

The SPND imbalance thresholds are shown in Table 10-2

10.1.2 *Uncertainty Inputs*

The uncertainty inputs used as a basis for the sample calculation is shown in Table 10-3. The cumulative distribution functions for the online algorithm uncertainties for

DNBR and exit quality are shown in Figure 10-1 and Figure 10-2, respectively. [

].

10.1.3 *Power Distribution Inputs*

Several thousand power distributions were considered, based upon a Cycle 1, 18-month core design for the U.S. EPR, encompassing the following core conditions:

- Variations of power level, axial offset, control rod insertion, taken at several points in the cycle and at various stages of a xenon oscillation.
- Dropped control rods and banks
- Bank withdrawals at power
- Undetected control rod misalignments
- Single rod withdrawals
- Asymmetric cooldown and heatup conditions

Each power distribution has both a sensed (based on SPND outputs generated using periodically determined calibration coefficients) and [

] Dropped bank events will cause a rod drop indication in multiple PS divisions, and as such the dropped bank power distributions were utilized in the $DNBR_{RD}$ setpoint assessment, as well as the exit quality trip (1st maximum value), and the High LPD Channel LSSS calculation. [

]

The same approach is used for the exit quality trip with regards to power distributions other than the dropped bank.

10.1.4 Thermal Hydraulic Statepoint Inputs

The RT calculations must cover the entire range of operating space (P, T, and Ω) that can be reached in transient events protected by the incore trip functions. The pressure range is dictated by the reactor trip setpoints for the pressurizer pressure. Temperature ranges are defined by the highest and lowest transient temperatures from the overcooling and overheating events. The thermal design flow is used in this calculation (i.e., a deterministic treatment of the flow uncertainties).

Statepoints used in the determination of the RT setpoints are shown in Table 10-5, based upon the bounds from Table 10-4.

10.1.5 Sample Calculation Results

[

]

Table 10-8 summarizes the results for the various LSSS setpoint calculations via the coverage method. These results indicate that a very rapid trip will occur once a dropped bank is detected, or an excessive imbalance.

It should be kept in mind that the coverage approach is very conservative because it establishes a 95/95 probability/confidence [

] These limits could be [

]

10.2 Static Setpoint Sample Calculation – LCO Functions

The following sample calculations exercise the coverage method for establishing new setpoints. Separate calculations are conducted for the following setpoints:

- DNB LCO
- LPD LCO (upper core half)
- LPD LCO (lower core half)

10.2.1 LCO Configuration Inputs

The DNB and LPD LCO configuration inputs (plant constants) are shown in Table 10-1. Only the setpoints corresponding to zero and five SPND (or SPND string) failures were considered.

Both the lower and upper core half LPD limits were set to a representative LOCA LPD limit of [] The DNB LCO was assumed to have a transient Δ (DNBR) allowance of [] incorporated in the setpoint.

10.2.2 Uncertainty Inputs

The same inputs provided in Table 10-3 for the LSSS sample problem were also used for the LCO sample problem. The main difference is that several of the signal uncertainties (i.e., pressure, temperature, flow) are reduced to reflect the averaging of the four loop signals prior to use by the online algorithm.

10.2.3 Power Distribution Inputs

The LPD and DNB LCO functions are designed to function within an operational envelope. For the purposes of restricting power distributions, APS LCO limits of $\pm 20\%$ were imposed upon the superset of power distributions. Additionally, all the power distributions in Section 10.1.3 based upon transient events were discarded, and only the distributions based upon normal power, AO, control rod insertion, burnup, and xenon swings were retained.

10.2.4 Thermal Hydraulic Statepoint Inputs

A reduced set of thermal-hydraulic conditions were used for the LCO calculation, reflecting normal operating conditions. These are provided in Table 10-7, and are based upon the parameter range bounds in Table 10-6.

10.2.5 Sample Calculation Results

[

]The results are shown in Table 10-9.

10.3 Transient DNBR Undershoot Evaluation

The following sample case corresponds to the following Bank Withdrawal at Power (SRP 15.4.2) for a 4.47 pcm/second reactivity insertion rate, with BOC reactivity coefficients, initiated from hot full power conditions. A DNB LCO setting of 2.50 and $DNBR_{RT}$ were imposed upon this calculation. The system response was evaluated using the Reference 4 methodology.

Figure 10-3 shows the comparative DNBR response for the event. The response for the design subchannel analysis code reflects the event when only the system trips were modeled (i.e., the incore trips were not included). The event reaches the excore flux

rate of change trip at 25.1 seconds, and results in minimum DNBR value of 1.98 at 27.4 seconds. The other two responses are those for the uncompensated and compensated Low DNBR Channel models (for DNBR). The compensated Low DNBR Channel response is quite conservative relative to the DNBR trace from the subchannel analysis code, reflecting filter settings that are quite aggressive relative to those needed for this particular case. The uncompensated Low DNBR Channel response much more closely follows the true DNBR as determined via the subchannel analysis code, but demonstrates that it would not be sufficient to afford protection without compensation.

The compensated Low DNBR Channel model reaches the Low DNBR Channel setpoint (MDNBR = 1.761) at 16.3 seconds. The uncompensated MDNBR then continues to fall until it reaches a MDNBR of 2.196 at 17.7 seconds.

This sample case demonstrates the benefits of monitoring directly upon the DNBR variable. In a Bank Withdrawal at Power analysis for a typical PWR, the case would be evaluated with the power distribution that gives the worst initial DNBR. This would likely be much lower than the DNB LCO value of 2.50 used in this analysis.

10.4 *Transient Δ (DNBR) Evaluation*

For the purposes of demonstrating the methods for establishing a Δ (DNBR) value for a potentially limiting event, a Complete Loss of Forced Reactor Coolant Flow event was evaluated. The system response was evaluated using Reference 4 methodology.

Figure 10-4 shows an example of the process for establishing a Δ (DNBR) for a potentially limiting case. The DNB LCO setpoint assumed in this case was 2.50. Because the DNB LCO is monitored using the compensated DNBR model, and uncompensated model uses different pressure measurement locations, the uncompensated model will predict a slightly higher initial DNBR value than the DNB LCO. Therefore, the uncompensated DNBR at transient initiation is approximately 2.65.

The overall DNBR response from the uncompensated online DNBR model produces a Δ (DNBR) of 0.635, when initiated from the DNB LCO. When the DNBR iteration

process is used to drive the MDNBR in the transient down to the DNB design limit, the $\Delta(\text{DNBR})$ remains essentially the same, 0.636. Since the online DNBR model is only an approximation, and this particular case was quite limiting overall with respect to $\Delta(\text{DNBR})$, it was rerun, using the same power distributions and thermal-hydraulic conditions, in the design subchannel analysis code. The resultant $\Delta(\text{DNBR})$ from this case was not as conservative as the online DNBR model, with a value of 0.568.

Table 10-1 Input Data for the Static Sample Problem

Parameter	Input Value		
Core flow area (cm ²)	59133.43		
Nominal volumetric flow rate (m ³ /hr)	108740.00		
Guide thimble OD (cm)	1.245		
Flow rate adjustment factor	0.945		
Fuel cell flow area (cm)	0.878778		
Heated perimeter (cm)	2.984513		
Enthalpy rise bias factors	-1.00	0.989832	
	-0.28	0.989832	
	-0.20	0.989871	
	-0.10	0.993044	
	-0.04	0.998359	
	-0.02	1.002842	
	0.00	1.008825	
	0.02	1.016287	
	0.04	1.025063	
	0.06	1.034774	
	0.20	1.104010	
0.32	1.129363		
1.00	1.129363		
Mass velocity bias factors	-1.00	0.94520	0.98677
	-0.28	0.94520	0.98677
	-0.16	0.94524	0.99768
	-0.12	0.94686	1.01112
	-0.10	0.95041	1.02260
	-0.08	0.95731	1.03678
	-0.06	0.96790	1.05319
	-0.04	0.98298	1.07077
	0.00	1.03017	1.10780
	0.04	1.09220	1.14477
	0.06	1.12284	1.16000
	0.10	1.16847	1.18534
	0.12	1.18252	1.20058
	0.14	1.19093	1.21462
	0.18	1.19839	1.22900
0.22	1.19965	1.23995	
0.26	1.19965	1.25000	
1.00	1.19965	1.25000	

Table 10-2 SPND Imbalance Thresholds for Sample Problem

A large, empty rectangular frame with a thin black border, centered on the page. It appears to be a placeholder for a table that is not present in the document.

Table 10-3 Input Uncertainties for the Sample Problem

Uncertainty	Type	Mean	Standard Deviation (σ)	Comments
PZR pressure	normal	0.00	2.35 bar	RT calculations
	normal	0.00	0.80 bar	LCO calculations
NR CL Temp	normal	0.00	1.30 °C	RT calculations
	normal	0.00	1.02 °C	LCO calculations
RCP speed	normal	0.0%	1.0%	
CHF correlation	inverse normal	[]	[]	[]
SPND I&C	normal	0%	0.6079%	
Thermal power	normal	0%	0.2918%	
$F_{\Delta H}$	normal	0%	2.4924%	
F_Q	normal	0.26%	2.9500%	
AO	normal	0%	0.0000%	
Cij sensitivity to power (DNBR)	normal	-0.0004736	0.00044	
Cij sensitivity to pressure (DNBR)	normal	0.0000456	0.0000782	
Cij sensitivity to temperature (DNBR)	normal	-0.0015176	0.0015913	
Cij sensitivity to flow (DNBR)	normal	0.0008358	0.0002666	
Cij sensitivity to power (LPD)	normal	-0.0001409	0.0003730	
Cij sensitivity to pressure (LPD)	normal	-0.0000157	0.0000755	
Cij sensitivity to temperature (LPD)	normal	-0.0007236	0.0017098	
Cij sensitivity to flow (LPD)	normal	0.0000855	0.0006380	
Burnup decalibration (DNBR)	normal	0.0008	0.0077	
Burnup decalibration (LPD)	normal	-0.0021	2.1500%	
F_Q^E	normal	0%	1.5198%	
$F_{\Delta H}^E$	normal	0%	1.8237%	
Epistemic	normal	0%	0.0000%	
Rod bow penalty on $F_{\Delta H}$	uniform	0%	0.0000%	min/max
Assembly bow penalty on $F_{\Delta H}$	uniform	0%	5.0000%	min/max
Rod bow penalty on F_Q	uniform	0%	3.0000%	min/max

Table 10-3 (continued) Input Uncertainties for the Sample Problem

Uncertainty	Type	Mean	Standard Deviation (σ)	Comments
Assembly bow penalty on F_Q	uniform	0%	6.0490%	min/max
DNBR algorithm	[]	Figure 1	Figure 1	[]
Quality algorithm	[]	Figure 2	Figure 2	
RCS flow	bias	2.3%	none	

Table 10-4 Parameter Ranges for LSSS Setpoint Sample Calculation

Parameter	Value
High PZR pressure trip setpoint	2415 psia
Nominal PZR pressure	2250 psia
Low PZR pressure trip setpoint	2005 psia
Upper CL temperature	590°F
Nominal CL temperature	563.68°F
Lower CL temperature	530°F
Upper RCP speed	105%
Nominal RCP speed	100%
Lower RCP speed	95%

Table 10-5 T/H Setpoint Statepoints for LSSS Sample Calculation

PZR Pressure (bar)	CL Temperature (°C)	RCP Speed
155	295	100%
167	295	100%
138	295	100%
155	310	100%
155	277	100%
138	310	100%
167	310	100%
167	277	100%
138	277	100%
155	295	105%
167	295	105%
138	295	105%
155	310	105%
155	277	105%
138	310	105%
167	310	105%
167	277	105%
138	277	105%
155	295	95%
167	295	95%
138	295	95%
155	310	95%
155	277	95%
138	310	95%
167	310	95%
167	277	95%
138	277	95%

Table 10-6 Parameter Ranges for LCO Setpoint Sample Calculation

Parameter	Value
PZR pressure control band	±36 psi
Tavg control band and EOC coastdown allowance	+ 2°F / -12°F

Table 10-7 T/H Setpoint Statepoints for LCO Sample Calculation

PZR Pressure (bar)	CL Temperature (°C)	RCP Speed
155	295	100%
151	295	100%
159	295	100%
155	288	100%
151	288	100%
159	288	100%
155	297	100%
151	297	100%
159	297	100%

Table 10-8 Results from Sample LSSS Coverage Calculation

--

Table 10-9 Results from Sample LCO Coverage Calculation

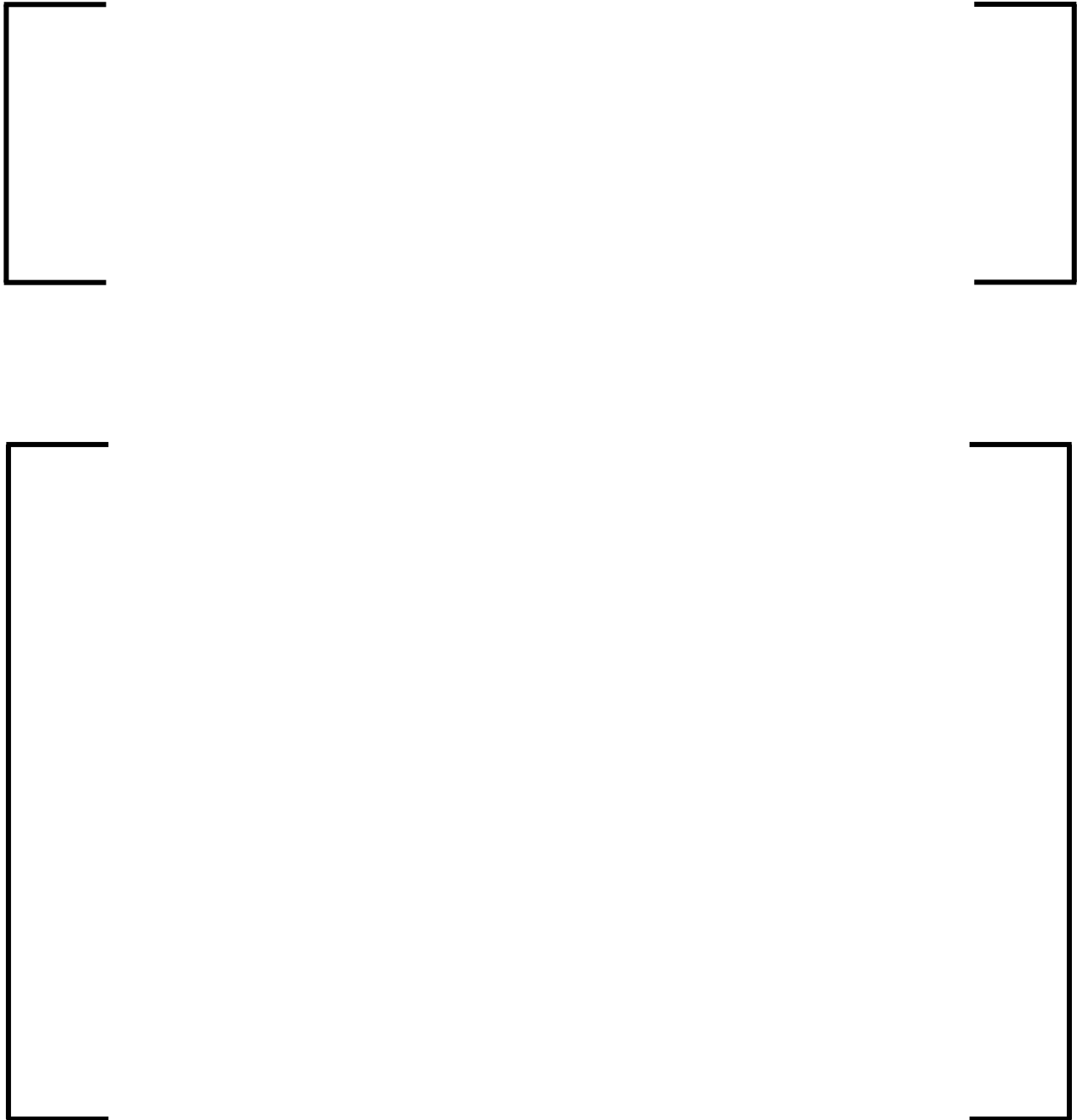


Figure 10-1 DNBR Algorithm Uncertainty



Figure 10-2 Exit Quality Algorithm Uncertainty

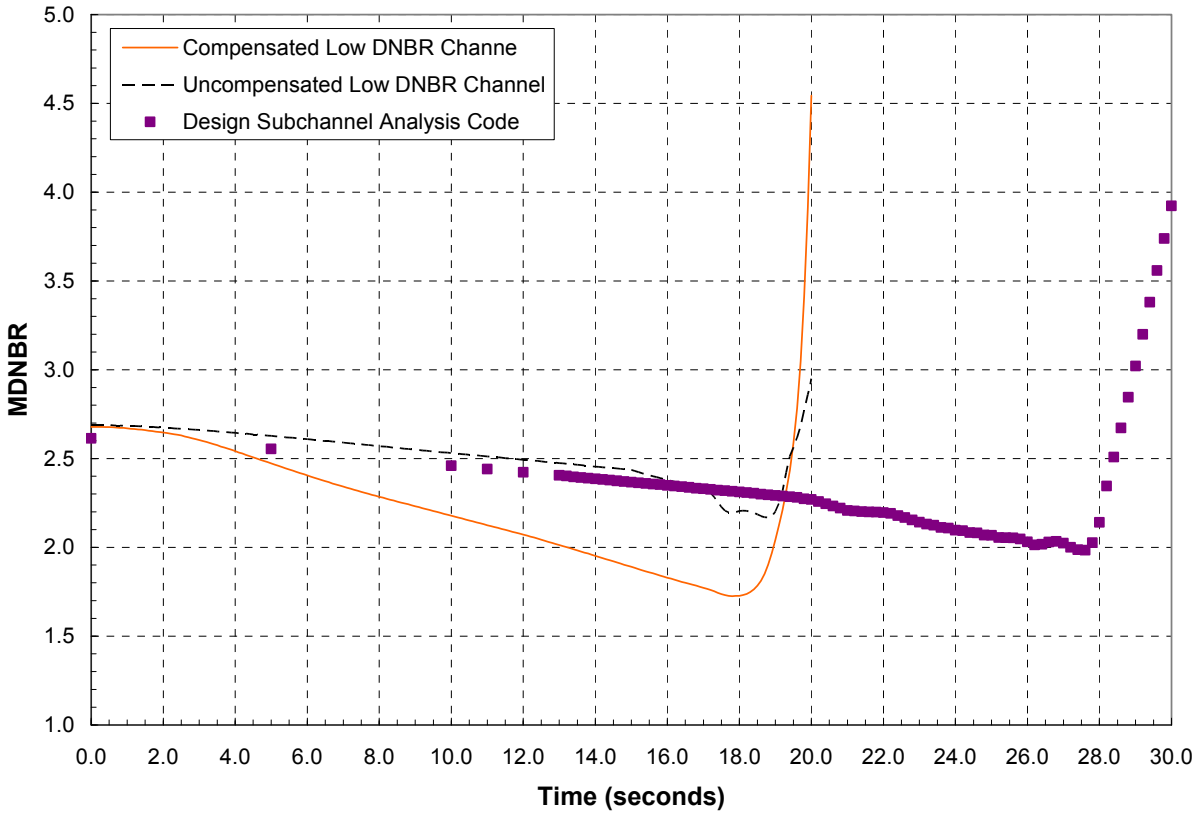


Figure 10-3 Bank Withdrawal At Power Considering Incore Trips

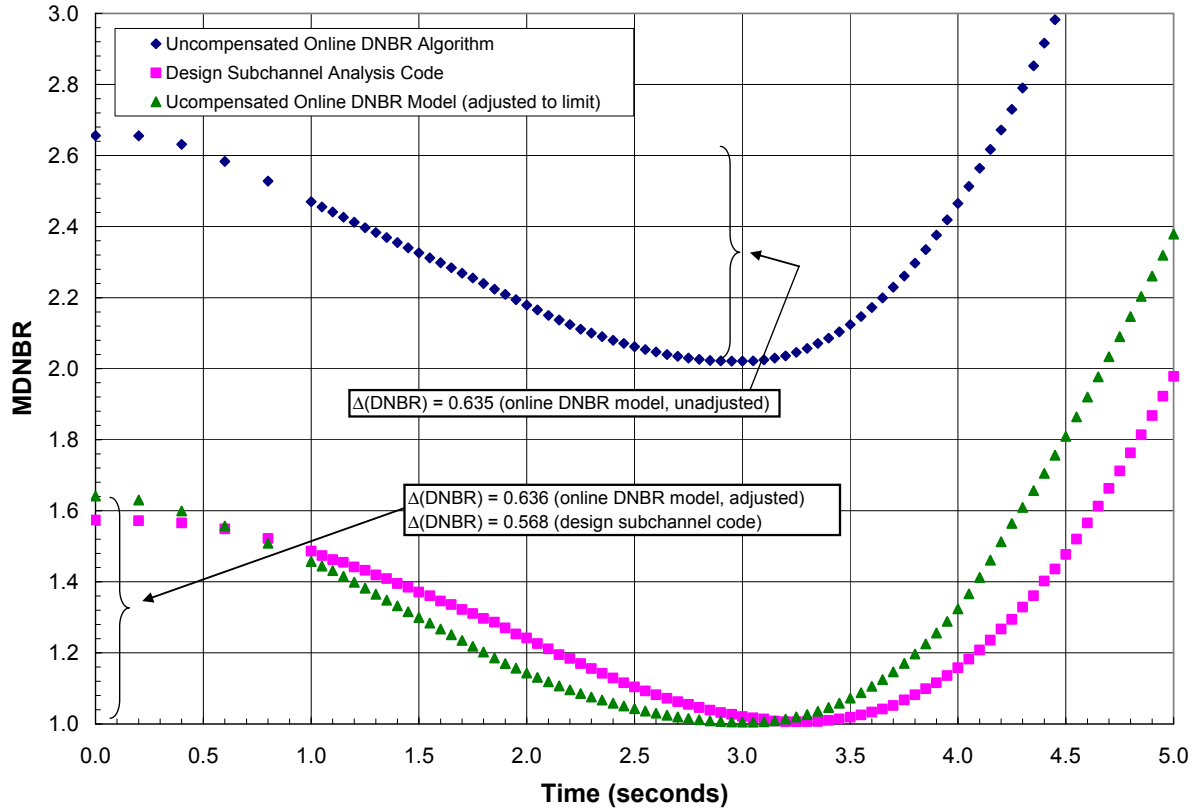


Figure 10-4 $\Delta(\text{DNBR})$ Calculation for Four-Pump Loss of Coolant Flow

11.0 REFERENCES

1. *U.S. Code of Federal Regulations*, Title 10, Section 50.
2. NUREG-0800, "Standard Review Plan for the Review of Safety Analysis Reports for Nuclear Power Plants (LWR Edition)," Nuclear Regulatory Commission, March, 2007 revision.
3. BAW-10186P-A, Revision 2, *Extended Burnup Evaluation*, June 2003.
4. EMF-2310(P)(A), Revision 1, *SRP Chapter 15 Non-LOCA Methodology for Pressurized Water Reactors*, Siemens Power Corporation, May 2004.
5. ANP-10275P, Revision 0, *U.S. EPR Instrument Setpoint Methodology Topical Report*, AREVA NP Inc., March 2007.
6. ANP-10282P, Revision 0, *POWERTRAX/E Online Core Monitoring Software for the U.S. EPR*, AREVA NP Inc., November 2007.
7. []
8. []
9. []
10. []

11. [

]

12. Regulatory Guide 1.126, Revision 1, "An Acceptable Model and Related Statistical Methods for the Analysis of Fuel Densification," U.S. Nuclear Regulatory Commission, March 1978.

13. [

]

14. [

]

15. [

]

16. [

]

17. ANP-10263PA, *Codes and Methods Applicability Report for U.S. EPR*, AREVA NP, Inc., August 2007.

18. EMF-96-029(P)(A), Volumes 1-2 and Attachment, *Reactor Analysis System for PWRs*, Siemens Power Corporation, January 1997.

19. EMF-93-164(P)(A) and Correspondence, Revision 0, *Power Distribution Measurement Uncertainty for INPAX-W in Westinghouse Plants*, Siemens Power Corporation, February 1995.
20. DOE/ET/34212-41, BAW-1810, *Urania Gadolinia: Nuclear Model Development and Critical Experiment Benchmark*, April 1984.
21. NUREG/CR-4604 (PNL-5849), *Statistical Methods for Nuclear Material Management*, Nuclear Regulatory Commission, December 1988.
22. EMF-1961(P)(A), *Statistical Setpoint Methodology for Combustion Engineering Type Reactors*, Siemens Power Corporation, July 2000.
23. EMF-92-081(P)(A), *Statistical Setpoint Methodology for Westinghouse Type Reactors*, Siemens Power Corporation, February 2000.

Appendix A Statistical Methodology

The statistical approach for establishing a setpoint utilizes [] considering the online DNBR and LPD algorithms, the uncertainties germane to the problem, and a broad range of power distributions and thermal hydraulic conditions. At each statepoint, the parameters being treated statistically are randomly varied based on their previously determined probability distribution or density, []

]

A.1 Description of Statistical Tolerance Limits

A.1.1 Overview

[

]

[

]

A.1.2 Coverage Approach for Single Setpoint

For a statistical process, there are two probabilities. The first, coverage, denotes the percentile of probability for the statistical variable and the second, confidence, denotes

the probability that an estimate of the coverage bounds the true coverage. [

]

[|] (A-1)

[

]

] (A-2)

[

]

The coverage approach finds a value of the random variable that bounds the true value, X. [

]

[

]

[

]

[

]

[

]

(A-3)

[

]

[

]

(A-4)

[

]

[

]



(A-5)

[

]

[

]

A.1.3 Testing Approach for Multiple Setpoints

[

]

[

]

[]

(A-6)

[

]

• [

]

• [

[

]

]

- [

]

[

] Therefore, the tabulated sample sizes given in Table A-1 also apply to the testing problem.

As an example of the process implementation for the testing process, [

]

[

]

A.1.4 Sample Size Considerations

In many applications of [

]

[

]

[

]

Table A-1 [

]

A large, empty rectangular frame with a black border, intended for the content of Table A-1. The frame is currently blank.

Table A-1 (continued) [Ordinal Rank of Estimators as Function of Sample Size]



Appendix B

Principles of SPND Calibration

B.1 Overview

Calibration of the SPNDs is typically performed at approximately 15 EFPD intervals via the use of the AMS and the incore monitoring system. A calibration by the AMS consists of using the aeroballs to measure the core power distributions at discrete locations, followed by a detailed reconstruction of the core-wide power distribution using the incore monitoring system software.

The results of this reconstruction provide the reference core conditions from which the specific calibration arrays are derived. The calibration array is a 6x12 array of factors which correlate the currents in individual detectors to the power applicable to either the DNBR or LPD evaluation. Distinct calibration arrays are used for the High LPD Channel and Low DNBR Channel trips. Details on these particular calibrations are discussed in subsequent subsections.

Throughout this Appendix, the index i will be used to indicate the number of an SPND within a detector string, from bottom to top. Therefore, the SPND denoted as $i=1$ will be the bottom SPND on a detector string. The range of i goes from 1 (the bottom-most SPND on a detector string) to 6 (the upper-most SPND on a detector string). Similarly, the index j will be used to denote the radial location of a SPND detector string. This will range from 1 to 12.

B.1.1 LPD Calibration Factors

The HLPD LSSS is based upon [

]

The HLPD calibration factor $C_{i,j}^{LPD}$ for the SPND can be defined as:

$$C_{i,j}^{LPD} = \frac{P_i^{AMS}}{I_{i,j}^{CAL}} \quad (B-1)$$

where $I_{i,j}^{CAL}$ is the current in SPND at the time of calibration, [

]

and $C_{i,j}^{LPD}$ is the SPND calibration factor array for LPD. See Appendix E for a discussion of the power distribution reconstruction.

In between calibrations, the HLPD Channel uses the SPND calibration array from Equation (B-1) to estimate the LPD as:

$$P_{i,j}^{LPD} = C_{i,j}^{LPD} \cdot I_{i,j} \quad (B-2)$$

where [$I_{i,j}$] is the measured current from each SPND.

Figure B-1 illustrates the HLPD calibration principle.

B.1.2 DNBR Calibration Factors

The Low DNBR Channel trip is [

]

The DNBR calibration array $C_{i,j}^{DNBR}$ for the SPND is:

$$C_{i,j}^{DNBR} = \frac{P_i^{AMS}}{I_{i,j}^{CAL}} \tag{B-3}$$

where $I_{i,j}^{CAL}$ is the current in SPND at the time of calibration, $C_{i,j}^{DNBR}$ is the SPND calibration factor array for DNBR, and [

$$\left[\right] \tag{B-4}$$

In this expression, [

] It is this

profile that the SPND strings are designed to estimate at all times. Figure B-2 graphically depicts the process for calculating a DNBR power for individual SPNDs.

Between calibrations, [] using the SPND calibration matrix for DNBR as:

$$P_{i,j}^{DNBR} = C_{i,j}^{DNBR} \cdot I_{i,j} \tag{B-5}$$

where [] and $I_{i,j}$ are the SPND currents. Figure B-3 graphically depicts the overall SPND calibration process for DNBR.

The DNBR calibration process is identical for both the LSSS and LCO, although the system is set up to store distinct $C_{i,j}^{DNBR}$ values for the LSSS and LCO functions.



Figure B-1 SPND Calibration for LPD

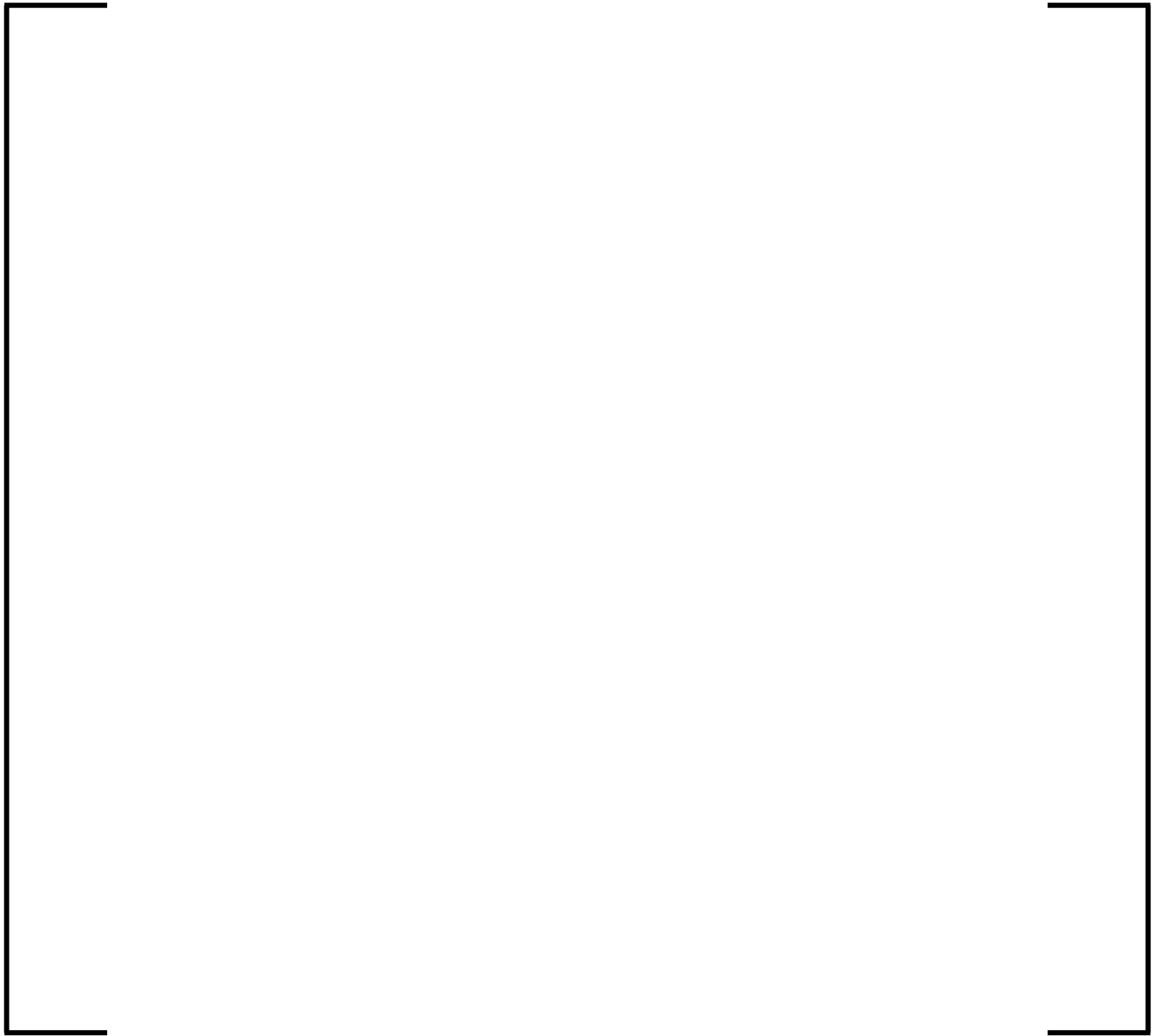


Figure B-2 Generation of SPND Power for DNBR

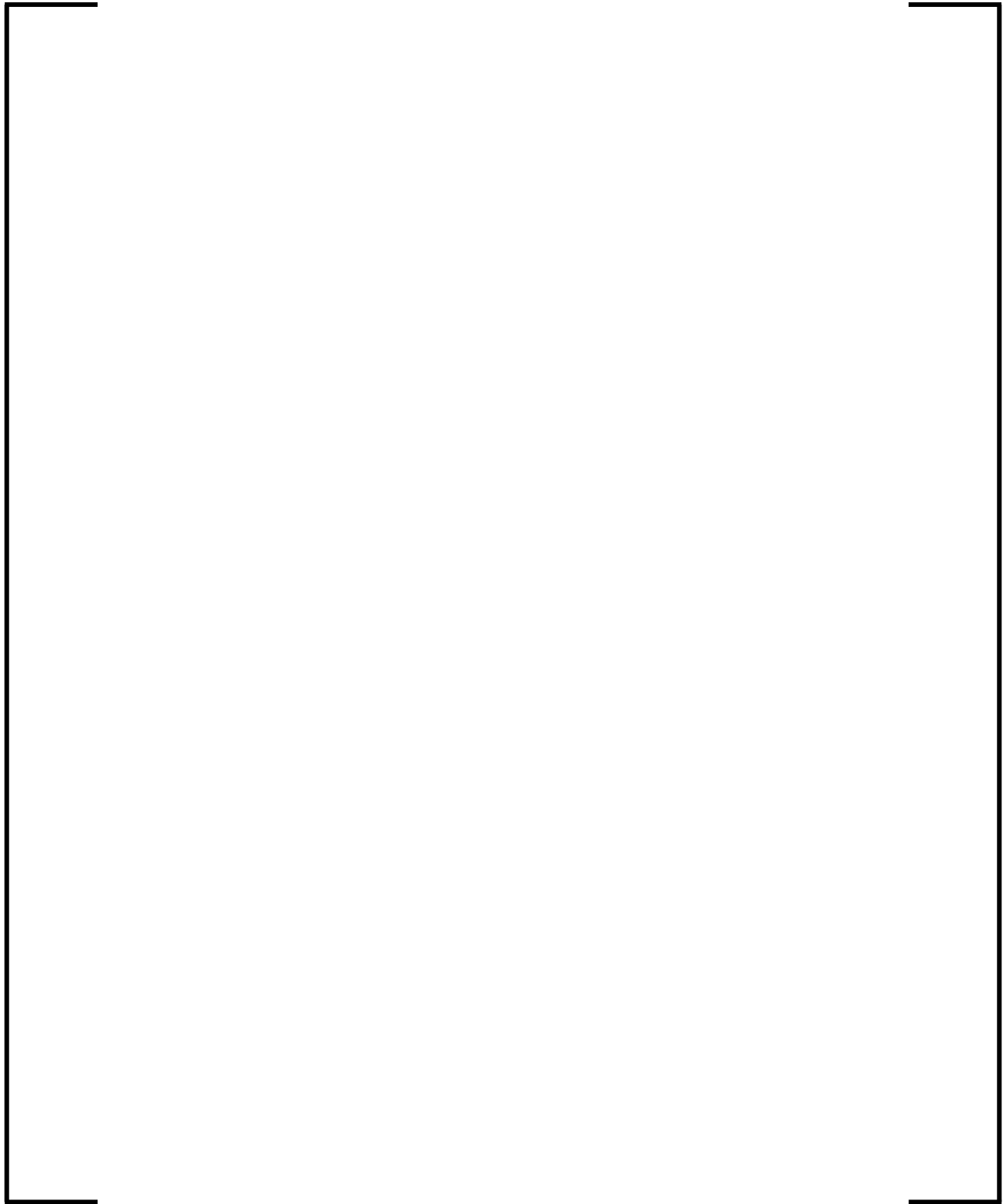


Figure B-3 SPND Calibration for DNBR

Appendix C

Description of Online DNBR Algorithm

The online thermal-hydraulic model used in the Low DNBR Channel LSSS and DNB LCO is a single closed-channel model. This appendix documents the flow of the online DNBR calculation.

C.1.1 Power Shape Reconstruction

As noted in the discussion in Appendix B, the power inputs to the Low DNBR Channel consist of all twelve (less those removed from the calculation due to detector failures) SPND strings, [

]

[

]

Lack of fit effects are taken into account via the use of the design code versus online algorithm uncertainty.

C.1.2 Filtering of Process Input Signals

In order to accommodate coolant transport times between the RTD location in the cold leg and the core inlet, as well as to reduce measurement noise, a second-order filter is used on the RTD signals. This takes the form:

$$TF_{\text{cold}} = \left(\frac{(1 + \tau_{\text{lead}}^{\text{Tcold}} S)}{(1 + \tau_{\text{lag1}}^{\text{Tcold}} S) \cdot (1 + \tau_{\text{lag2}}^{\text{Tcold}} S)} \right) \cdot T_{\text{cold}} \quad (\text{C-1})$$

where TF_{cold} is the filtered T_{cold} signal, T_{cold} is the unfiltered cold leg temperature signal, the tau values are time constants (see Table 3-2), and S is the Laplace transform operator.

In order to reduce noise associated with RCP speed measurement, a lag filter is applied. This takes the form:

$$\Omega F = \left(\frac{1}{(1 + \tau_{RCP} S)} \right) \cdot \Omega \tag{C-2}$$

where ΩF is the filtered RCP speed signal, Ω is the unfiltered signal, and τ_{RCP} is the lag time constant on the filter.

C.1.3 Calculation of the Inlet Mass Velocity

The inlet mass velocity at the core is derived [

] The inlet mass

flow rate is calculated as:

$$\tag{C-3}$$

where:

[

A_{core} = Fluid flow area of the core, in cm^2

Ξ = Units conversion factor (m^3/hr to cm^3/sec)

Θ = Flow rate adjustment factor

[

]

Of these values, Q_{ref} , Ω_{ref} , A_{core} , Ξ , and Θ are stored in the plant computer as constants, although these are updated when surveillance measurements are taken.

C.1.4 []

[

]

[]

[]

(C-4)

where:

[

]

[

]

$$[\quad]$$

(C-5)

where[

]

$$[\quad]$$

(C-6)

[

]

$$[\quad]$$

(C-7)

The outlet quality is then calculated as:

$$[\quad]$$

(C-8)

where:

$$[\quad]$$

C.1.5 []

Once the thermal-hydraulic balance on the hot channel is achieved, [

]

- [

]

$$[]$$

(C-9)

- [

]

$$[]$$

(C-10)

- [

]

$$[]$$

(C-11)

- [

]

$$[\quad]$$

(C-12)

[

]

$$[\quad]$$

(C-13)

and

$$[\quad]$$

(C-14)

[

]

[

]

C.1.6 [

]

[

]

$$[\quad] \quad (C-15)$$

In this expression, [

]

C.1.7 []

$$[\quad]$$

$$[\quad] \quad (C-16)$$

$$[\quad] \quad (C-16)$$

and

$$[\quad] \quad (C-17)$$

$$[\quad]$$

C.1.8 Calculate Uniform Critical Heat Fluxes

[] If any of the applicable CHF correlations change, then the online algorithm must necessarily be updated, and the uncertainty describing the differences in MDNBR predictions between the design code and the online algorithm must be reevaluated.

The particular expression evaluated for the uniform flux shape critical heat flux depends upon the form of the correlation,

$$[] \tag{C-18}$$

In this expression, a uniform critical heat flux calculation []

C.1.9 Calculate Non-Uniform Flux Factors

As with the CHF for uniform flux shapes discussed in the previous section, the form of the non-uniform flux factor correction factor will correspond to an NRC-approved critical heat flux correlation applicable to the fuel type in the core. Typically the non-uniform flux factor takes a Tong-like form as:

$$CHF_{\text{non-uniform}} = \frac{CHF_{\text{uniform}}}{FNU} \tag{C-20}$$

where the non-uniform flux factor FNU takes the general form:

$$FFNU = \frac{K}{\phi(ZH) \cdot (1 - e^{-K \cdot ZH})} \int_0^{ZH} dz \phi(z) \cdot e^{-K(ZH-z)} \quad (C-21)$$

with

$$K = \frac{K_{FNU1} (1 - \chi)^{K_{FNU2}}}{G^{K_{FNU3}}} \quad (C-22)$$

where

$\phi(i)$ = Local heat flux at elevation i

ZH = Distance from entry (bottom of heated length) to point where DNBR is calculated

χ = Equilibrium thermodynamic quality (at elevation ZH)

G = Local mass velocity (at elevation ZH)

K_{FNU1} = Fitting constant (inverse meters)

K_{FNU2} = Fitting constant

K_{FNU3} = Fitting constant

As in the calculation of the CHF for uniform flux shapes, the non-uniform flux factor is calculated for each available SPND string, at each spacer grid location within the heated length, and for both fuel and thimble cells.

C.1.10 Calculate DNBRs

The DNBR is calculated as:

$$DNBR = \frac{PCY \cdot CHF_{uniform}}{FNU \cdot P_{local}} \quad (C-23)$$

where:

PCY = Fuel rod heated perimeter

P_{local} = Local power density

[

]

C.1.11 Filter MDNBR and Exit Quality Signals

[

]

[

]

(C-24)

[

]

(C-25)

[

]

(C-26)

and

[

]

(C-27)

C.2 Calculation of SPND Imbalance

The SPND imbalance is calculated [

]

$$[\quad] \quad (C-28)$$

where IMB is the SPND imbalance in W/cm, P_{ij} is the calibrated (for imbalance) LPD signal from the SPND at radial location j (or radially symmetric location j -sym), [

]

$$[\quad]$$

Additionally, the term in parentheses is evaluated prior to the evaluation of the portion outside of the parentheses (the index k , although also representing the radial location of the detector, is used to differentiate it from the term outside of the parentheses).

This may be interpreted as follows. [

]

[
]

$$[\quad]$$

(C-29)

[

]

Appendix D

Random Sampling from Cumulative Distribution Functions

Recalling that the definition of a probability distribution function is that the probability that some selected value x is greater than some random variable X

$$P(x \geq X) = \int_{-\infty}^x f(y) dy = F(x) \quad (D-1)$$

where 'y' is the variable of integration, and $f(y)$ is the density of the random variable X . To directly sample a CDF, the probability at the point of the CDF is equated with the cumulative probability of the uniform distribution at the point of the random sample.

An as example, consider a random number z drawn from a uniform distribution. The cumulative probability for that draw is just:

$$P = \int_0^z dy = z \quad (D-2)$$

Since the probability for Equations (D-1) and (D-2) are the same, they are equated to get:

$$z = F(x) \quad (D-3)$$

Applying inversion, the value of x corresponding to the specified probability z is:

$$x = F^{-1}(z) \quad (D-4)$$

This expression maps the zero-to-one uniform distribution to the variable x .

Appendix E

Methodology for Assessing Measured Power Distribution Uncertainties

This appendix describes the processes used to generate the required data and, where applicable, the uncertainties associated with the data. Although the following discussion utilizes POWERTRAX/E as the incore monitoring system, the methodology is applicable to other incore monitoring software.

E.1 Aeroball Measurement System

The AMS is an electromechanical, computer-controlled, on-line flux mapping measurement system based on movable activation probes which operates on demand. The function of the AMS is consistent with that of current moveable incore detector systems currently employed in the U.S.

The aeroballs are steel balls containing vanadium which produce a gamma decay signature readily discernable by the measurement software. Moveable probes use aeroball stacks, in a column length that spans the active core height, at fixed assembly positions. On demand, a nitrogen gas driving medium transports the aeroball stacks to the core, where they become irradiated. After irradiation, the balls leave the core and pass into the measuring table in the AMS room inside the containment. The AMS computer controls the entire measuring process. It also calculates adjusted count rates from the measured pulse counts by applying correction factors, such as decay of the activity during the measuring procedure, residual activities, and scattering effect.

The AMS system to be employed in the U.S. EPR is based on 30 years of operation for 220 fuel cycles in 12 plants. This includes the 10 cycles of plant operation used to perform the sample power distribution reconstruction methodology uncertainty analysis described in Section E-3 of this Appendix.

A diagram illustrating the locations of the 40 probes to be utilized in the U.S. EPR design is provided in Figure E-1. The axial resolution of the U.S. EPR AMS is 36 equidistant nodes.

Additional information concerning the AMS can be found in Reference 6.

E.2 MEDIAN Power Distribution Reconstruction Methodology

During plant operation a three dimensional core power distribution is periodically derived from a combination of measured and calculated data. The power distribution so calculated is referred to as the “inferred” power distribution to differentiate it from the specific measured and calculated data utilized by the reconstruction methodology. The AMS described in Section E.1 is the source of the measured data. The core simulator PRISM provides calculated theoretical three dimensional power, burnup and neutron flux distributions and detector signals based on a physical core model which is continuously updated online in order to account for actual state parameters such as thermal reactor power, bank configurations, inlet temperature, etc. The PRISM methodology is described in Reference 17. The number of axial nodes used in the PRISM model for incore monitoring corresponds to the axial resolution of the AMS, although the boundaries generally will not be identical due to consideration of the axial material boundaries of the fuel assemblies.

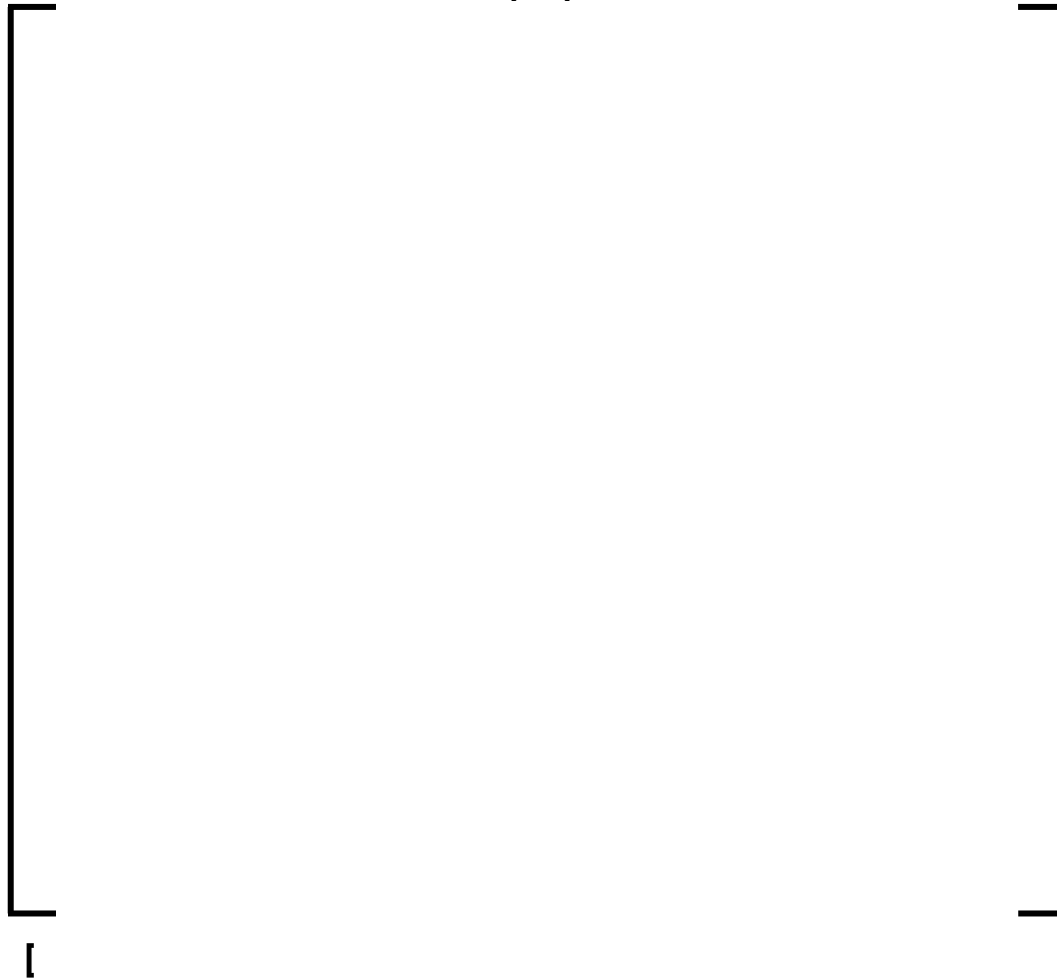
The inferred power distribution is generated by the PRISM module MEDIAN (**M**easurement **D**ependent Interpolation **A**lgorithm using **NEM**). MEDIAN is a calculation module in PRISM and is only used for reconstructing the inferred relative power distribution in the presence of measured data from the AMS. Because it is a module within PRISM, the PRISM calculated theoretical solution is directly available to it.

Radially the measured activation distribution corresponds exactly to the geometry of the calculation model. Axially the measured activation distribution is interpolated appropriately to match the nodal geometry of the calculation model.

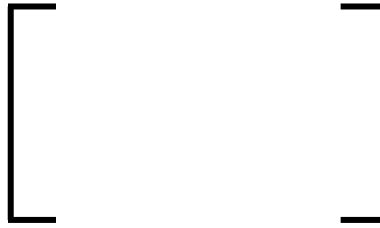
The inferred power distribution is determined in 3 steps:

- MEDIAN adapts the group-wise neutron fluxes at the measured nodes to achieve optimal consistency between theoretical results and measurement.
- MEDIAN extrapolates the instrumented location group-wise fluxes to the non-instrumented locations by use of the nodal balance equation.
- Spacer grid axial form functions (SGFF) are applied to the reconstructed 3D power distribution in non-instrumented locations.

E.3 Determination of Two-Group Optimal Fluxes



]



E.4 Extrapolation of the Node Fluxes

After the optimal fluxes have been calculated in the instrumented nodes, the fluxes in the remaining non-instrumented nodes are determined. The flux extrapolation is calculated by the physical models involved in the NEM method and not by a purely mathematical variance minimization approach. Therefore fuel assembly (FA) quantities like cross sections, flux and burnup gradients remain unchanged. By means of the optimal neutron fluxes in the instrumented FAs the nodal balance equation is modified and the flux distribution for the non-instrumented nodes n is determined by solving the following equation (see Section 4.2 of Ref. 5):



$$[\quad] - [\quad]$$

Using the spatial coupling coefficients from the PRISM calculated theoretical flux solution an inhomogeneous equation system for the fluxes in the non-instrumented nodes is derived:

$$[\quad]$$

This inhomogeneous linear equation system in ϕ_g is solved conserving the eigenvalue from the PRISM calculated theoretical solution and the optimal fluxes in the instrumented nodes by the iterative usage of the Gauss-Seidel algorithm. The result is a core wide node-wise 2-group flux distribution. From this distribution other quantities such as nodal powers and pin powers can be derived.

E.5 Application of Spacer Grid Axial Form Functions

The 3D inferred power distribution in the instrumented nodes include the flux depression effect due to the presence of grid spacers since the measured activation distributions

include this effect. For the 3D inferred power distributions in the non-instrumented nodes, the flux depression effect becomes diluted since the cross sections and coupling coefficients of the PRISM calculated theoretical solution do not include this effect. In order to capture the flux depression effect due to the presence of grid spacers, CALFAX applies Spacer Grid Form Functions (SGFF) to the axial power distributions in non-instrumented locations.

The SGFF are generated using SCALE Version 4.4a (Ref. 3). CSASIX is run to obtain macroscopic cell weighted fuel region cross section libraries in 44 groups based on ENDF/B5 data. These cross sections are used in XSDRNPM (discrete-ordinates transport method) using S8-P3 in slab geometry. In these calculations a spacer grid (SG) + fuel zone and a fuel only zone describe the spacer grid axial zone surrounded by a zone of pure fuel material. The slab geometry consists of 87 layers over 35 cm. Reflective boundary conditions are used at both edges. The resultant axial power density distribution, normalized to a value of 1.0 at the rightmost boundary, can then be approximated with analytical functions. The following sketch shows the qualitative behavior of the form function $F(z)$ as a function of the curve parameters DISTH, DISTI, PREDZ, PREDH, and PREDI:



where:

$$\begin{bmatrix} \\ \\ \\ \\ \end{bmatrix}$$

For each grid in the active fuel zone the corresponding SGFF are applied to the assembly nodal powers and the $F_{\Delta H}$ pin axial powers over all axial nodes. The nodal average value is reduced by the integrated $F(z)$ effect over the node and the top and bottom edge values are reduced by the $F(z)$ effect directly. A renormalization is then performed such that the 2D FA powers and 2D $F_{\Delta H}$ pin powers are unchanged.

Application of the SGFF effect to nodal F_Q values is a 2 step process. It is assumed that the F_Q shape within a node follows the same quadratic axial profile of the assembly power within the node. The three knowns (node average, top surface, and bottom surface) define the quadratic. With this formulation the maximum can be found. The peak assembly power within the node is found before and after grid factors are applied and renormalization occurs. The ratio of the after-to-before peak power is applied to F_Q to obtain the F_Q with grid factor applied.

E.6 Inferred Relative Power Distribution Uncertainties

The data reduction and statistical treatment techniques used to derive inferred relative power distribution uncertainties (calculated plus measured) for $F_{\Delta H}$, F_Q , assembly power AO, and local peaking factor (LPF) are essentially the same as those described in Section 5.0 of Reference 19 and further applied in Reference 18.

To summarize the Reference 19 methodology, for each parameter of interest the statistics which form the basis of the corresponding uncertainty are derived from

differences between the values when the detector is failed (the “inferred” value) and when a given detector is operable (the “measured” value). For each available map the measured/inferred power distribution is calculated with all operable detectors. Each operable detector is then singularly “failed” and the measured/inferred power distribution is recalculated. The percentage difference or difference (inferred minus measured) in the parameter of interest is calculated for the “failed” location. This process is repeated for each operable detector, and for multiple maps, multiple cycles and multiple plants. The cumulative data base forms the basis for the uncertainty.

This methodology is used to obtain uncertainty distributions for the following inferred relative power distribution parameters:

- Peak power (F_Q) for HLPD calibration
- Peak pin ($F_{\Delta H}$) for DNBR calibration
- Assembly power axial offset (AO) for DNBR calibration

As noted before, one-sided 95/95 uncertainties are not required, rather the distributions which would be used to obtain these uncertainties are required.

The uncertainty distributions for items F_Q and $F_{\Delta H}$ are further combined with the local peaking factor (LPF) uncertainty to derive one-sided 95/95 tolerance limits for F_Q and $F_{\Delta H}$.

E.7 Sample Power Distribution Uncertainty Calculation

The purpose of this section is to provide a representative demonstration of Reference 18 and 19 methodologies for generating power distribution uncertainties, based upon measurement data from plants using the AMS. This data is based upon 147 measurements taken over 10 cycles of operation at two independent reactors:

1. Plant G1 is a 177 assembly core with a 15x15 fuel lattice (see Figure E-2) and an active fuel height of 9.83 feet. The G1 AMS includes 24 columns divided into 30

axial layers. G1 measured data from 76 maps in Cycles 26 through 30 are used in the analysis. These maps are at or near hot full power conditions and include gadolinia fuel.

2. Plant G2 is a 193 assembly core with an 18x18 fuel lattice (see Figure E-3) and an active fuel height of 12.85 feet. The G2 AMS includes 28 columns divided into 32 axial layers. G2 measured data from 71 maps in Cycles 1 through 5 are used in the analysis. These maps are at or near hot full power conditions and include gadolinia fuel.

The standard deviation of the relative uncertainty in the LPF was determined by comparisons of calculated pin-by-pin fission rate distributions with critical experiment measurements (Reference 20).

E.7.1 F_Q Power Distribution Uncertainty

The database is generated by considering locations where the measured assembly average power is greater than 0.90 times the core average. In addition, only those axial nodes whose measured nodal power is greater than 0.90 times the core average are used. In the Reference 18 and 19 applications the top and bottom 10% or 15% of nodes were excluded per plant Technical Specifications. This approach is not applicable to the U.S. EPR. This resulted in 81486 data points over 2968 assemblies.

This uncertainty does not include the calculated LPF uncertainty described in Section E.7.4.

In Table E-2 the statistics (mean and standard deviation) are compiled by map, cycle, plan, and overall. The degrees of freedom associated with the overall standard deviation are conservatively assumed to be 2967. In Figure E-4 a histogram of the combined (both plants, all maps) relative difference data is presented compared to a normal distribution of the same mean and standard deviation. Conservatively, no credit is taken for the small positive bias (0.256 percent) observed for F_Q .

E.7.2 $F_{\Delta H}$ Power Distribution Uncertainty

The database is generated by considering locations where the measured assembly average power is greater than 0.90 times the core average. This resulted in 2968 data points.

This uncertainty does not include the calculated LPF uncertainty described in Section E.7.4.

In Table E-2 the statistics (mean and standard deviation) are compiled by map, cycle, plan, and overall. The degrees of freedom associated with the overall standard deviation is 2967. In Figure E-5 a histogram of the combined relative (percent) difference data is presented compared to a normal distribution of the same mean and standard deviation.

To account for both the small negative bias (0.18 percent) and the small burnup dependence of this bias (bounded by -0.10 percent), a conservative total adjustment of 0.28 percent is used for $F_{\Delta H}$.

E.7.3 Assembly Axial Offset Distribution Uncertainty

The database is generated by considering locations where the measured assembly average power is greater than 0.90 times the core average. The assembly axial offset uncertainties are used to characterize the uncertainty in the axial shape of the reconstructed $F_{\Delta H}$ pin.

In Table E-2 the statistics (mean and standard deviation) are compiled by map, cycle, plan, and overall.

In Figure E-6 a histogram of the combined difference data is presented compared to a normal distribution of the same mean and standard deviation.

E.7.4 Local Peaking Factor Uncertainty

The standard deviation of the relative uncertainty in the calculated local peaking factor was determined by comparisons of calculated pin-by-pin fission rate distributions with critical experiment measurements performed by (Reference 20). These comparisons included six distributions which cover a variety of lattice configurations, various enrichments and the inclusion of burnable absorbers.

Only UO₂ pin powers were used for the LPF uncertainty component because the very low gadolinia pin powers skewed the statistics when differences (C-M) were converted to relative differences (% C-M). The gadolinia pin power differences did behave similarly to the UO₂ pin power differences. As the gadolinia burns out and the relative gadolinia pin power increases, the gadolinia pin power relative differences would behave like the UO₂ pin power relative differences. From comparisons of the calculated to measured pin-by-pin fission rate distributions, values for the combined uncertainties in calculation and measurement were determined. The following table summarizes the mean and standard deviation for each of the six cores analyzed.

A χ^2 test of normality (mean -0.004 percent, standard deviation 1.186 percent) was performed on the 183 data points using 10 intervals. The χ^2 statistic (O-E)²/E has nine degrees of freedom. Since \bar{x} and s were used to approximate the statistics μ and σ , respectively, two additional degrees of freedom are lost, resulting in seven degrees of freedom. The resultant χ^2 value of 12.40 is < 14.07 which corresponds to a five percent significance level, i.e., at this significance level there is no clear evidence that this distribution is not normal, and thus the hypothesis that the distribution is normal is accepted. The results are summarized in Table E-3.

E.7.5 Combined Power Distribution Uncertainties

Two methods were used to combine the uncertainties associated with the assembly (F_{ΔH}) and nodal (F_Q) power distributions and the local peaking factor:

- A Monte Carlo method was utilized to combine the uncertainties associated with the assembly ($F_{\Delta H}$) and nodal (F_Q) power distributions, respectively, and the local peaking factor. The Monte Carlo simulation randomly sampled data from each of the two components of the error terms for both the inferred value and the measured or reference value. The two inferred values were multiplied together to simulate the inferred calculation. Similarly the resultant reference value was obtained and divided into the inferred value. This result is the multiplier to apply to the inferred value to obtain the reference value. The nonparametric tolerance equation (Reference 11) was used to determine the point on the simulated distribution that represents the one-sided 95/95 statistical tolerance/confidence limit for when the inferred power distribution under predicts the reference value.
- An analytical method assuming normality was also used as a cross-check of the Monte Carlo results. The uncertainty factors that multiply the peaking factors calculated from the inferred power distribution are of the form $(1 + K_x S_x)$, where S_x is the standard deviation in the variable of interest, i.e., $F_{\Delta H}$ or F_Q . The one-sided 95/95 tolerance factor is a function of the number of degrees of freedom associated with the relative standard deviation. The degrees of freedom can be calculated from Satterthwaite's formula (Reference 21), given below:

For a variance defined as:

$$S_0^2 = a_1 S_1^2 + a_2 S_2^2 + \dots + a_k S_k^2 \quad (\text{E-1})$$

the degrees of freedom are given by:

$$df_0 = \frac{S_0^4}{\left(\frac{a_1^2 S_1^4}{df_1} + \frac{a_2^2 S_2^4}{df_2} + \dots + \frac{a_k^2 S_k^4}{df_k} \right)} \quad (\text{E-2})$$

The one-sided tolerance factor may then be computed by:

$$k_f = z_p + \frac{\sqrt{z_p^2 - ab}}{a} b \quad (E-3)$$

where $a = 1 - \frac{z_\gamma^2}{2 \cdot (n-1)}$, $b = z_p^2 - \frac{z_\gamma^2}{n}$ and n is the number of degrees of freedom. For a 95/95 tolerance the z_γ and z_p are equal to 1.645.

Any negative biases are accounted for in the final relative uncertainty factors whereas positive biases are conservatively ignored.

The Monte Carlo simulation resulted in an F_Q uncertainty of [] percent. The analytical method results in an F_Q uncertainty of [] percent. A value of [] percent is assumed.

The Monte Carlo simulation resulted in an $F_{\Delta H}$ uncertainty of [] percent. The analytical method results in an $F_{\Delta H}$ uncertainty of [] percent, which includes a [] percent burnup dependence bias. A value of [] percent is assumed.

E.7.6 Summary

Table E-4 summarizes the inferred relative power distribution uncertainties based on data representative of the U.S. EPR core design.

Table E-1 Inferred Relative Power Distribution Summary Statistics

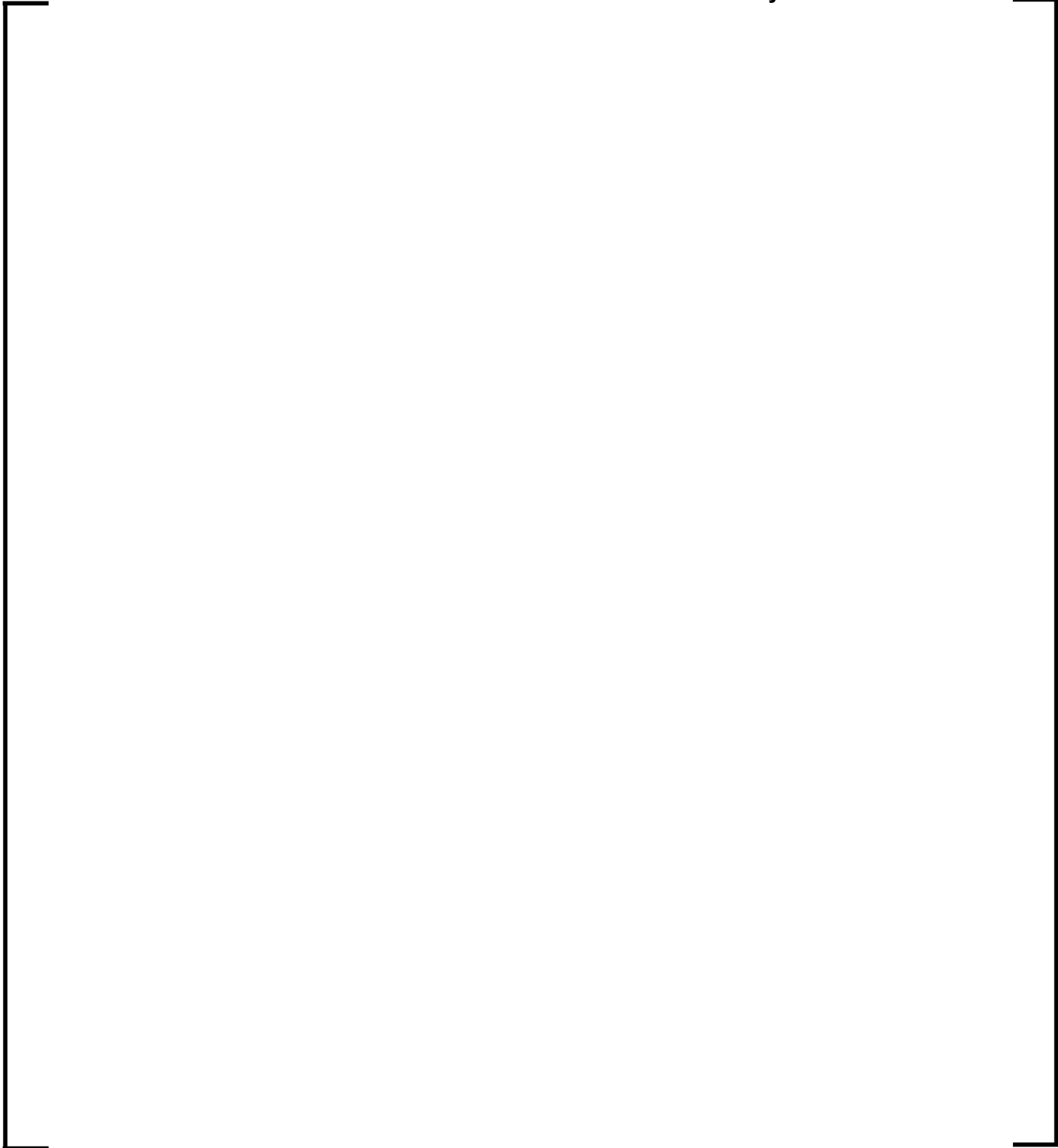
A large, empty rectangular frame with a thin black border, occupying most of the page below the title. It is intended for the content of Table E-1.

Table E-1 (Continued)

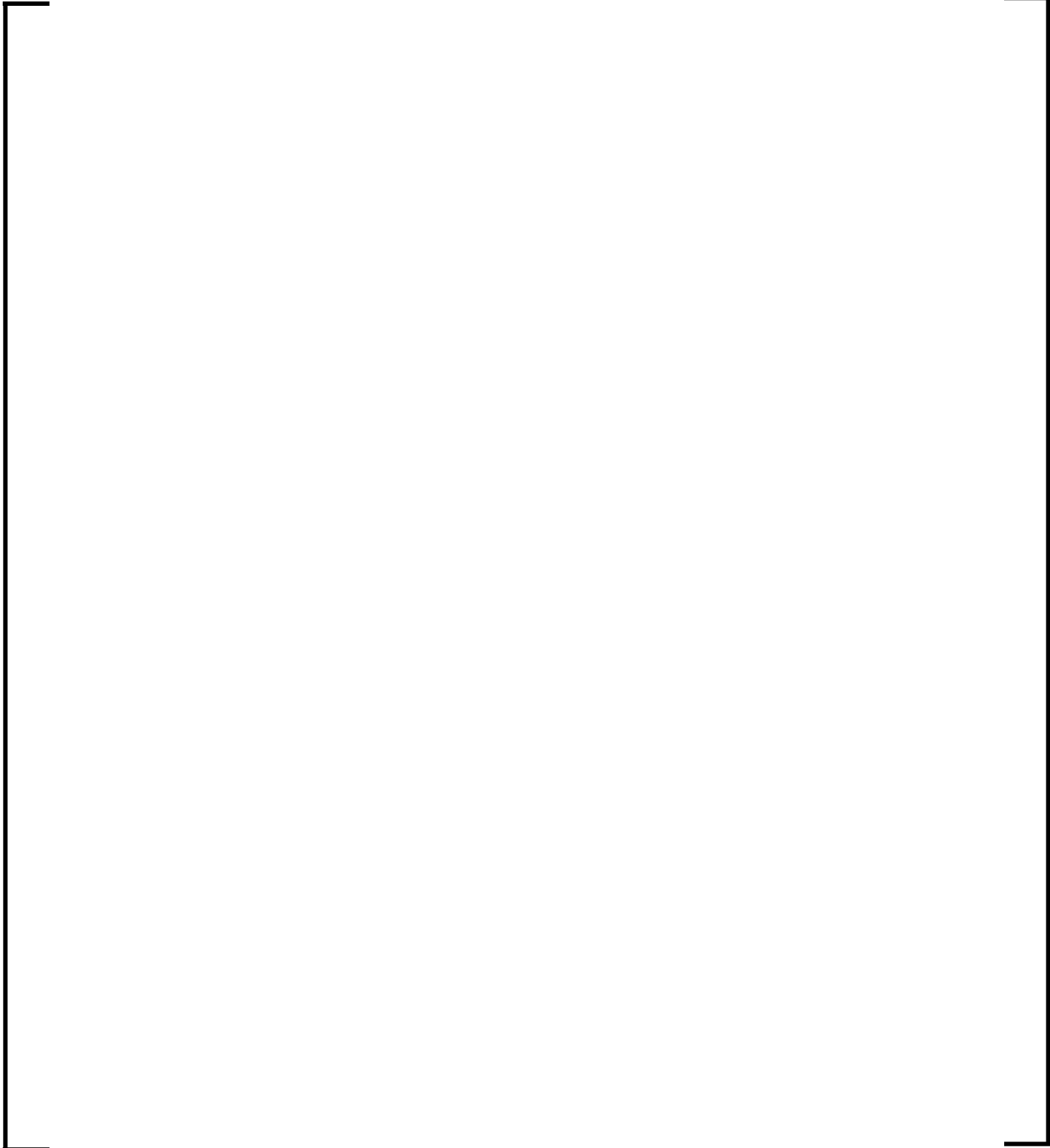
A large, empty rectangular frame with a thin black border, occupying most of the page. It is positioned centrally below the section header and above the footer area. The frame is currently empty, suggesting that the table content is either missing or has been redacted.

Table E-1 (Continued)

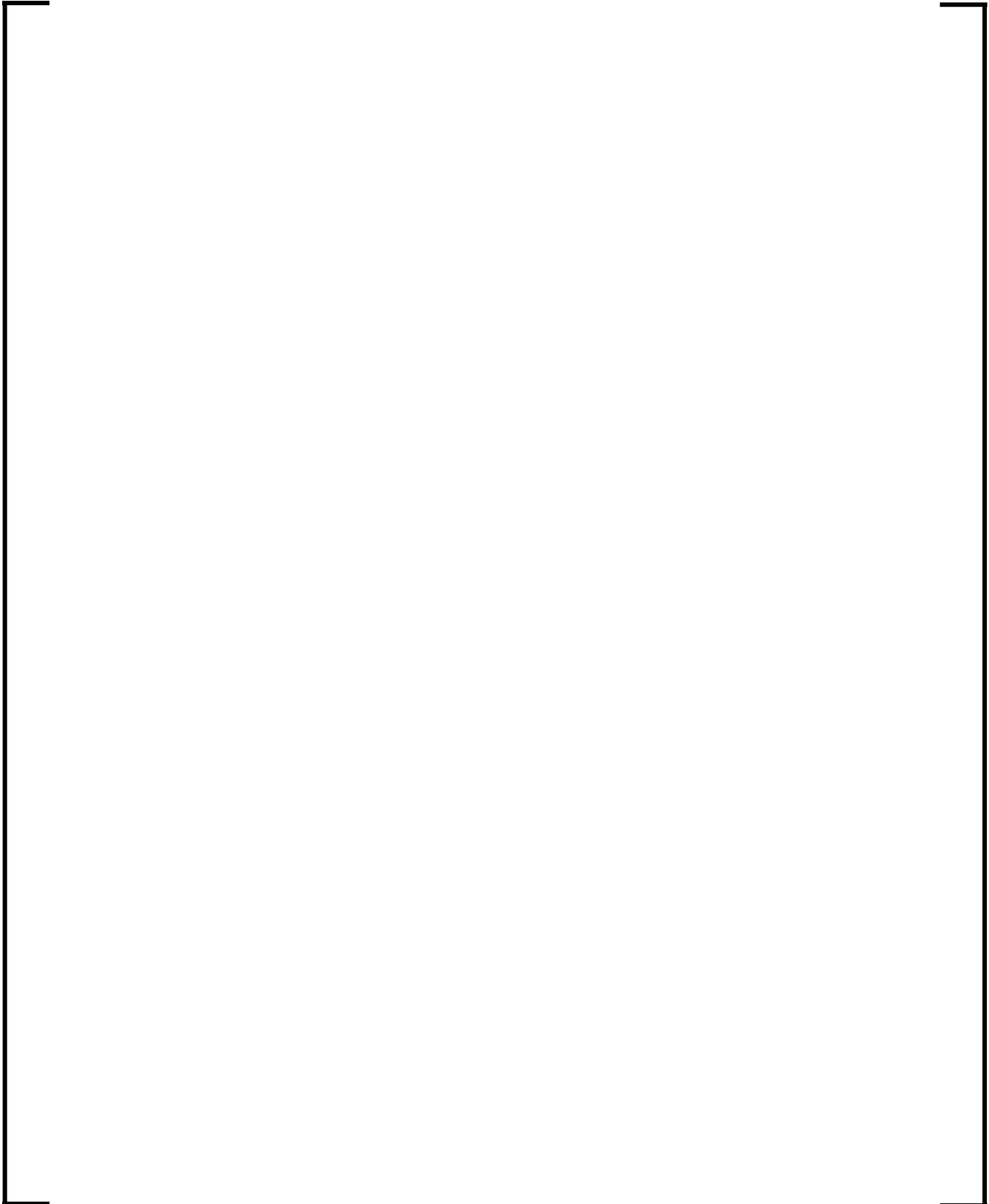
A large, empty rectangular frame with a thin black border, occupying most of the page. It is positioned below the section header and above the footer area, indicating that the table content is either missing or has been redacted.

Table E-1 (Continued)

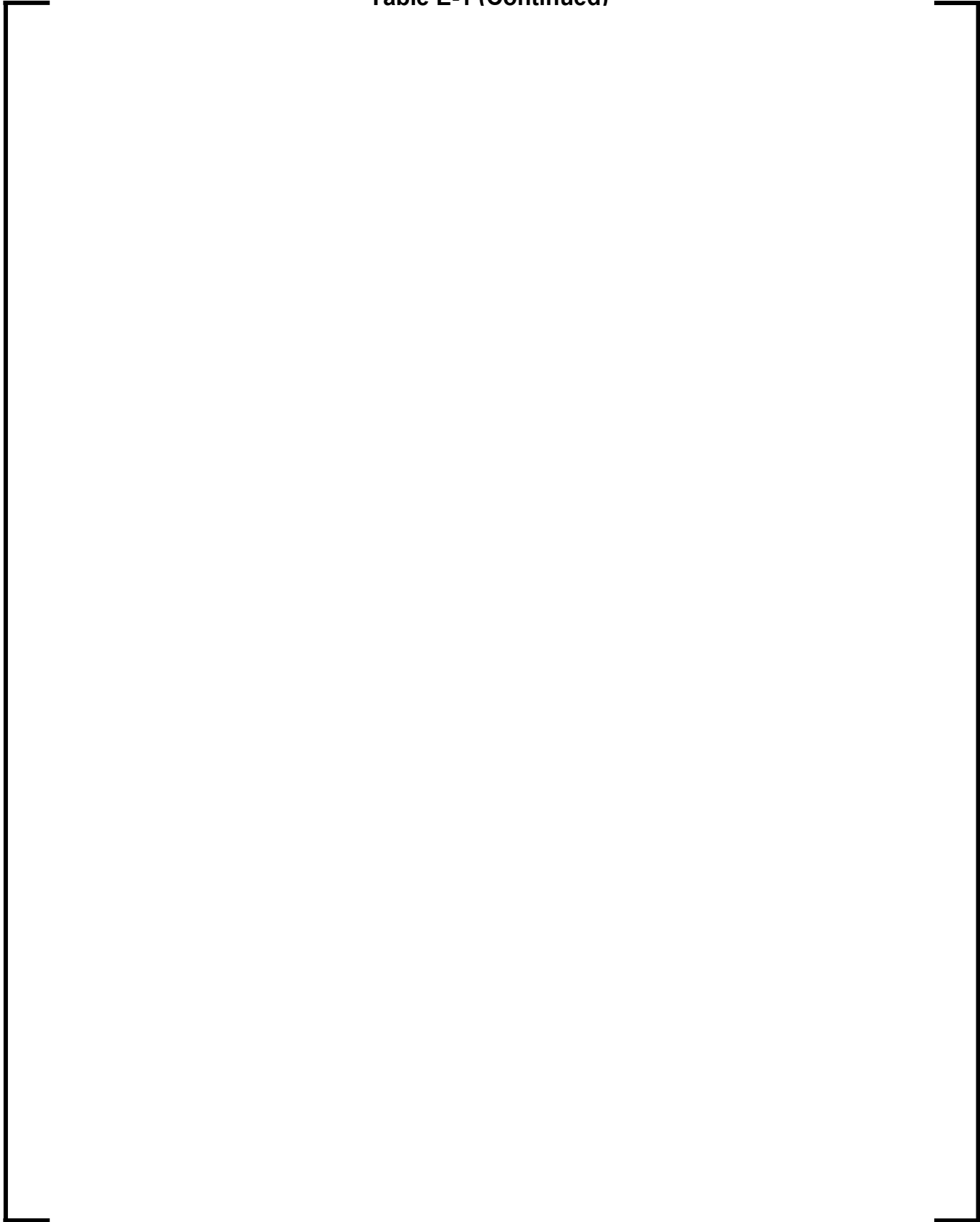
A large, empty rectangular frame with a thin black border, occupying most of the page. It is positioned centrally below the section header and above the bottom margin. The frame is intended for a table, but it is currently blank.

Table E-2 χ^2 Test of Normality, Local Peaking Factor Data

Interval	Core						Observed (O)	Expected (E)	$\frac{(O-E)^2}{E}$
	1	5	12	14	18	20			
-100.000 to -1.773	0	7	3	3	1	2	16	12.26	1.14
-1.773 to -1.330	2	0	0	0	0	4	6	11.71	2.79
-1.330 to -0.887	1	1	2	5	4	2	15	17.57	0.38
-0.887 to -0.443	3	1	6	4	7	1	22	23.61	0.11
-0.443 to 0.000	4	2	8	4	3	2	23	26.35	0.43
0.000 to 0.443	17	1	4	3	6	9	40	26.35	7.07
0.443 to 0.887	4	6	4	2	5	2	23	23.61	0.02
0.887 to 1.330	0	5	2	3	5	2	17	17.57	0.02
1.330 to 1.773	0	4	1	3	1	2	11	11.71	0.04
1.773 to 100.000	1	2	2	2	0	3	10	12.26	0.42
Total							183	183	12.42

Table E-3 Summary of Mean and Standard Deviations (%C-M)

Table E-4 Inferred Relative Power Distribution Uncertainties

Description	Results	Comments
Incore Monitoring System		AMS and POWERTRAX/E
Number of Reactors	2	G1 and G2
Number of cycles	10	5 cycles from Plant G1 5 cycles from Plant G2
Number of Maps	147	76 from Plant G1 71 from Plant G2
Standard deviation of the relative uncertainty in the assembly and nodal power distributions	[] for assembly, [] for nodal	Comparisons used all available measured data
Number of pin-by-pin fission rate distributions used to calculate local peaking factor uncertainty	6	Included various guide tube configurations, variety of enrichments, and burnable absorbers
Standard deviation of the relative uncertainty in the local peaking factor	[]	
Standard deviation of the combined relative uncertainty in assembly power and local peaking factor	[]	
Standard deviation of the combined relative uncertainty in nodal power and local peaking factor	[]	
One-sided 95/95 upper tolerance limit for $F_{\Delta H}$	[]	Includes [] bias
One-sided 95/95 upper tolerance limit for F_Q	[]	

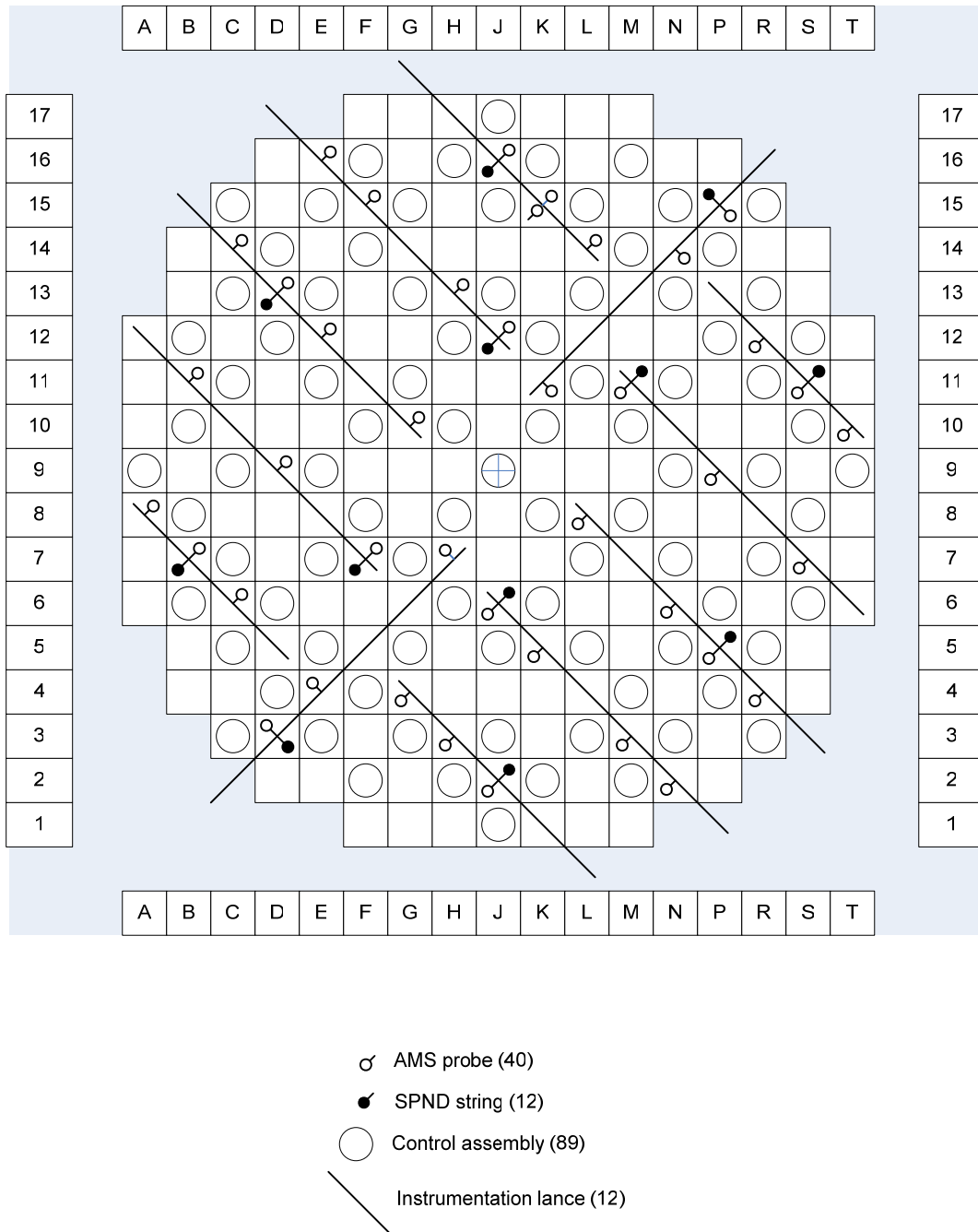


Figure E-1 Layout of Incore Nuclear Instrumentation in U.S. EPR

1	1	1	1	1	1	1	1	1	1	1	1	1	1	1
1	1	1	1	1	1	1	1	1	1	1	1	1	1	1
1	1	3	1	1	3	1	1	1	3	1	1	3	1	1
1	1	1	1	1	1	1	1	1	1	1	1	1	1	1
1	1	1	1	3	1	1	3	1	1	3	1	1	1	1
1	1	3	1	1	1	1	1	1	1	1	1	3	1	1
1	1	1	1	1	1	1	1	1	1	1	1	1	1	1
1	1	1	1	3	1	1	1	1	1	3	1	1	1	1
1	1	1	1	1	1	1	1	1	1	1	1	1	1	1
1	1	3	1	1	1	1	1	1	1	1	1	2	1	1
1	1	1	1	3	1	1	3	1	1	3	1	1	1	1
1	1	1	1	1	1	1	1	1	1	1	1	1	1	1
1	1	3	1	1	3	1	1	1	3	1	1	3	1	1
1	1	1	1	1	1	1	1	1	1	1	1	1	1	1
1	1	1	1	1	1	1	1	1	1	1	1	1	1	1

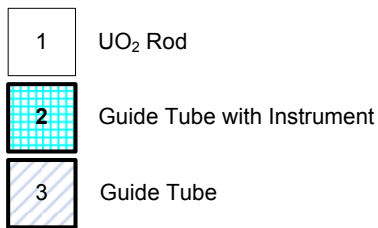


Figure E-2 Plant G1 Assembly Guide Tube Configuration

1	1	1	1	1	1	1	1	1	1	1	1	1	1	1	1	1	1
1	1	1	1	1	1	1	1	1	1	1	1	1	1	1	1	1	1
1	1	1	1	1	1	3	1	1	1	1	3	1	1	1	1	1	1
1	1	1	3	1	1	1	1	1	1	1	1	1	1	3	1	1	1
1	1	1	1	1	1	1	3	1	1	3	1	1	1	1	1	1	1
1	1	1	1	1	3	1	1	1	1	1	1	3	1	1	1	1	1
1	1	3	1	1	1	1	1	1	1	1	1	1	1	1	3	1	1
1	1	1	1	3	1	1	1	1	1	1	1	1	3	1	1	1	1
1	1	1	1	1	1	1	1	1	1	1	1	1	1	1	1	1	1
1	1	1	1	1	1	1	1	1	1	1	1	1	1	1	1	1	1
1	1	1	1	3	1	1	1	1	1	1	1	1	3	1	1	1	1
1	1	3	1	1	1	1	1	1	1	1	1	1	1	1	3	1	1
1	1	1	1	1	3	1	1	1	1	1	1	3	1	1	1	1	1
1	1	1	1	1	1	1	3	1	1	3	1	1	1	1	1	1	1
1	1	1	3	1	1	1	1	1	1	1	1	1	1	3	1	1	1
1	1	1	1	1	1	3	1	1	1	1	2	1	1	1	1	1	1
1	1	1	1	1	1	1	1	1	1	1	1	1	1	1	1	1	1
1	1	1	1	1	1	1	1	1	1	1	1	1	1	1	1	1	1

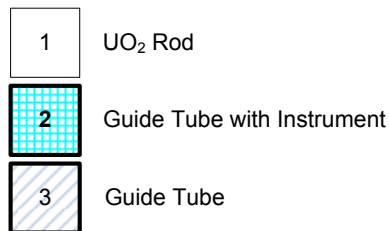


Figure E-3 Plant G2 Assembly Guide Tube Configuration



Figure E-4 FQ Relative Difference Compared to Normal Distribution



Figure E-5 $F\Delta H$ Relative Difference Compared to Normal Distribution



Figure E-6 AO Relative Difference Compared to Normal Distribution